STRESS ANALYSIS OF PRISMATIC AND CYLINDRICAL SHELLS

Thesis by

Lars Skjelbreia

In Partial Fulfillment of the Requirements

For the Degree of

Doctor of Philosophy

California Institute of Technology

Pasadena, California

1953

ACKNOWLEDGMENT

It is with pleasure that the writer takes this opportunity to express his appreciation to Professor G. W. Housner. His interest in this research and his high scientific standards have influenced in a most important way the writer's progress during his graduate studies at the California Institute of Technology.

The writer also wishes to thank Professor R. R. Martel for the pleasant cooperation and fruitful exchange of ideas in the early part of the research. Thanks are also due to Professor D. E. Hudson, Mr. M. J. Wood and Mr. M. E. Jessey for their assistance in all phases of the experimental work.

ABSTRACT

This thesis consists essentially of two distinct parts. The first part deals with the development of the theory and the second part deals with experimental verification of the theory.

The theory developed in this paper applies to the analysis of prismatic shells, also called hipped-plate structures or "Faltwerke", and uses only techniques commonly employed in structural engineering analysis. A cylindrical shell is approximated by a prismatic shell and analysed as such. In the analysis, extensive use is made of a relaxation or distribution method. Both simply supported and continuous shells are treated.

For the purpose of verifying the theory several test models were built, both prismatic and cylindrical. Stresses were measured with electric strain gages, and close agreement was found between theory and experiments.

TABLE OF CONTENTS

TABLE OF CONTENTS (Cont'd)

I. INTRODUCTION

The cylindrical and prismatic shells treated in this paper have a wide application as reinforced concrete roofs for hangars, industrial buildings, auditoriums and similar structures where large floor areas are needed. Construction of this kind is not a new development as the first such structures were erected in Europe as early as 1920; however they were hardly known in this country until the early forties. The number of concrete shell structures built in recent years has increased some, since no other structural system makes such an economical use of materials, but the lack of a fairly simple design theory has retarded the general use of these structures.

The majority of shell roofs used are cylindrical barrels. The prismatic shells, which are similar to the cylindrical shells, consist of several thin plates intersecting at parallel edges. Compared with cylindrical shells, prismatic shells require simpler formwork and are less likely to buckle, but, due to their greater bending moments on an axial section, they are heavier and thus less adaptable to extremely large spans.

Both types of shells are supported by two or more diaphragms normal to the surface as shown in Figure 1. These structures can therefore be considered as a special kind of simply supported or continuous beam. The shell can be analysed as an ordinary beam only if it is rigid enough to maintain the shape of the cross-section under load. However, since the thickness normal to the surface of the shell is generally small, the cross-section will deform and a more elaborate theory is needed in analysing the shell.

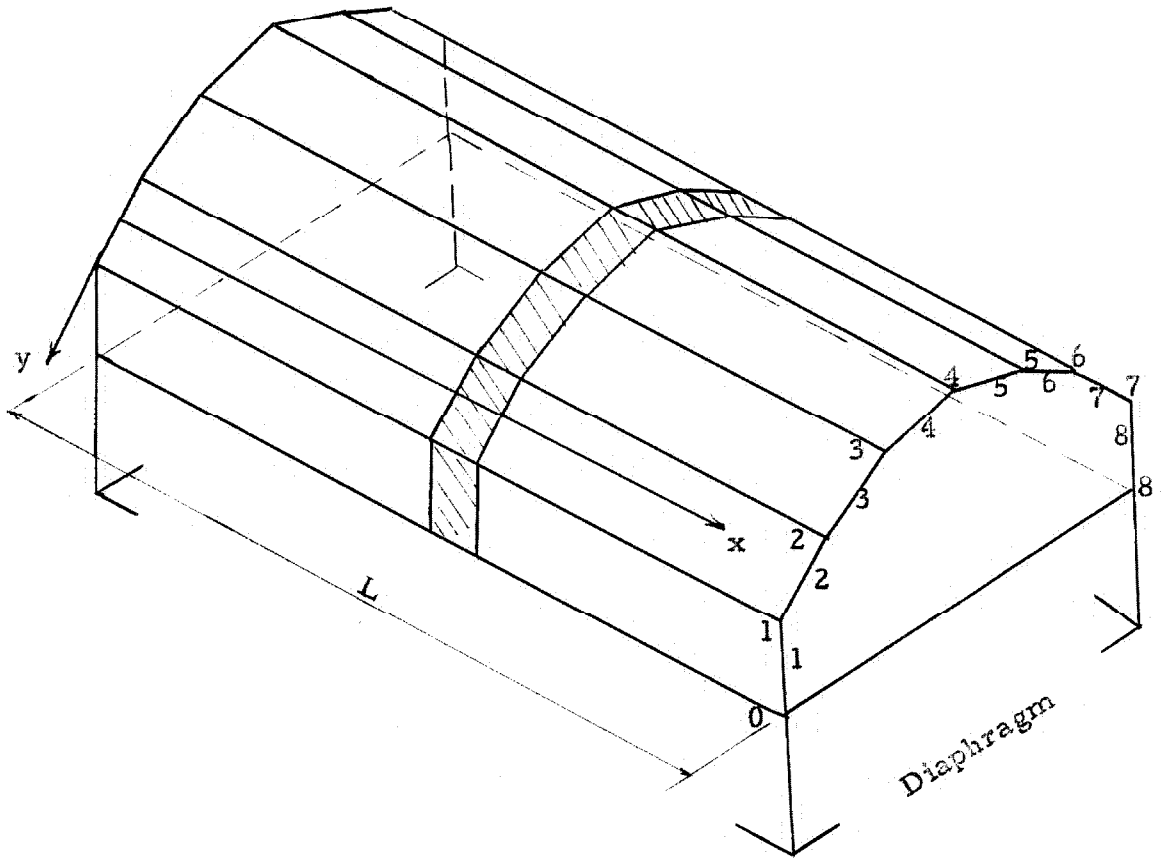

Figure 1

Prismatic Shell

The first analytical solution of cylindrical shell stresses was published by Lame and Clapeyron[18]* in the early parts of the nineteenth century. They neglected the moments and transverse shearing forces and supposed that only membrane forces (i.e. normal forces and tangential shearing forces) act on the shell. In this case the stresses in the shell are calculated according to the membrane theory, which will give an approximate analysis for shells whose lengths are of the same order of magnitude as their widths.

In 1892 Love[19] presented the first general mathematical theory of elasticity for cylindrical shells. This has afforded a basis for the subsequent development in this field. Using this theory the problem reduces in each particular case to the solution of a system of three partial differential equations of second order. The solution of these equations, however, is very complicated and is not practical for engineering design. The first practical solution available for shell roof design was developed by Finsterwalder[21] who gave an approximate solution of the problem. In this, the solution furnished by the membrane theory is taken as a first approximation and the general bending theory used only to satisfy the boundary conditions. The cylindrical shells used in engineering practice are supported in such a manner that the tangential and transverse displacements at the ends vanish. For such shells experiments have shown that the twisting moments, the bending moment and shearing force normal to the shell surface on a section perpendicular to the axis of the shell are small and can be neglected. In doing so the system of three simultaneous partial differential equations can be reduced to the following single

---

*The numbers refer to the bibliography.

partial differential equation of eighth order[39]

$$\frac{\partial^8 M_\phi}{\partial \phi^8} + (2+\nu)\, a^2 \frac{\partial^8 M_\phi}{\partial x^2 \partial \phi^6} + 2 \frac{\partial^6 M_\phi}{\partial \phi^6} + (1+2\nu)\, a^4 \frac{\partial^8 M_\phi}{\partial x^4 \partial \phi^4}$$

$$+2(2+\nu) a^2 \frac{\partial^6 M_\phi}{\partial x^2 \partial \phi^4} + \frac{\partial^4 M_\phi}{\partial \phi^4} + \nu a^6 \frac{\partial^8 M_\phi}{\partial x^6 \partial \phi^2} + (1+\nu)^2\, a^4 \frac{\partial^6 M_\phi}{\partial x^4 \partial \phi^2} \qquad (1)$$

$$+ (2+\nu)\, a^2 \frac{\partial^4 M_\phi}{\partial x^2 \partial \phi^2} + 12\,(1-\nu^2) \frac{a^6}{h^2} \frac{\partial^4 M_\phi}{\partial x^4} = 0$$

where,

M_ϕ = bending moment per unit length of an axial section (cross-bending)

h = thickness of shell

ν = Poisson's ratio

a, ϕ, x as shown in Figure 2.

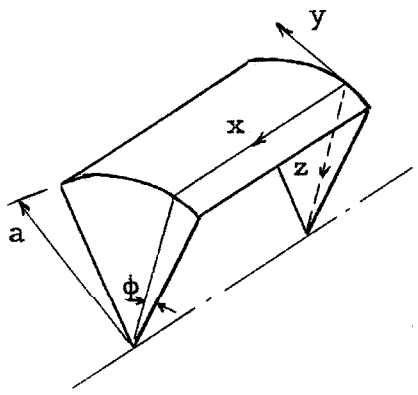

Figure 2

The solution of the eighth order differential equation is obtained by use of Fourier series and the results obtained by this method are quite satisfactory.

The first attempt to give a solution of the stress analysis of prismatic shells was by W. Ehlers[4]. He considered that each plate acts as a beam having large resistance to bending in its plane. Ehlers also assumed the plates were hinged along the common edges so that only shear could be transmitted from one plate to another. This corresponds to the membrane theory of the cylindrical shell.

Later E. Gruber[5][8] considered the effect of the cross-bending moment (the moment on an axial section) and found that the deflection of the hinged shell may be 3-4 times that of the rigidly connected shell and that the axial stresses on a cross-section differed as much as 100°/o. In developing the theory Gruber neglected the twisting moments, bending moment and shearing force normal to the shell surface on a section perpendicular to the axis of the shell, as was done in the case of the cylindrical shell. The membrane solution is taken as the basic solution; however, the cross-bending moments are accounted for by applying statically equivalent correction loads at the joints. Using this theory the problem reduces in each particular case to the solution of the following r simultaneous differential equations of the fourth order, where r is the number of sides of the shell[5].

$$S'_{n-1,n}\frac{d^4M_{n-1}}{dx^4} + 2(S'_{n-1,n} + S'_{n,n+1})\frac{d^4M_n}{dx^4} + S'_{n,n+1}\cdot\frac{d^4M_n}{dx^4} - 6E\left[\sum_{\nu=0}^{\nu=r-1}\delta_\nu \; p_{\nu,\nu+1} + \sum_{\nu=0}^{\nu=r} g_\nu \cdot M_\nu\right] = \frac{d^4N_{n,n-1}}{dx^4} + \frac{d^4N_{n,n+1}}{dx^4} \qquad (2)$$

where :

$p_{\nu,\nu+1}$ = load in direction of the plate

M_{n-1} = cross-bending moment (moment on an axial section) at joint n-1

N_{nn-1} = Normal force on section of plate n, n-1 perpendicular to axis of the shell

E, J, s = constants

By introducing Fourier series the above system of differential equations are reduced to the same number of simultaneous linear algebraic equations. By solving these equations the solution of the problem is obtained.

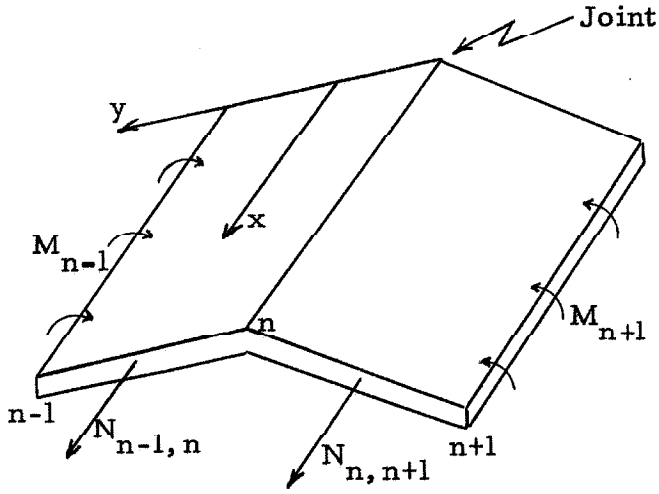

Section of Prismatic Shell

Figure 3

The development of the analytical methods of calculating stresses in cylindrical and prismatic shell has been outlined above. The results obtained by these methods are satisfactory for engineering purposes. The inherent drawback of these methods, aside from their being intricate and requiring very lengthy calculations, is that the mathematical processes they utilize are such that they do not

afford any insight into the physical processes involved. Also, even if the calculations are systematized and use is made of tables computed in advance, the designer must have more mathematical facility than is customarily possessed.

In developing the theory described in this paper the following restrictions are imposed on the problem:

1) The cross-section of the shell is constant along the axis.

2) The shell is restrained so that there is no tangential displacement in the cross-section of the shell at the ends.

3) Displacements of the shell are sufficiently small so that stresses produced by twisting can be neglected.

4) Displacements of the shell are sufficiently small so that stresses produced by axial plate-bending can be neglected.

5) Displacements due to shear are sufficiently small so that shear strain can be neglected.

The restrictions listed above are the same as those Finsterwalder and Gruber imposed in the development of their theories for cylindrical and prismatic shells. The purpose of this paper is, therefore, to present a new method of analysis, that an engineer can handle by making use only of the ordinary techniques employed in structural analysis. The procedure used in the following analysis will apply to such cases where the loading is of the form $f(x)h(y)$, where x is the axial coordinate and y is the transverse coordinate, and where the variation of loading along the span is continuous. It will be seen that if the loading is not continuous some small inaccuracies will be introduced.

In the case of prismatic shells the side plates are very flexible in bending perpendicular to their planes, but are extremely rigid and act as beams between the end diaphragms as regards deflection in their planes. An externally applied joint load P will therefore resolve itself into components parallel to the two adjoining plates. These load components will be defined as plate loads. In accordance with this all the external load will be reduced to plate loads.

If the stress distribution is independent of the distortion of the cross-section from its original form, the shell is said to be a membrane. The computation of the stresses is then a relatively simple matter. For the shell considered here the stress distribution is strongly dependent upon the distortion of the cross-section. First, the external load applied to the surface of the shell is distributed to the joints by bending in the shell. During distortion of the cross-section a cross-bending is developed that has the effect of redistributing the plate loads. From this point of view it is seen that the distribution of axial stresses is identical with that of a prismatic membrane with appropriately adjusted panel point or joint loads. The appropriate load at each joint is $(P_n + \Delta P_n' + \Delta P_n'')$, where P_n is the tributary joint load from externally applied forces, $\Delta P'$ is obtained by replacing the cross-bending moments due to the distribution of the load by statically equivalent joint loads, and $\Delta P_n''$ is obtained by replacing the cross-bending moments due to the relative displacement of the joints by statically equivalent joint loads. P_n and $\Delta P_n'$ can be computed from the external loads. The $\Delta P_n''$

must be computed from the deflections of the plates. When $\Delta P_n''$ is known for each joint the axial stresses and the cross-bending moments can be computed easily. The $\Delta P_n''$ will be called the correction loads and it is their determination that is essential to the solution of the problem.

Consider now a cylindrical shell. The curved cross-section is the limiting case of an inscribed polygon as the number of sides increases. In principle the same method of analysis can be used for the cylindrical shell as for the polygonal shell. In fact, as the length of sides approaches zero the mathematical formulation of the prismatic shell goes into the partial differential equations of the cylindrical shell. If this convergence is rapid, the stresses in a polygonal shell with a relatively small number of sides will give an adequate representation of the stresses in the cylindrical shell. It will be shown that this is the case and that a cylindrical shell can be approximated adequately by a prismatic shell with a small number of sides. However, in obtaining the cross-bending moments a somewhat different train of thought has to be followed. Since the characteristic feature of a cylindrical shell is that it transmits the loads primarily by direct stresses, no cross-bending moments are produced due to the distribution of the load, as was the case for the prismatic shell, but there are cross-bending moments induced by the distortion of the cross-section. Consequently, the resultant cross-bending moment can be calculated from $\Delta P_n''$.

II. METHOD OF ANALYSIS

The nomenclature used in the analysis is shown in Figure 4 where each joint and plate is given a number. The direction of the plates is given by the angle α_n with the following sign convention: Draw a horizontal line through the joint n extending to the right. Angle α_n is then measured from this line to the plate n + 1, counter-clockwise being considered positive and clockwise negative. The following terminology is used:

h_n = width of plate n

t_n = thickness of plate n

L = span of shell

N = total number of side plates

2:1 External loading

Given a shell and loading, the first step is to resolve all external loads into their components perpendicular (q_n) and parallel ($p'_{n,n-1}$) to the respective surfaces on which they act. The shell is then loaded with perpendicular load components q_n as shown in Figure 5 (the tangential load components not being shown). Considering, then, a transverse slice of unit width as a continuous framework with pin supported joints, the end moments at each joint are computed by the method of moment distribution. The number of slices for which this must be done depends upon how rapidly the loading varies along the span of the shell. The following exposition is for a loading uniform along the span in which case the analysis of a single slice is sufficient. The actual moment distribution is the same as for the continuous beam shown in Figure 6 and from the computed bending

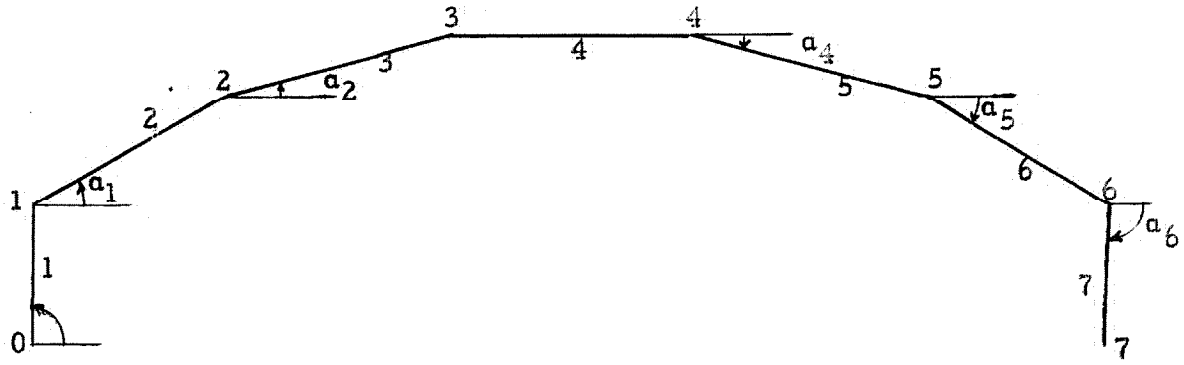

Figure 4

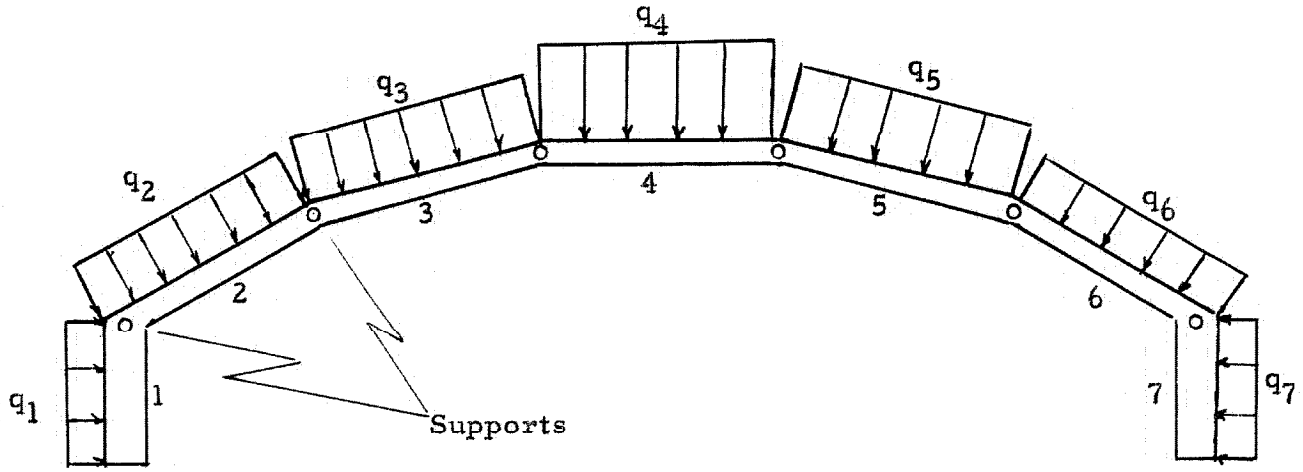

Figure 5

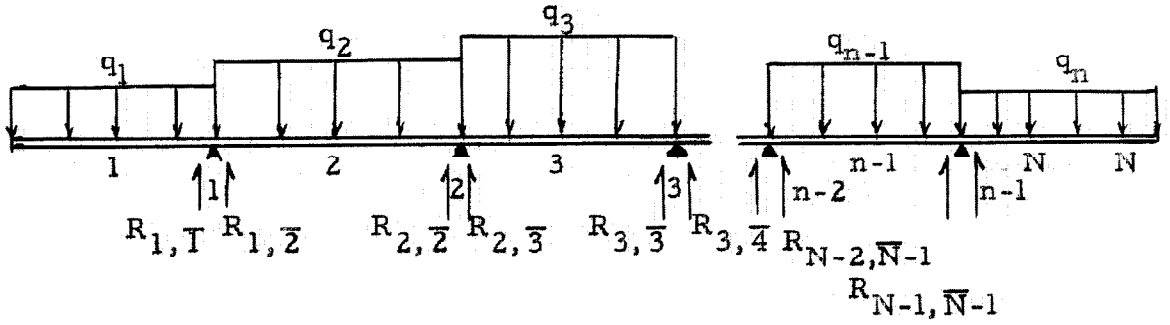

Figure 6

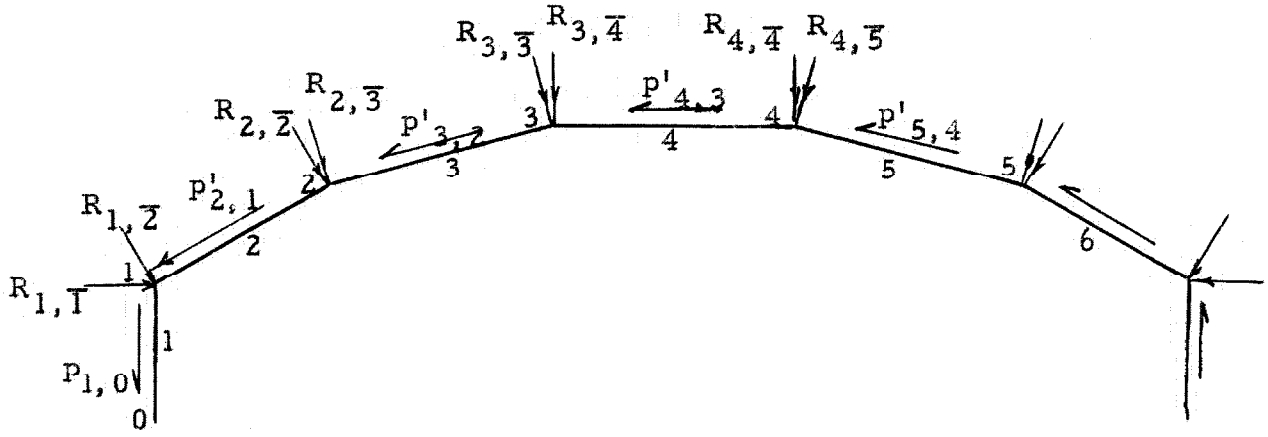

Figure 7

moments at the supports and the loads q_n the end reactions $R_{1,\overline{2}}$ etc., are computed. The following sign convention is adopted for the bending moments at the supports. A clockwise moment acting on the end of a member is considered to be negative and a counterclockwise moment is considered to be positive. With this convention the fixed-end moment $\overline{Y}'_{n-1,n}$ at the (n-1) end of member (n-1,n) is positive for a positive load q_n, and the fixed-end moment $\overline{Y}'_{n,n-1}$ is negative. The bar over the letter indicates a fixed-end moment and the prime indicates that the moment is associated with the distribution of the q_n to the joints. The distributed end moments are designated by the same letter but with the bar omitted.

The reactions $R_{1,\overline{2}}$ etc., are carried by the pin supports at the joints. If the pin supports are removed, the forces $R_{1,\overline{2}}$ etc., with directions reversed must be considered to be acting on the joints of the shell. These loads act on the shell as shown in Figure 7. Denote the plate loads due to the reactions $R_{n-1,\overline{n}}$ etc. by $p''_{n,n-1}$. The tangential forces $p_{3,2}$, $p_{n,n-1}$ are considered positive when directed from joint n to n-1, hence $p_{n-1,n} = -p_{n,n-1}$. The forces $p'_{n-1,n}+p''_{n,n-1}$ are then the plate loads corresponding to the $P_n + \Delta P'_n$.

2:2 Plate loads due to forces at the joints.

a) Joint loads perpendicular to plates

A portion of the shell to be considered is shown in Figure 8 with the joint loads acting. From Figure 8 it is seen that the plate loads $p''_{n+1,n}$ due to the R loads are:

$$p''_{n+1,n} = -\frac{R_{n,\overline{n}}}{\sin(a_{n-1}-a_n)} - \frac{R_{n,\overline{n+1}}}{\tan(a_{n-1}-a_n)} + \frac{R_{n+1,\overline{n+1}}}{\tan(a_n-a_{n+1})} + \frac{R_{n+1,\overline{n+2}}}{\sin(a_n-a_{n+1})} \quad (3)$$

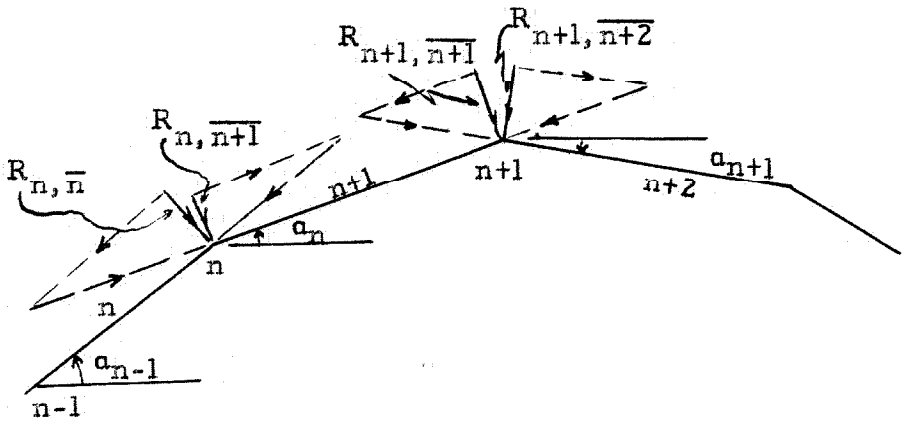

Figure 8

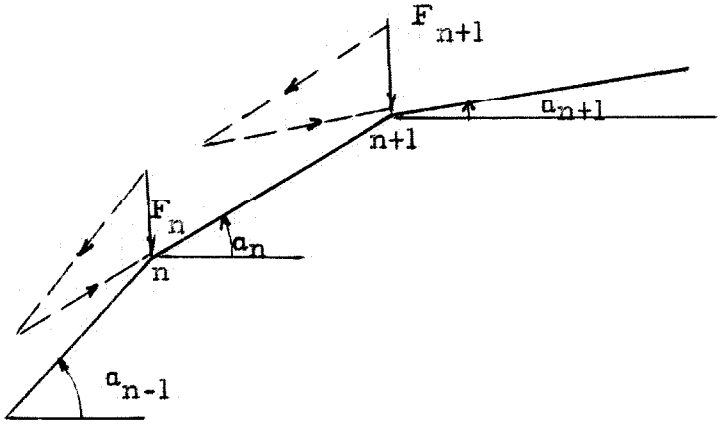

Figure 9

b) Vertical joint loads

If concentrated vertical loads act at the joints, the plate loads can be found from Figure 9. The plate loads in terms of the vertical loads are:

$$p'''_{n+1,n} = \frac{\cos \alpha_{n+1}}{\sin(\alpha_{n+1}-\alpha_n)} F_{n+1} - \frac{\cos \alpha_{n-1}}{\sin(\alpha_n-\alpha_{n-1})} F_n \qquad (4)$$

where F_n = vertical joint load, considered positive when directed inward, as shown, and $p'''_{n+1,n}$ are plate loads due to the F-loads considered positive when directed from joint n+1 to n.

2:3 Correction loads

Each plate in the shell is now loaded with a uniform plate load along the span. Because of these plate loads the shell will deflect approximately as shown in Figure 10. Since the joints at a particular cross-section do not deflect the same amounts the side plates will rotate and induce cross-bending moments. These have a variation along the span proportional to the deflections of the side plates. The reversed end reactions corresponding to these moments are the joint loads $Q_{n-1,\bar{n}}$ shown in Figure 10 c.

The Q-loads in terms of the cross-bending moments are:

$$Q_{n-1,\bar{n}} = \frac{Y''_n - Y''_{n-1}}{h_n} = - Q_{n,\bar{n}} \qquad (5)$$

$Q_{n-1,\bar{n}}$, $Q_{n,\bar{n}}$ etc. are considered positive when directed inward. Y''_n is the moment at joint n at the center of the span due to deflection of the shell, positive when producing compression on the outside surface.

The plate loads, $w_{n,n-1}$, at the center of the span, due to the

(a)

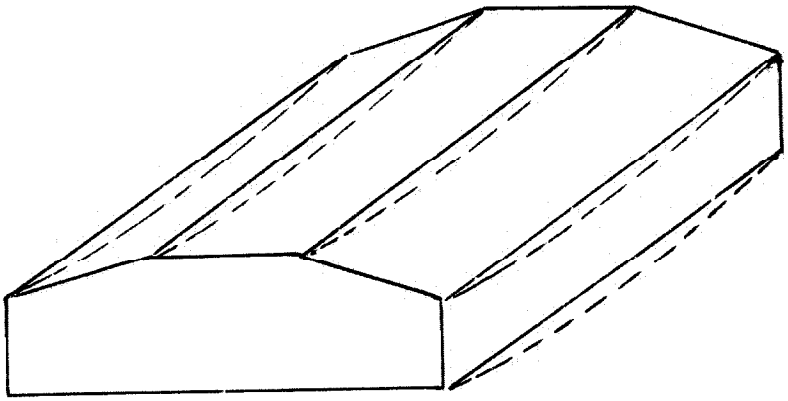

(b)

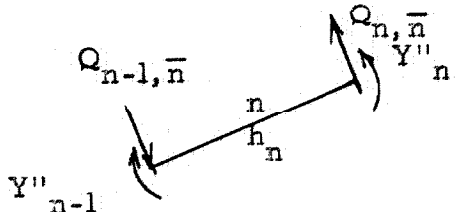

(c)

Figure 10

correction loads are given by Equation (3).

The problem now is to analyse a shell, hinged at the joints but capable of resisting shear and loaded with the following plate loads:

$$t_{n,n-1}(x) = p_{n,n-1} + w_{n,n-1} F(x) \tag{6}$$

where $p_{n,n-1}$ is the total uniformly distributed plate load:

$$p_{n,n-1} = p'_{n,n-1} + p''_{n,n-1} + p'''_{n,n-1} + \text{----} \tag{7}$$

The axial stresses computed thus will be those of the continuous shell under the externally applied loads.

2:4 Shear Equations (Membrane solution)

If the plates of the prismatic shell were not joined along their common edges they would deflect as ordinary beams under their respective plate loads, and sliding would occur along the joints. However the continuity at the joint prevents relative shift along the edges, and consequently shear forces will be induced along the common edges.

Consider a portion of the shell, Figure 11a, where internal forces and moments produced by the arbitrary plate loads are indicated. Figure 11c shows positive shear and normal forces. Figure 11b shows the free body diagram of two adjoining plates.

The stress distribution over the cross-section of the plate can be written,

$$\sigma_n(x) = \frac{N_{n(x)}}{a_n} \pm \frac{M_n(x) y_n}{I_n} \tag{8}$$

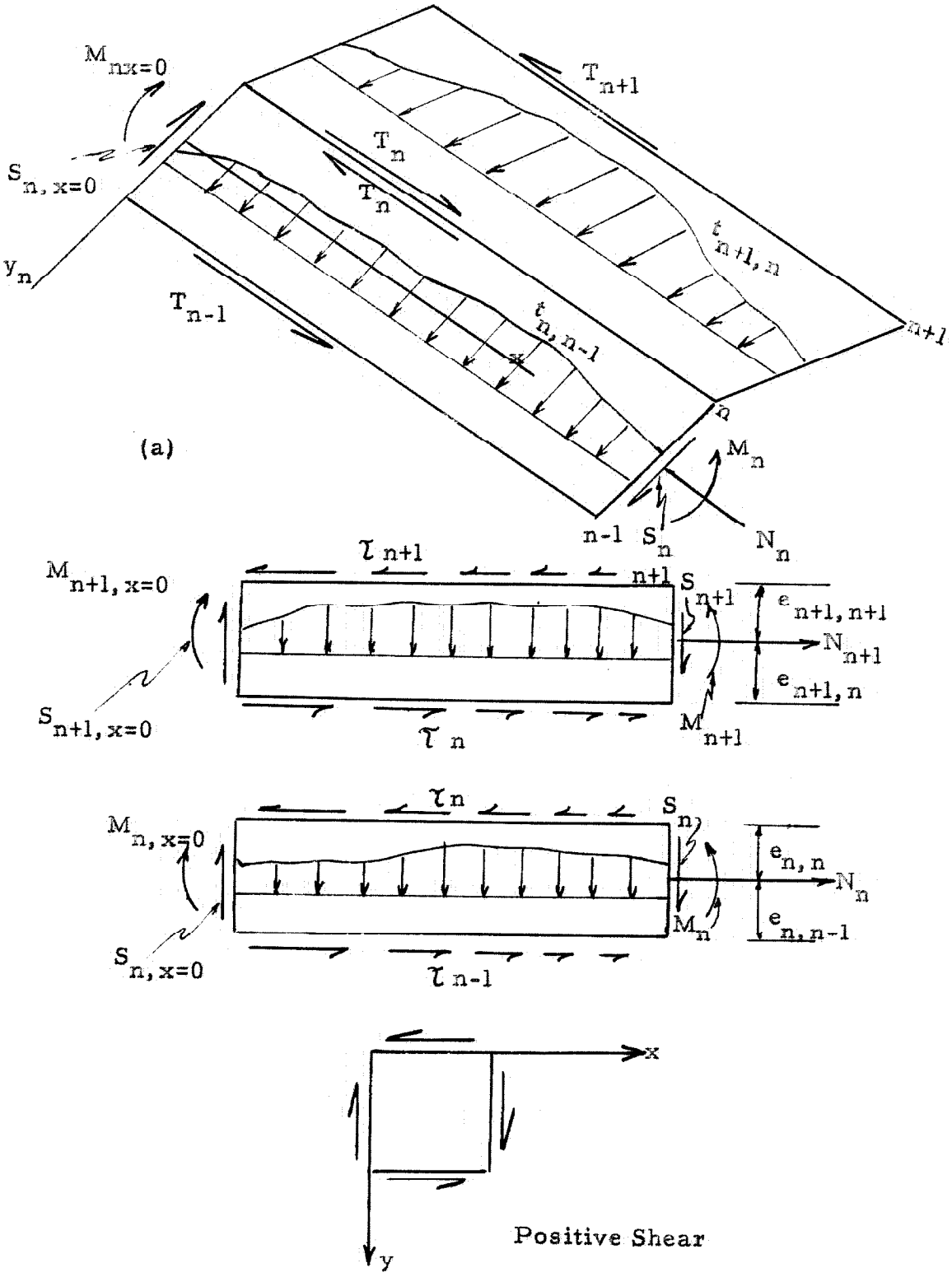
$M_{nx=0}$
$S_{n,x=0}$
y_n
T_{n+1}
T_n
T_n
T_{n-1}
$t_{n+1,n}$
$t_{n,n-1}$
x
n+1
n
n-1
S_n
M_n
N_n
(a)
τ_{n+1}
n+1
$M_{n+1,x=0}$
$S_{n+1,x=0}$
S_{n+1}
$e_{n+1,n+1}$
N_{n+1}
$e_{n+1,n}$
M_{n+1}
τ_n
(b)
τ_n
$M_{n,x=0}$
$S_{n,x=0}$
S_n
$e_{n,n}$
N_n
$e_{n,n-1}$
M_n
τ_{n-1}
x
y
Positive Shear
(c)

Figure 11

where a_n, I_n and y_n are, respectively, the area, moment of inertia, and distance to the fiber where stress is desired, of the cross-section of the n th plate.

From Figure 11c,

$$M_n(x) = \int_0^x \tau_n dx - \int_0^x \tau_{n-1}\, dx$$

Set $$T_n(x) = \int_0^x \tau_n dx \quad , \qquad T_{n-1}(x) = \int_0^x \tau_{n-1}\, dx$$

Then $$N_n(x) = T_n(x) - T_{n-1,}(x) \quad . \tag{9}$$

$$M_n(x) = M_n^0(x) - T_n(x)\, e_{n,n} - T_{n-1}(x)\, e_{n,n-1} \tag{10}$$

$M_n^0(x)$ is the moment that would exist at the section x of the n th plate if the plate were to act as a beam under the plate loads only. Depending on the end conditions (simply supported, fixed at the ends, continuous etc.) this moment would of course vary for the same load.

Along the common edge the stresses in two adjoining plates must be equal for reasons of continuity, therefore,

$$(\sigma_{n,x})_{y_n = -\, e_{n,n}} = (\sigma_{n+1,x})_{y_{n+1} = e_{n+1,n}} \tag{11}$$

In the case of a rectangular cross-section of the plates,

$$e_{n,n} = e_{n,n-1} = \frac{h_n}{2} \; , \; I_n = 1/12\; t_n h_n^3 = 1/12\; a_n h_n^2 = Z_n \frac{h_n}{2} \tag{12}$$

or $a_n = \dfrac{6Z_n}{h_n}$ $\qquad Z_n$ = section modulus

Substituting Equations (9) and (10) into Equation (8) and making use of condition equation (11) one obtains

$$\frac{T_n(x)-T_{n-1}(x)}{a_n} - \frac{M_n^0(x)-T_n(x)\frac{h_n}{2}-T_{n-1}(x)\frac{h_n}{2}}{Z_n\frac{h_n}{2}}\frac{h_n}{2} =$$

$$\frac{T_{n+1}(x)-T_n(x)}{a_{n+1}} + \frac{M_{n+1}^0(x)-T_{n+1}(x)\frac{h_n}{2}-T_{n-1}(x)\frac{h_n}{2}}{Z_n\frac{h_n}{2}}\frac{h_n}{2}$$

Rearranging the terms the equation becomes

$$T_{n-1}(x)\frac{h_n}{Z_n} + 2T_n(x)\left(\frac{h_n}{Z_n}+\frac{h_{n+1}}{Z_{n+1}}\right)+T_{n+1}(x)\frac{h_{n+1}}{Z_{n+1}}=3\left(\frac{M_n^0(x)}{Z_n}+\frac{M_{n+1}^0(x)}{Z_{n+1}}\right) \qquad (13)$$

It is seen that as many equations of this type can be written as there are common joints in the structure or unknown shear forces. The numerical solutions of these equations can be obtained by a distribution method as pointed out by Winter and Pei[16].

For a continuous beam with uniform loads of various magnitude on the spans the Three Moment Equation is

$$M_{n-1}\frac{L_n}{I_n} + 2M_n\left(\frac{L_n}{I_n}+\frac{L_{n+1}}{I_{n+1}}\right) + M_{n+1}\frac{L_{n+1}}{I_n} = -\frac{w_nL_n^3}{4I_n} - \frac{w_{n+1}L_{n+1}^3}{4I_{n+1}} \qquad (14)$$

It is seen that the form of Equation (14) is identical with that of Equation (13) and that the following correspondence of terms can be established:

$$T_n \sim M_n$$

$$h_n \sim L_n$$

$$Z_n \sim I_n$$

$$3M_n^0 \sim -\frac{w_nL^3}{4}$$

The value of the shear forces at any section x can be obtained readily by loading a conjugate continuous beam of spans h_n and moment of inertia equal to $1/6\ t_n \cdot h^2_n$ with the uniform loads

$$w_n = -\frac{12M^0_{n,x}}{h_n^3} \quad .$$

By performing a moment distribution the end moments obtained will be equal in magnitude and sign to the shear forces at the respective joints at section x.

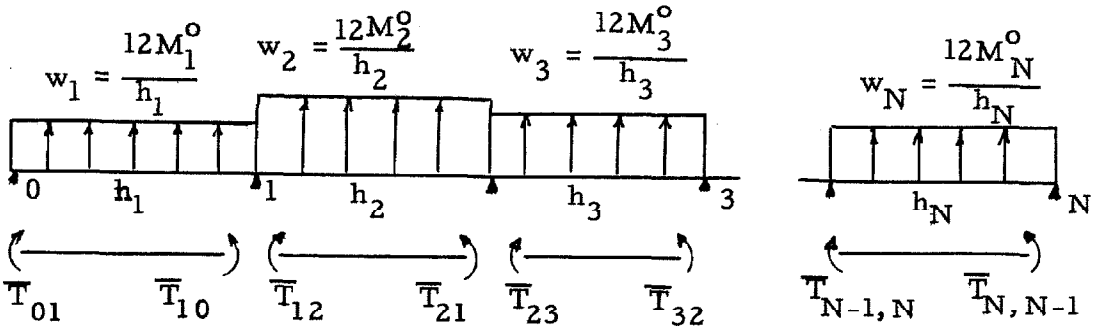

Figure 12

Figure 12 shows the conjugate continuous beam with the uniform load (M^0_n assumed positive) and the fixed end conjugate moments $\overline{T}_{n-1,n}$, $\overline{T}_{n,n-1}$ (i.e. $\overline{T}_{n,n-1}$ the fixed end moments at the end n of member n-1, n) due to these loads.

With the sign convention adopted for moment distribution, counterclockwise positive, the fixed end moments will be (the bar over $\overline{T}_{n,n-1}$ indicates fixed end moment):

$$-\overline{T}_{n-1,n} = \overline{T}_{n,n-1} = \frac{1}{12} h_n^2 \frac{12 M^0_n}{h_n} = \frac{M^0_n}{h_n} \tag{15}$$

The stiffness factor for the n th span is

$$K_n = \frac{t_n h_n}{6} \tag{16}$$

When the load is of the form f(x) h(y) only one distribution process need be carried out in order to determine the variation of the joint shear force along the span. This is easily seen since for each plate the moment $M^0_n(x) = C_n g(x)$ where g(x) is the same function of x for each plate depending on the magnitudes of the plate loads. For instance, for uniform plate loads $g(x) = \frac{4x}{L} - \frac{4x^2}{L^2}$ and $C_n = p_{n,n-1} \frac{L^2}{8}$. The fixed end moments will be:

$$-\overline{T}_{n-1,n}(x) = \overline{T}_{n,n-1}(x) = \frac{C_n}{h_n} g(x) \tag{17}$$

Since g(x) is a common factor for the fixed end moments for each span of the conjugate beam, all that is necessary is to distribute $\frac{C_n}{h_n}$ and multiply the result with g(x) and the variation of the shear is known. The shear forces are then maximum at the same place $M^0_n(x)$ is maximum.

2:5 Deformation of the shell

Consider now the deformation of the shell and assume that the hinged shell is cut along the joint so that each plate n can deflect in its plane. Let the deflection of the n th plate at the center be y_n. As shown in Figure 13 the joint n will move to n' as a point on the plate n, and to n'' as a point on plate n+1. The plates n and n+1

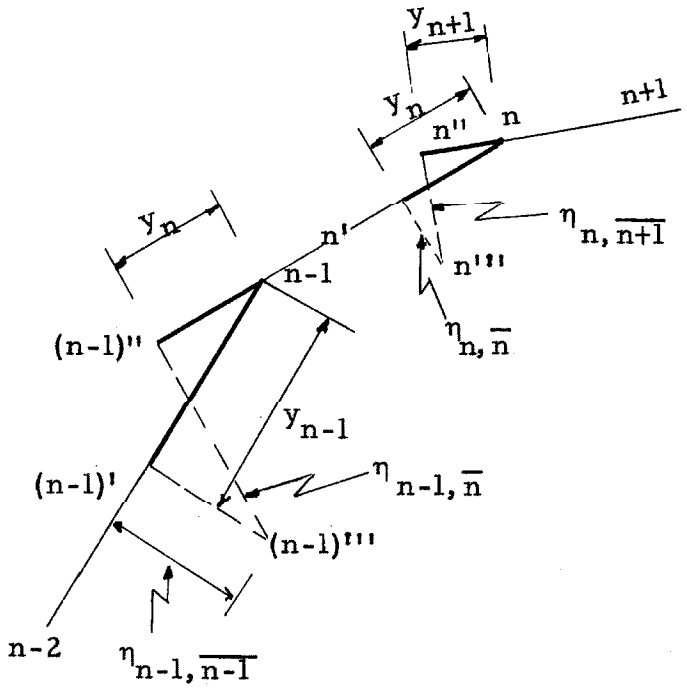

Figure 13

can be rotated and translated until n' and n'' coincide at n'''. From Figure 13 the deflections perpendicular to the plates are:

$$\eta_{n,\overline{n+1}} = \left(\frac{y_n}{\cos(\alpha_{n-1}-\alpha_n)} - y_{n+1}\right)\cot g\,(\alpha_{n-1}-\alpha_n) \tag{18}$$

$$\eta_{n,\overline{n}} = \left(y_n - \frac{y_{n+1}}{\cos(\alpha_{n-1}-\alpha_n)}\right)\cot g\,(\alpha_{n-1}-\alpha_n) \tag{19}$$

$\eta_{n,\overline{n+1}}$ and $\eta_{n,\overline{n}}$ are considered positive when joint n moves inward. The total relative deflection perpendicular to plate n is then:

$$d_n = \eta_{n,\overline{n}} - \eta_{n-1,\overline{n}} \tag{20}$$

Substituting Equations (18) and (19) into Equation (20)

$$d_n = -y_{n-1}\,\mathrm{cosec}(a_{n-2}-a_{n-1}) + y_n\left\{\cot(a_{n-1}-a_n) + \cot(a_{n-2}-a_{n-1})\right\}$$

$$-y_{n+1}\,\mathrm{cosec}(a_{n-1}-a_n) \qquad (21)$$

As was shown in Section 2:3 the fixed end moments due to relative displacement of the joints are:

$$\overline{Y}''_{n-1,n} = \overline{Y}''_{n,n-1} = \frac{6EJ_n}{h_n^2(1-\nu^2)}\,d_n = \frac{E\,t_n^3}{2\,h_n^2(1-\nu^2)}\,d_n\;; \qquad (22)$$

where $J_n = 1/12\ t_n^3$ and $\overline{Y}''_{n-1,n}$ and $\overline{Y}'_{n,n-1}$ are positive counterclockwise when d_n is positive.

Substituting Equation (21) into (22) the fixed end moment at the center of the span is obtained

$$\overline{Y}''_{n-1,n} = \overline{Y}''_{n,n-1} = \frac{1}{\Delta}\left[-y_{n-1}\,\mathrm{cosec}\,(a_{n-2}-a_{n-1})\right.$$

$$\left. + y_n\left\{\cot(a_{n-1}-a_n) + \cot(a_{n-2}-a_{n-1})\right\} - y_{n+1}\mathrm{cosec}\,(a_{n-1}-a_n)\right] \qquad (23)$$

$$\frac{1}{\Delta} = \left[\frac{Et_n^3}{2h_n^2(1-\nu^2)}\right] \qquad (24)$$

Equation (23) shows that the fixed end moments at the joints due to relative displacement of the joints can be expressed as a function of y_n, the beam deflection of the side plates. The beam deflections are produced by the uniform plate load $p_{n,n-1}$ plus the correction load $w_{n,n-1}$. The variation of $w_{n,n-1}$ along the span is proportional to the deflections of the side plates; however, it will be assumed that the correction loads ($w_{n,n-1}$) have the same variation along the span as the beam deflection of the side plates due to a uniform load. For

finding the deflection this amounts to replacing the actual correction load with an equivalent uniformly distributed load that will give the same deflection at the center of the span. It is therefore necessary to know the deflection at the center of the span due to the actual correction load. Let F(x) be the variation of the deflection of the side plate due to uniform load; then the correction load will be:

$$w_{n,n-1}(x) = w_{n,n-1}F(x) \tag{25}$$

Since the true correction loads are to be replaced by $w_{n,n-1}F(x)$, the deflection at the center of the span can be obtained by using this load. For uniform load F(x) is a polynomial of fourth order and the deflection from this load is an eighth order polynomial. However, since the deflection of a beam is relatively insensitive to small variations of the load distribution, in what follows F(x) is taken to be a sine curve for convenience. This simplification introduces negligible errors.

Thus, two approximations have been made. The first, which takes

$$w_{n,n-1}(x) = w_{n,n-1}F(x)$$

is essential in this method of analysis. The second, that F(x) can be approximated by a sine curve, is not a necessity, but it simplifies the algebra considerably. Hereafter M, Y, T, N, y or σ with single prime (') refer to external loads and with a double prime (") refer to correction loads. Without any prime they refer to the total effect of external and correction loads. (Note: p without a prime is the total plate load due to the external loads, whereas w is the plate correction load at the center).

III. ANALYSIS OF PRISMATIC SHELLS WITH DIFFERENT END CONDITIONS

To demonstrate how this analysis is applied, three particular cases with different end conditions will be considered. A numerical example is given at the end of the chapter for the case of simply supported ends.

As shown in the preceding discussion, only one conjugate moment distribution is necessary for calculating the shear forces. These forces will be determined at the center of the span and the following notation will be used for convenience:

$$M_n^{0,\prime} = \frac{p_{n,n-1}L^2}{8}$$
$$M_n^{0,\prime\prime} = \frac{w_{n,n-1}L^2}{\pi^2} \qquad (26)$$

The shear forces corresponding to $M_n^{0,\prime}$ and $M_n^{0,\prime\prime}$ will be denoted by T_n' and T_n'' respectively. The value of any quantity such as $M_n^{0,\prime}$ at a point x will be denoted by $M_n^{0,\prime}(x)$.

3:1 Simply supported

a) Uniform plate load

Figure 14a shows the n th plate loaded with uniform plate load $p_{n,n-1}$ and Figure 14b the corresponding moment curve $M_n^{0,\prime}(x)$. Figure 14c and 14d show the shear force and shear intensity distribution.

First the bending moments at the center of each plate produced by $p_{n,n-1}$ must be found. For simply supported ends, these are

$$M^{0,\prime}_{n,x=\frac{L}{2}} = \frac{p_{n,n-1}L^2}{8} \quad \left[g_1(x)\right]_{x=\frac{L}{2}} \qquad (27)$$
$$= M_n^{0,\prime}$$

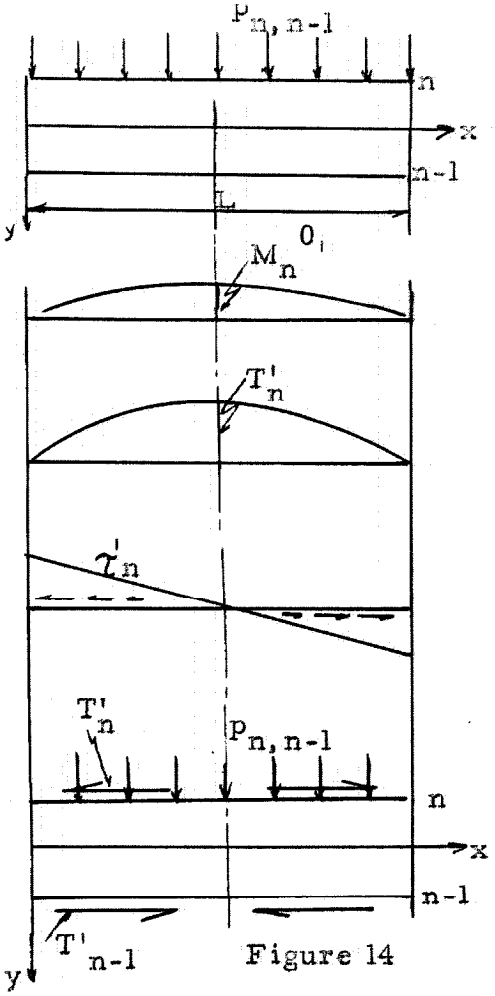

Figure 14

(a) $p_{n,n-1}$ (constant)

(b) $M_n^{0'}(x) = \frac{p_{n,n-1} L^2}{8} g_1(x)$

(c) $T'_n(x) = T'_n \, g_1(x)$

(d) $\tau'_n(x) = \frac{T'_n}{L}\left(4 - \frac{8x}{L}\right)$,

where

$$g_1(x) = \frac{4x}{L^2} - \frac{4x^2}{L^2}$$

(e)

$$w_{n,n-1}(x) = w_{n,n-1} \sin\frac{\pi x}{L}$$ (a)

$$M_n^{0''}(x) = \frac{w_{n,n-1} L^2}{\pi^2} g_1(x)$$ (b)

$$T''_n(x) = T''_n \, g_1(x)$$ (c)

$$\tau''_n(x) = \frac{\pi T''_n}{L} \cos\frac{\pi x}{L}$$ (d)

where

$$g_1(x) = \sin\frac{\pi x}{L}$$

(e)

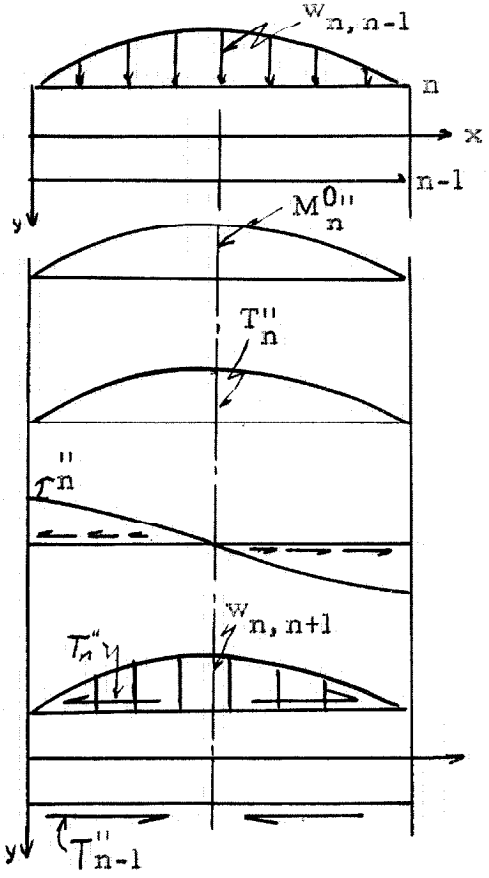

Figure 15

where

$$g_1(x) = \frac{4x}{L} - \frac{4x^2}{L^2} \tag{28}$$

Hence, the corresponding fixed end conjugate moments for determining the shears at the center of the span are:

$$-\overline{T}'_{n-1,n} = \overline{T}'_{n,n-1} = \frac{M^{0}_{n}}{h_n} = \frac{p_{n,n-1}L^2}{8h_n} \tag{29}$$

From the results of the conjugate moment distribution, the shear force at the n th joint can then be written:

$$T'_n(x) = T'_n\, g_1(x) \tag{30}$$

where $g_1(x)$ is defined by Equation (28).

The moment $M'_n(x)$ due to the uniform load $p_{n,n-1}$ and the shear forces $T'_n(x)$ and $T'_{n-1}(x)$ is from Figure 15e:

$$M'_n(x) = \frac{L^2}{8}\left[p_{n,n-1} - \frac{4T'_n h_n}{L^2} - \frac{4T'_{n-1}h_n}{L^2}\right] \quad g_1(x)$$

or

$$M'_n(x) = \frac{A_{n,n-1}L^2}{8} \quad g_1(x) \tag{31}$$

where

$$A_{n,n-1} = p_{n,n-1} - \frac{4T'_n h_n}{L^2} - \frac{4T'_{n-1}h_n}{L^2} \tag{32}$$

The deflection of the n th plate is:

$$y'_n(x) = \frac{5A_{n,n-1}L^4}{384\, EI_n}\, F_1(x) \tag{33}$$

where

$$F_1(x) = \left(\frac{16x}{5L}\right)\left(1 - \frac{2x^2}{L^2} + \frac{x^3}{L^3}\right), \tag{34}$$

and $\quad I_n = 1/12\; t_n h_n^3$

The moment and deflection at any section x due to the uniform plate load $p_{n,n-1}$ plus the shear forces at the edges are thus equal to the moment and deflection in the same beam loaded with an equivalent uniform load $A_{n,n-1}$ only.

b) Correction loads

Figures 15a and b show the sine distributed plate load and the corresponding moment curve $M_n^{0''}(x)$ respectively. Figure 15c and Figure 15d show the shear force and shear intensity respectively.

For the purpose of finding the bending moment and the deflection of the plates approximate $F_1(x)$ (Equation 34)) with a sine curve. The correction load may then be written as:

$$w_{n,n-1}(x) = w_{n,n-1} F_1(x) \doteq w_{n,n-1} \sin \frac{\pi x}{L}$$

The bending moments at the center of the span produced by the $w_{n,n-1} \sin \frac{\pi x}{L}$ are:

$$M^{0''}_{n,x=\frac{L}{2}} = \frac{w_{n,n-1} L^2}{\pi^2} \left[g_2(x)\right]_{x=\frac{L}{2}} \tag{35}$$

where $$g_2(x) = \sin \frac{\pi x}{L} \tag{36}$$

Hence, the fixed end conjugate moments at the center of the span corresponding to $M_n^{0''}$ are

$$-\overline{T}''_{n-1,n} = \overline{T}''_{n,n-1} = \frac{M^{0''}}{h_n} = \frac{w_{n,n-1} L^2}{\pi^2 h_n} \tag{37}$$

The shear force at the nth plate will be:

$$T_n''(x) = T''_n g_2(x) \tag{38}$$

The moment $M''_n(x)$ due to the sine distributed $w_{n,n-1}(x)$ load and the shear forces $T''_{n-1}(x)$ and $T''_n(x)$ is then from Figure 15e

$$M''_n(x) = \frac{L^2}{\pi^2}\left(w_{n,n-1} - \frac{T''_{n-1}\,\pi^2 h_n}{2L^2} - \frac{T''_n\,\pi^2 h_n}{2L^2}\right) g_2(x)$$

or

$$M''_n(x) = \frac{L^2}{\pi^2}\, B_{n,n-1} \cdot g_2(x) \tag{39}$$

where

$$B_{n,n-1} = \left(w_{n,n-1} - \frac{T''_{n-1}\,\pi^2 h_n}{2L^2} - \frac{T''_n\,\pi^2 h_n}{2L^2}\right) \tag{40}$$

The moment and deflection at any section x produced by a sine distributed plate correction load and the corresponding joint shears are then equal to the moment and deflection in the same beam loaded with an equivalent sine distributed plate load $B_{n,n-1}$ only. The deflection of the nth plate is:

$$y''_n(x) = \frac{B_{n,n-1} L^4}{\pi^4 E I_n} F_2(x) \tag{41}$$

where

$$F_2(x) = \sin\frac{\pi x}{L}$$

$$I_n = \frac{1}{12}\, t_n h_n^3 \tag{42}$$

The total deflection due to both the uniform plate load and the correction load will then be:

$$y = \frac{5 A_{n,n-1} L^4}{384\, E I_n} F_1(x) + \frac{B_{n,n-1} L^4}{\pi^4 E I_n} F_2(x) \tag{43}$$

It is now necessary to approximate $F_2(x)$ by $F_1(x)$. This amounts to replacing the correction load with an equivalent uniform load, as discussed in the previous chapter.

Then

$$y_n = \frac{5}{384}\frac{L^4}{EI_n}\left(A_{n,n-1} + 0.7885\, B_{n,n-1}\right) F_1(x) \tag{44}$$

$$= \frac{5}{384}\frac{L^4}{EI_n} E_{n,n-1} F_1(x) = \frac{5}{32}\frac{L^4 E_{n,n-1}}{E t_n h_n^3} F_1(x) \tag{45}$$

where $$E_{n,n-1} = A_{n,n-1} + 0.7885\, B_{n,n-1} \tag{46}$$

Substituting Equation (45) into Equation (23) the general expression for the fixed end cross-bending moments is

$$\overline{Y}''_{n-1,n}(x) = \overline{Y}''_{n,n-1}(x) = \frac{1}{\beta} H_{n,n-1} F_1(x) \tag{47}$$

where

$$H_{n,n-1} = \frac{E_{n-1,n-2}}{t_{n-1} h_{n-1}^3} \operatorname{cosec}(a_{n-2} - a_{n-1}) + \frac{E_{n,n-1}}{t_n h_n^3}\left\{\cot(a_{n-1} - a_n) + \cot(a_{n-2} - a_{n-1})\right\} - \frac{E_{n+1,n}}{t_{n+1} h_{n+1}^3} \operatorname{cosec}(a_{n-1} - a_n) \tag{48}$$

and

$$\frac{1}{\beta} = \frac{5 L^4 t_n^3}{64\, h_n^2 (1-\nu^2)} \tag{49}$$

$F_1(x)$ is defined by Equation (34).

3:2 <u>One end fixed, the other simply supported</u>

The method of solving this problem is the same as for the case of simply supported ends. As before the shear forces and the deflection of the plates at the center of the span will be found.

a) Uniform plate load (See Figure 16)

Moments at the center of the span are:

$$M^{0'}_{n,\,x=\frac{L}{2}} = \frac{p_{n,n-1}L^2}{8} \left[g_1(x)\right]_{x=\frac{L}{2}} \tag{50}$$

where

$$g_1(x) = \frac{3x}{L} - \frac{4x^2}{L^2} \tag{51}$$

Hence, the fixed end conjugate moments at the center of the span corresponding to $M^{0'}_n$ are given by Equation (29). The shear force at the n th joint will be:

$$T'_n(x) = T'_n\, g_1(x) \tag{52}$$

where $g_1(x)$ is defined by Equation (51).

The moment $M'_n(x)$ due to the uniform load $p_{n,n-1}$ and the shear forces $T'_n(x)$ and $T'_{n-1}(x)$ are then

$$M'_n(x) = \frac{L^2}{8}\left(p_{n,n-1} - \frac{4\,T'_{n-1}h_n}{L^2} - \frac{4\,T_n\,h_n}{L^2}\right) g_1(x) \tag{53}$$

or

$$M'_n(x) = A_{n,n-1}\frac{L^2}{8}\, g_1(x) \tag{54}$$

where

$$A_{n,n-1} = p_{n,n-1} - \frac{4\,T'_{n-1}\,h_n}{L^2} - \frac{4\,T'_n\,h_n}{L^2} \tag{55}$$

The deflection of the n th plate will then be:

$$y'_n(x) = \frac{A_{n,n-1}L^4}{192\,EI_n}\, F_1(x) \tag{56}$$

where

$$F_1(x) = \left(\frac{4x}{L}\right)\left(1 - \frac{3x^2}{L^2} + \frac{2x^3}{L^3}\right)$$

$$I_n = \frac{1}{12}\, t_n h_n^3 \tag{57}$$

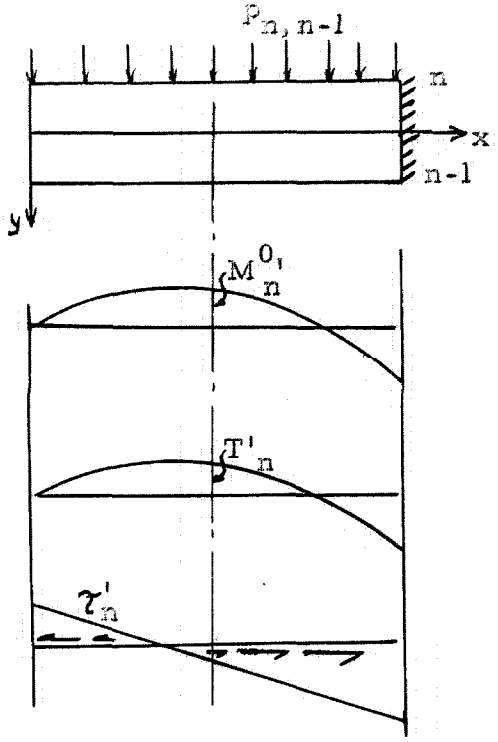

Figure 16

$p_{n,n-1}$ (constant

$$M^{0}_{n}(x) = \frac{p_{n,n-1} L^2}{8} g_1(x)$$

$$T'_n(x) = T'_n g_1(x)$$

$$\tau'_n(x) = \frac{T'_n}{L} (3 - \frac{8x}{L}),$$

where

$$g_1(x) = (\frac{3x}{L} - \frac{4x^2}{L^2})$$

$$w_{n,n-1}(x) = w_{n,n-1} \sin \frac{\pi x}{L}$$

$$M^{0}_{n}''(x) = \frac{w_{n,n-1} L^2}{\pi^2} g_2(x)$$

$$T''_n(x) = T''_n g_2(x)$$

$$\tau''_n(x) = \frac{T''_n}{L} (\pi \cos \frac{\pi x}{L} - \frac{3}{\pi}),$$

where

$$g_2(x) = \sin \frac{\pi x}{L} - \frac{3\pi}{xL}$$

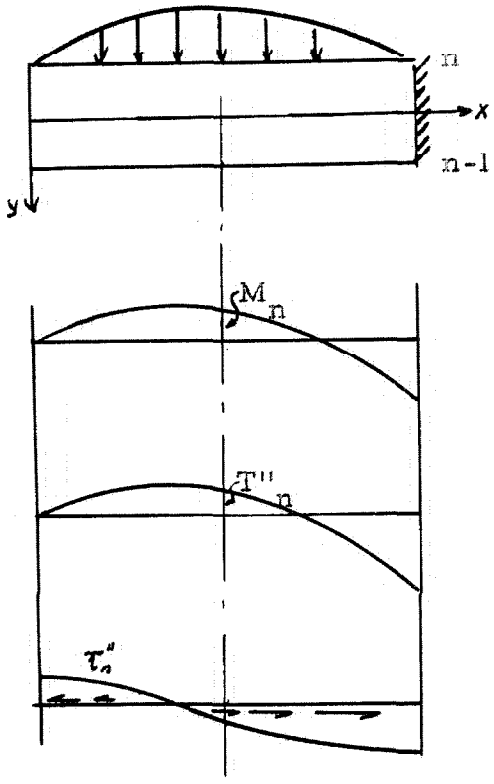

Figure 17

b) Correction loads (See Figure 17)

$$w_{n,n-1}(x) = w_{n,n-1} F_1(x) \doteq w_{n,n-1} \sin \frac{\pi x}{L},$$

where $F_1(x)$ is defined by Equation (57).

The bending moments at the center of the span produced by $w_{n,n-1} \sin \frac{\pi x}{L}$

$$M^{0''}_{n,x=\frac{L}{2}} = \frac{w_{n,n-1} L^2}{\pi^2} \left[g_2(x)\right]_{x=\frac{L}{2}} \tag{58}$$

$$\text{where} \quad g_2(x) = \sin \frac{\pi x}{L} - \frac{3x}{\pi L} \tag{59}$$

The fixed end conjugate moments at the center of the span corresponding to $M^{0''}_n$ are then given by Equation (37).

The shear forces will be:

$$T''_n(x) = T''_n \; g_2(x) \tag{60}$$

where $g_2(x)$ is defined by Equation (59).

The moment $M''_n(x)$ due to the sine distributed $w_{n,n-1}(x)$ and the shear forces $T''_n(x)$ and $T''_{n-1}(x)$ are then,

$$M''_n(x) = \frac{L^2}{\pi^2}\left(w_n - \frac{\pi^2 T''_{n-1} h_n}{2L^2} - \frac{\pi^2 T''_n h_n}{2L^2}\right) g_2(x) \tag{61}$$

$$\text{or} \quad M''_n(x) = \frac{B_{n,n-1} L^2}{\pi^2} \; g_2(x) \tag{62}$$

$$\text{where} \quad B_{n,n-1} = \left(w_{n,n-1} - \frac{\pi^2 T''_{n-1} h_n}{2L^2} - \frac{\pi^2 T''_n h_n}{2L^2}\right) \tag{63}$$

The deflection of the nth plate is,

$$y''_n(x) = \frac{0.411\, B_{n,n-1} L^4}{\pi^4 E I_n} F_2(x) \tag{64}$$

where

$$F_2(x) = \frac{1}{0.411}\left(\sin\frac{\pi x}{L} + \frac{\pi x^3}{2L^3} - \frac{\pi x}{2L}\right) \tag{65}$$

$$I_n = \frac{1}{12} t_n h_n^3$$

Now, take $F_2(x) = F_1(x)$; then the total deflection due to both the uniform plate load and the correction load will be:

$$y_n = \frac{L^4}{192\, E I_n} (A_{n,n-1} + 0.810\, B_{n,n-1})\, F_1(x) \tag{66}$$

$$= \frac{E_{n,n-1} L^4}{195\, E I_n} F_1(x) \tag{67}$$

where

$$E_{n,n-1} = A_{n,n-1} + 0.810\, B_{n,n-1} \tag{68}$$

Substituting Equation (67) into Equation (23) the general expression for the fixed end cross-bending moments is,

$$\overline{Y}''_{n-1,n}(x) = \overline{Y}''_{n,n-1}(x) = \frac{1}{\beta} H_{n,n-1} F_1(x) \tag{69}$$

where $H_{n,n-1}$ and $F_1(x)$ are defined by Equation (48) and (57), respectively and

$$\frac{1}{\beta} = \frac{L^4 t_n^3}{32\, h_n^2 (1-\nu^2)} \tag{70}$$

3:3 Continuous Shells

The case with moments applied at both ends of a span will be treated in this section. Let the moment at the left end be $M_{n,a}$ and at the right end be $M_{n,b}$.

a) Uniform plate load (See Figure 18).

The moments at the center of the span are:

$$M^{0,}_{n,\,x=\frac{L}{2}} = \frac{p_{n,n-1}L^2}{8} \left[g_1(x)\right]_{x=\frac{L}{2}} \tag{71}$$

where

$$g_1(x) = \frac{4x}{L} - \frac{4x^2}{L^2} + c\left(1-\frac{x}{L}\right) + b\,\frac{x}{L} \tag{72}$$

$$c = \frac{M'_{n,a}8}{p_{n,n-1}L^2} \qquad b = \frac{M'_{n,b}8}{p_{n,n-1}L^2} \tag{73}$$

The fixed end conjugate moments at the center of the span corresponding to $M^{0,}_{n}$ are given by Equation (29). The shear force at the nth joint will be:

$$T'_n(x) = T'_n\ g_1(x) \tag{74}$$

where $g_1(x)$ is defined by Equation (72).

The moment $M'_n(x)$ due to the uniform load $p_{n,n-1}$, the end moments M'_{na} and M'_{nb} and the shear forces $T'_n(x)$ and $T'_{n-1}(x)$ is then

$$M'_n(x) = A_{n,n-1}\frac{L^2}{8}\ g_1(x) \tag{75}$$

where

$$A_{n,n-1} = p_{n,n-1} - \frac{4\,T'_{n-1}\,h_n}{L^2} - \frac{4\,T'_n\,h_n}{L^2} \tag{76}$$

The deflection of the nth plate will then be:

$$y'_n(x) = \frac{A_{n,n-1}L^4}{48\ EI_n}\ G_1(x) = \frac{A_{n,n-1}L^4 G_1(L/2)}{48\quad EI}\ F_1(x) \tag{77}$$

where

$$G_1(x) = \frac{2x^4}{L^4} - \frac{4x^3}{L^3} - c\left(\frac{3x^2}{L^2} - \frac{x^3}{L^3}\right) - \frac{bx^3}{L^3} + 2(1+c+b/2)\frac{x}{L} \tag{78}$$

$$\text{and} \qquad F_1(x) = \frac{G_1(x)}{G_1(L/2)} \tag{79}$$

b) Correction loads (See Figure 19)

$$w_{n,n-1}(x) = w_{n,n-1} F_1(x) \doteq w_{n,n-1} \sin\frac{\pi x}{L}$$

where

The bending moments at the center of the span produced by $w_{n,n-1} \sin\frac{\pi x}{L}$ is: (where $F_1(x)$ is defined by Equation (57)

$$M^{0}{}''_{n,x=\frac{L}{2}} = \frac{w_{n,n-1} L^2}{\pi^2} \left[g_2(x)\right]_{x=\frac{L}{2}} \tag{80}$$

where

$$g_2(x) = \sin\frac{\pi x}{L} + s\left(1 - \frac{x}{L}\right) + u\frac{x}{L} \tag{81}$$

$$s = \frac{M''_{na}\pi^2}{w_n L^2}, \qquad u = \frac{M''_{nb}\pi^2}{w_n L^2} \tag{82}$$

The fixed end conjugate moments at the center of the span corresponding to $M^{0}{}''_{n}$ are then given by Equation (37).

The shear forces will be:

$$T''_n(x) = T''_n g_2(x) \tag{83}$$

where $g_2(x)$ is defined by Equation (81).

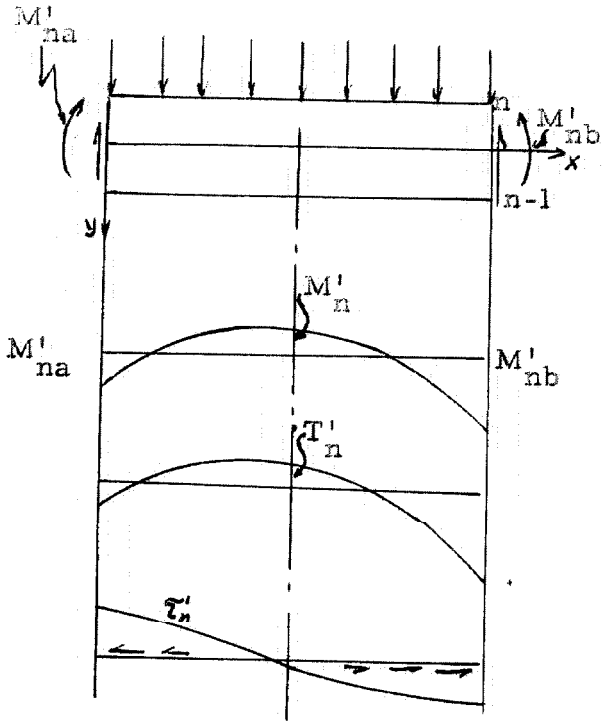

Figure 18

$p_{n,n-1}$ (constant)

$$M'^{0}_{n}(x) = \frac{p_{n,n-1} L^2}{8} g_1(x)$$

$$T'_n(x) = T'_n g_1(x)$$

$$\tau'_n = \frac{T'_n}{L} \left(4 - \frac{8x}{L} \right) - c + b \text{ , where}$$

$$g_1(x) = \frac{4x}{L} - \frac{4x^2}{L^2} + c\left(1 - \frac{x}{L}\right) + b\frac{x}{L}$$

$$c = \frac{M'_{na}\, 8}{p_{n,n-1} L^2} \qquad b = \frac{M'_{nb}\, 8}{p_{n,n-1} L^2}$$

$$w_{n,n-1}(x) = w_{n,n-1} \sin\frac{\pi x}{L}$$

$$M''^{0}_{n}(x) = \frac{w_{n,n-1} L^2}{\pi^2} g_2(x)$$

$$T''_n(x) = T''_n g_2(x)$$

$$\tau''_n(x) = \frac{T''_n}{L} \pi \cos\frac{\pi x}{L} - s + u$$

where

$$g_2(x) = \sin\frac{\pi x}{L} + s\left(1 - \frac{x}{L}\right) + u\frac{x}{L}$$

$$s = \frac{M''_{na}\, \pi^2}{w_{n,n-1} L^2}, \quad u = \frac{M'_{nb}\, \pi^2}{w_{n,n-1} L^2}$$

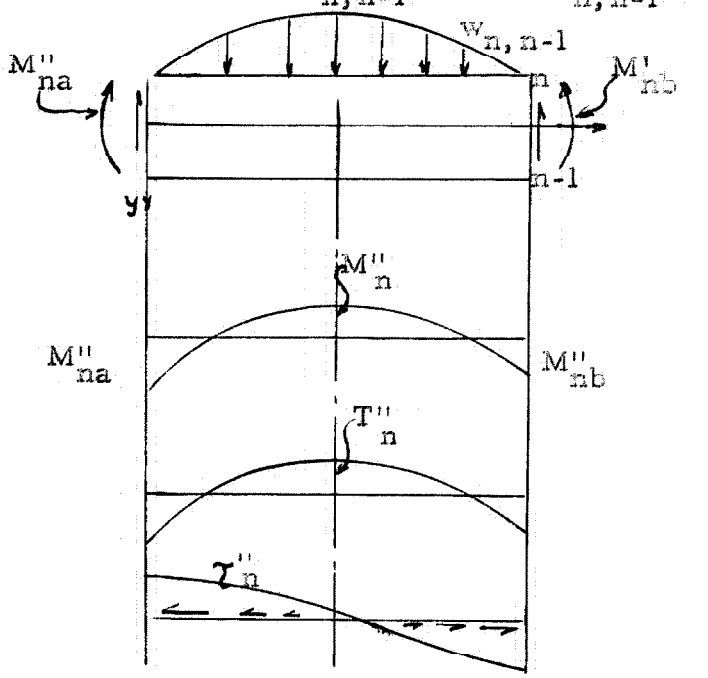

Figure 19

The moment $M''_n(x)$ due to the sine distributed load $w_{n,n-1}(x)$, the end moments M''_{na} and M''_{nb} and the shear forces are then,

$$M''_n(x) = B_{n,n-1}\frac{L^2}{\pi^2}\, g_2(x) \tag{84}$$

where

$$B_{n,n-1} = (w_{n,n-1} - \frac{\pi^2 T''_{n-1} h_n}{2L^2} - \frac{\pi^2 T''_n h_n}{2L^2}) \tag{85}$$

The deflection of the n th plate will then be:

$$y''_n(x) = \frac{B_{n,n-1}L^4}{\pi^4 EI_n}\, G_2(x) = \frac{B_{n,n-1}L^4 G_2(L/2)}{\pi^4 EI_n}\, F_2(x) \tag{86}$$

where

$$G_2(x) = \sin\frac{\pi x}{L} - \frac{s\pi^2}{2}(\frac{x^2}{L^2} - \frac{x^3}{3L^3}) - \frac{u\pi^2 x^3}{6L^3} + \frac{1}{3}\pi^2(s+u/2)\frac{x}{L} \tag{87}$$

$$F_2(x) = \frac{G_2(x)}{G_2(L/2)} \tag{88}$$

Approximating $F_2(x)$ by $F_1(x)$, Equation (86) becomes:

$$y''_n(x) = \frac{B_{n,n-1}L^4 G_2(L/2)}{\pi^4 EI_n}\, F_1(x) \tag{89}$$

The total deflection will then bc,

$$y_n(x) = \frac{L^4 G_1(L/2)}{48\, EI_n}\, A_{n,n-1} + \frac{48 G_2(L/2)}{\pi^4 G_1(L/2)} B_{n,n-1}\, F_1(x)$$
$$= \frac{L^4 G_1(L/2)}{48\, EI_n}\, E_{n,n-1}\, F_1(x) \tag{90}$$

where

$$E_{n,n-1} = A_{n,n-1} + \gamma B_{n,n-1} \tag{91}$$

$$\gamma = \frac{48G_2(L/2)}{\pi^4 G_1(L/2)} \tag{92}$$

Substituting Equation (90) into Equation (23), the general equation for the fixed end cross-bending moments is

$$\overline{Y}''_{n-1,n}(x) = \overline{Y}''_{n,n-1}(x) = \frac{1}{\beta} H_{n,n-1} F_1(x) \tag{93}$$

where $H_{n,n-1}$ and $F_1(x)$ are defined by Equations (48) and (79) respectively, and

$$\frac{1}{\beta} = \frac{L^4 t_n^3 G_1(L/2)}{8h_n^2 (1-\nu^2)} \tag{94}$$

Summary of Formulas

Plate bending moments:

$$M_n(x) = \frac{A_{n,n-1}L^2}{8} g_1(x) + \frac{B_{n,n-1}L^2}{\pi^2} g_2(x) \tag{95}$$

Joint shear forces:

$$T_n(x) = T'_n g_1(x) + T''_n g_2(x) \tag{96}$$

Since $N_n = T_n - T_{n-1}$

$$N_n(x) = N'_n g_1(x) + N''_n g_2(x) \tag{97}$$

Longitudinal stress:

Since $$\sigma_{n-1} = \frac{N_n}{A_n} \pm \frac{M_n}{Z_n} \tag{98}$$

$$\sigma_n(x) = \sigma'_n g_1(x) + \sigma''_n g_2(x) \tag{99}$$

Cross bending moment:

$$Y_n = Y'_n + Y''_n \; F_1(x) \tag{100}$$

$$A_{n,n-1} = p_{n,n-1} - \frac{4T'_{n-1}h_n}{L^2} - \frac{4T'_n h_n}{L^2} \tag{101a}$$

$$B_{n,n-1} = w_{n,n-1} - \frac{\pi^2 T''_{n-1}h_n}{2L^2} - \frac{4T''_n h_n}{2L^2} \tag{101b}$$

The fixed end bending moments at the center of the span due to rotation of the plates are:

$$\overline{Y}''_{n-1,n} = \overline{Y}''_{n,n-1} = \frac{1}{\beta} \; H_{n,n-1} \tag{102}$$

$$\frac{1}{\beta} = \frac{L^4 t_n^3 G_1(L/2)}{8h_n^2(1-\nu^2)} \tag{103a}$$

$$H_{n,n-1} = - \frac{E_{n-1,n-2}}{t_{n-1}h^2_{n-1}} \operatorname{cosec}(a_{n-1} - a_{n-1}) \tag{103b}$$

$$+ \frac{E_{n,n-1}}{t_n h_n^3} \left\{\cot(a_{n-1}-a_n) + \cot(a_{n-2}-a_{n-1})\right\} - \frac{E_{n+1,n}}{t_{n+1}h_{n+1}} \operatorname{cosec}(a_{n-1}-a_n)$$

where

$$E_{n,n-1} = A_{n,n-1} + \gamma B_{n,n-1}$$

$$\gamma = \frac{48 \; G_2(L/2)}{\pi^4 \; G_1(L/2)} \tag{104}$$

$G_1(x)$ and $G_2(x)$ are defined by Equations (78) and (87) respectively.

3:4 Procedure in solving a problem

First, a moment distribution must be performed on the fixed

end cross-bending moments, $\overline{Y}_{n,n-1}$, caused by the rotation of the plates, as given by Equation (102). Since Equation (102) contains the unknown $E_{n,n-1}$, the distributed moments Y''_n will also depend on the unknown $E_{n,n-1}$. Thus it is necessary to distribute the coefficients of $E_{n,n-1}$ and this is most conveniently done by performing separate distributions for the coefficients of each unknown $E_{n,n-1}$ occurring in the set of Equations for $\overline{Y}''_{n,n-1}$. (See example in Section 3:5, Figure 21). From the superposition of the results of the moment distributions one can now write the expressions for the moments Y''_n at the joints and the correction loads $Q_{n-1,\overline{n}}$ in terms of the $E_{n,n-1}$ by Equation (5).

Let C_2^{10} be the moment at joint 2 from the distribution of the coefficients of the E_{10}'s. In general, let $C_n^{m,m-1}$ be the moment at n due to the distribution of the coefficients of the $E_{m,m-1}$. Then, from Equation (102)

$$Y''_n = C_n^{10} E_{10} + C_n^{21} E_{21} + C_n^{32} E_{32} + -- C_n^{m,m-1} E_{m,m-1} +-- \quad (105)$$

From Equation (5)

$$h_n \beta Q_{n-1,\overline{n}} = Y''_n - Y''_{n-1} = \left[C_n^{10} - C_{n-1}^{10}\right] E_{10} + \left[C_n^{21} - C_{n-1}^{21}\right] E_{21} + --$$

$$---+ \left[C_n^{m,m-1} - C_{n-1}^{m,m-1}\right] E_{m,m-1} +-- \quad (106)$$

where β is defined by Equation (103a) $E_{n,n-1} = A_{n,n-1} + \gamma B_{n,n-1}$

where γ is defined by Equation (104).

The next step is to determine the $A_{n,n-1}$ from the actual loading on the shell. This requires one distribution process to determine the

plate loads, and one to determine the shear forces.

After determining the $A_{n,n-1}$ it is necessary to determine the $B_{n,n-1}$. This is done by applying the correction loads $Q_{1\bar{2}} = 1$ and $Q_{2\bar{2}} = -1$ (if the cross-section is symmetrical, also apply the loads symmetrical to these), and finding the shear forces produced by these loads. This is done by the conjugate moment distributions. From the plate load w and the shear due to $Q_{1\bar{2}} = 1$ and $Q_{2\bar{2}} = -1$ only the equivalent correction plate loads, $B_{n,n-1}$, are determined by Equation (106b). Then applying $Q_{2\bar{3}} = 1$ and $Q_{3\bar{3}} = -1$, their equivalent correction plate loads are determined, and so forth for the other Q's. Let the equivalent correction plate loads produced by $Q_{1\bar{2}} = 1$ and $Q_{2\bar{2}} = -1$ be $B^{12}_{n,n-1}$ etc. In general, let $B^{m-1,m}_{n,n-1}$ be the equivalent correction plate load of the $Q_{m-1,\bar{m}}$ and $Q_{m,m} = -1$. Then the actual correction load is expressed by

$$B_{n,n-1} = B^{12}_{n,n-1}\, Q_{1\bar{2}} + B^{23}_{n,n-1}\, Q_{2\bar{3}} + \cdots + B^{m-1,m}_{n,n-1} Q_{m-1,m} + \cdots \qquad (107)$$

and it follows then that

$$E_{n,n-1} = A_{n,n-1} + \gamma\left(B^{12}_{n,n-1}\, Q_{1\bar{2}} + B^{23}_{n,n-1}\, Q_{2\bar{3}} + \cdots + B^{m-1,m}_{n,n-1} Q_{m-1,m} + \cdots\right) \qquad (108)$$

Substituting Equations (108) into Equations (106) a set of simultaneous equations in $Q_{n-1,\bar{n}}$ are obtained. The solution of these equations gives the actual correction loads. Knowing the correction loads, the cross-bending moments, the loads $B_{n,n-1}$ and the shear T''_n can be computed and these determine the longitudinal stresses. The values for $Q_{n-1,\bar{n}}$, $B_{n,n-1}$, T''_n and σ''_n are determined at the center of the

span and the variation along the span is found by multiplying with the appropriate function of x. (See page 54).

The same procedure also applies for any different end conditions. In fact, if the solution for the simply supported shell is known, a shell of any span and end condition with the same type of loading and cross-section can be solved readily since all the moment distributions over the cross-section are unchanged.

For the continuous shell, the end moments M'_{na}, M'_{nb}, M''_{na} and M''_{nb} shown in Figures 18 and 19, may be obtained by performing a moment distribution in the longitudinal direction, over the total length of the structure. The fixed end moments are:

Uniform load $\quad M_{Fixed} = -1/12\ pL^2$

Sine load $\quad M_{Fixed} = -\frac{2}{\pi^3} wL^2$

Since the value of the Q's (correction loads) is quite sensitive to small changes in the coefficients of Equations (106) and (108) it is necessary to carry out the calculations using a calculating machine. For the same reason, when approximating the cylindrical shell with a prismatic shell, the angles between the side plates $(a_n - a_{n-1})$ should not be less than 10 degrees.

3:5 Example, simply supported shell

To illustrate the applications of the method the stresses will be investigated for a simply supported shell having the cross-section shown in Figure 20. Poisson's ratio is taken to be zero and the loading on the shell is as follows.

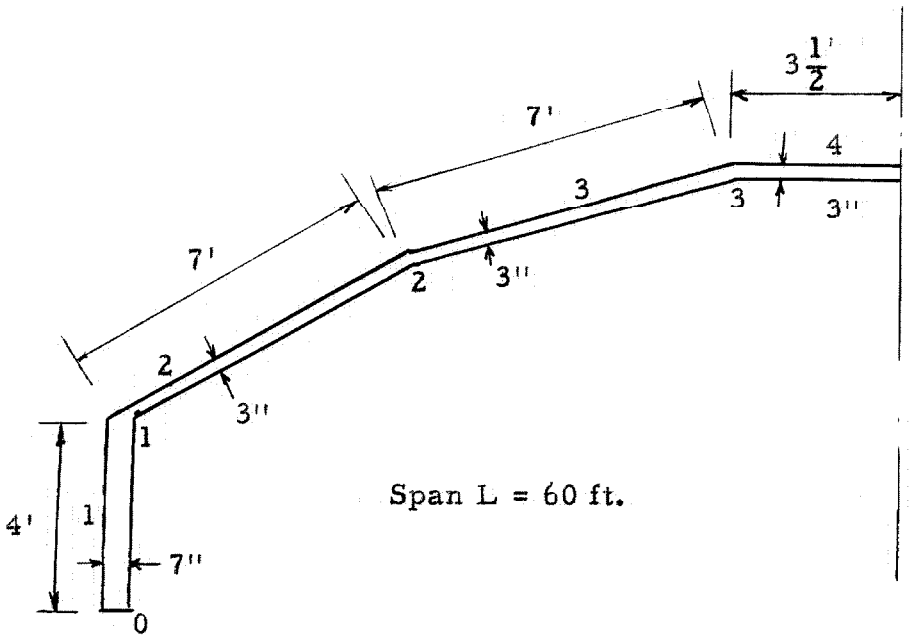

Figure 20

Dead Load per ft^2 of plate 1: 90 lb./$ft.^2$

Dead Load per $ft.^2$ of plates 2, 3 and 4: 52 lb./$ft.^2$

The cross-section and loading are symmetrical about the centerline.

TABLE 1

Joint No. n	(1) α_n	(2) $\cos\alpha_n$	(3) $\sin\alpha_n$	(4) $\alpha_{n-1}-\alpha_n$	(5) $\cot(\alpha_{n-1}-\alpha_n)$	(6) $\operatorname{cosec}(\alpha_{n-1}-\alpha_n)$
0	90	0	1			
1	30	0.8660	0.5000	60	0.5774	1.1547
2	15	0.9659	0.2588	15	3.7321	3.8637
3	0	1	0	15	3.7321	3.8637
4	-15	0.9659	-0.2588	15	3.7321	3.8637

From Equation (3) and Table 1 the equations for the plate loads in terms of the joint loads (R-loads or Q-loads) are:

$$p''_{10} = 1.1547\, R_{1\overline{2}}$$

$$p''_{21} = -0.5774\, R_{1\overline{2}} + 3.7321\, R_{2\overline{2}} + 3.8637\, R_{2\overline{3}} \qquad (109)$$

$$p''_{32} = -3.8637\, R_{2\overline{2}} - 3.7321\, R_{2\overline{3}} + 3.7321\, R_{3\overline{3}} + 3.8637\, R_{3\overline{4}}$$

From Equation (47) and Table 1 the fixed end moments due to deflection in terms of the loads $E_{n,n-1}$ are:

$$\overline{Y}''_{12} = \overline{Y}''_{21} = -9.9860\, E_{10} + 16.2258\, E_{21} - 14.5474\, E_{32}$$

$$\overline{Y}''_{23} = \overline{Y}''_{32} = -14.5474\, E_{21} + 28.1040\, E_{32} \qquad (110)$$

Equations (109) and (110) are the basic equations in the solution of this problem.

By distributing the coefficient of each $E_{n,n-1}$ term the moment Y''_n at the joints are determined as functions of the $E_{n,n-1}$ loads as shown below.

Distribution of coefficient of E_{10}

1		2		3		4	
1	1/2	1/2	1/2	1/2	1/2	1/2	
-9.9860	-9.9860	0	0	0	0	0	
0	-2.6319	+2.6319	0.5193	-0.5193	0.5193	-0.5193	

(a)

Distribution of coefficient of E_{21}

1		2		3		4	
1	1/2	1/2	1/2	1/2	1/2	1/2	
16.2258	16.2258	-14.5474	-14.5474	0	0	14.5474	
0	8.8668	-8.8668	-4.6780	+4.6780	-4.6780	+4.6780	

(b)

Distribution of coefficients of E_{32}

1		2		3		4	
1	1/2	1/2	1/2	1/2	1/2	1/2	
-14.5474	-14.5474	28.1040	28.1040	0	0	-28.1040	
0	-12.7022	12.7022	8.1633	-8.1633	-8.1633	8.1633	

(c)

From the result of the moment distribution Y''_n is obtained.

$$Y''_1 = 0$$

$$Y''_2 = -2.6319\, E_{10} + 8.8668\, E_{21} - 12.7022\, E_{32} \qquad (111)$$

$$Y''_3 = 0.5193\, E_{10} - 4.6780\, E_{21} + 8.1633\, E_{32}$$

The correction loads are

$$Q_{1\overline{2}} = \frac{Y''_2}{7} = -0.3750\, E_{10} + 1.2667\, E_{21} - 1.8146\, E_{32}$$

$$Q_{2\overline{3}} = \frac{Y''_3 - Y''_2}{7} = 0.4502\, E_{10} - 1.9350\, E_{21} + 2.9808\, E_{32} \qquad (112)$$

Where $E_{n,n-1} = A_{n,n-1} + 0.7885\, B_{n,n-1}$

The next step is to determine the $A_{n,n-1}$ as follows.

Load perpendicular to plates:

$q_2 = 52 \cos 30^\circ = 45.0$ lb./ft.^{2}

$q_3 = 52 \cos 15^\circ = 50.2$ lb./ft.^{2}

$q_4 = 52 \cos 0^\circ = 52.0$ lb./ft.^{2}

Load parallel to plates:

$p'_{10} = 90 \times 4 = 360$ lb./ft.

$p'_{21} = 52 \times 7 \sin 30^\circ = 182$ lb./ft.

$p'_{32} = 52 \times 7 \sin 15^\circ = 94.2$ lb./ft.

The fixed end moments are

$$\overline{Y}'_{12} = -\overline{Y}'_{21} = 1/12\, q_2 7^2 = 183.9;\quad \overline{Y}'_{23} = -\overline{Y}'_{32} = 205.1;\quad \overline{Y}'_{34} = -\overline{Y}'_{43} = 212.3$$

The result of the moment distribution is shown below:

1		2		3		4
1	1/2	1/2	1/2	1/2	1/2	
183.9	-183.9	205.1	-205.1	212.3	-212.3	
0	-241.1	241.1	-202.2	202.2	-202.2	

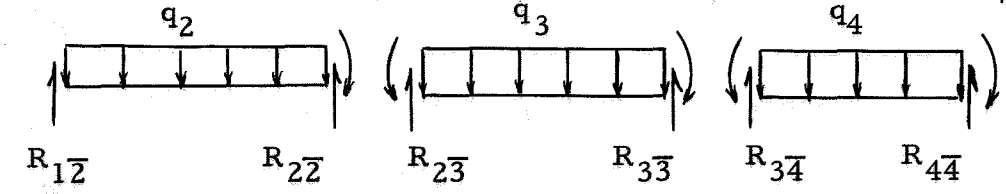

Figure 22

Thus,

$$Y'_1 = 0,\ Y'_2 = -241.1,\ Y'_3 = -202.2 \text{ ft.-lbs.}$$

$$R_{1\overline{2}} = 123.2,\quad R_{2\overline{2}} = 192.1,\quad R_{2\overline{3}} = 181.4 \text{ lbs.}$$

$$R_{3\overline{3}} = 170.2,\quad R_{3\overline{4}} = 182.0,\quad R_{4\overline{4}} = 182.0 \text{ lbs.}$$

From Equation (109)

$$p''_{10} = 142.2,\quad p''_{21} = 1346.6,\quad p''_{32} = -80.7 \text{ lbs.}$$

Then, since $p_{n,n-1} = p'_{n,n-1} + p''_{n,n-1}$

$$p_{10} = 502.2,\quad p_{21} = 1528.5,\quad p_{32} = 13.7 \text{ lbs.}$$

It is now necessary to determine the shear produced by $p_{n,n-1}$ as follows:

The fixed end conjugate moments given by $\overline{T}'_{n,n-1} = \frac{p_{n,n-1}L^2}{8h_n}$ are

$$\overline{T}'_{10} = 56,500,\quad \overline{T}'_{21} = 98,258,\quad \overline{T}'_{32} = 884$$

The result of distributing the fixed end "shears" and the equivalent loads are shown below

	0	1		2		3	
	1	0.5712	0.4286	1/2	1/2	1/2	1/2
	-56,500	56,500	-98,258	98,258	-884	884	0
	0	105,446	-105,446	52,080	-52,080	-16,456	16,456
T'		105,446		52,080		-16,456	
$\frac{4T'_n h_n}{L^2}$	0	468.6	820.1		405.1		-128

Figure 23

Then from Equation (32) and Figure 23

$$A_{10} = 502.2 - 468.6 = 33.6$$

$$A_{21} = 1528.5 - 820.1 - 405.1 = 303.3$$

$$A_{32} = 13.7 - 405.1 + 128.0 = -263.4$$

Since $T_1' = 105,446$, $T_2' = 52,080$, $T_3' = -16,456$ lbs.

$$N_1' = 105,446,\ N_2' = -53,366,\ N_1' = -68,536,\ N_4' = 32,912 \text{ lbs.}$$

$$(M_n')_{max} = \frac{A_{n,n-1} L^2}{8} \qquad M_1' = 15,200,\ M_2' = 136,500,$$

$$M_3' = -118,500 \text{ ft./lbs.}$$

Then axial stresses are:

$$\sigma_{n-1} = \frac{N_n}{a_n} \pm \frac{M_n}{Z_n},$$

where

$a_n = 336$ in. $a_2 = a_3 = a_4 = 252$ in.

$Z_1 = 2688$ in. $Z_2 = 3528$ in.

For plate 1

$$\sigma_o' = \frac{105,466}{336} + \frac{15,200 \times 12}{2688} = 314 + 68 = 382 \text{ lbs./in.}^2$$

$$\sigma_1' = 314 - 68 = 246$$

For plate 2

$$\sigma_1' = \frac{-53,366}{252} + \frac{136,500 \times 12}{3528} = -212 + 464 = 242$$

$$\sigma_2' = -212 - 464 = -676$$

For plate 3

$$\sigma_2' = -272 - 403 = -675$$

$$\sigma_3' = -272 + 403 = 131$$

For plate 4

$$\sigma_3' = \frac{32,912}{252} = 131$$

The stress at the extreme fiber of each individual plate is now calculated. Comparing the stress at a joint calculated for two adjacent plates will give a check on the accuracy of the moment distribution performed in obtaining the shear forces.

The above stresses are plotted in Figure 26 as the broken line labeled "hinged".

To determine the $B_{n,n-1}$ the procedure is as follows:

a) Apply correction loads $Q_{1\overline{2}} = 1$, $Q_{2\overline{2}} = -1$ (also $Q_{6\overline{6}} = 1$, $Q_{5\overline{6}} = -1$).

From Equation (109)

$$w_{10} = 1.1547, \quad w_{21} = -4.3095, \quad w_{32} = 3.8637$$

From these loads the following shears are computed and a moment distribution performed.

$$\overline{T}''_{n,n-1} = \frac{L^2 \times w_{n,n-1}}{\pi^2 xh}, \quad \overline{T}''_{10} = 105.3, \quad \overline{T}''_{21} = -224.57, \quad \overline{T}''_{32} = 201.34$$

0	1		2		3	
1	0.5714	0.4286	1/2	1/2	1/2	1/2
-105.30	105.30	224.57	-224.57	-201.34	201.34	0
0	-112.73	112.73	-42.74	42.74	215.15	-215.15
T''_n	-112.73		-42.74		215.15	
$\frac{\pi^2 T''_n h_n}{2L^2}$	-0.6210	-1.0817	-0.4101		2.0644	

Figure 24

b) Apply correction loads $Q_{2\overline{3}} = 1$, $Q_{3\overline{3}} = -1$ (also $Q_{5\overline{-}} = 1$, $Q_{4\overline{5}} = -1$)

From Equation (109)

$w_{10} = 0$, $w_{21} = 3.8637$, $w_{32} = -7.4642$

From these loads the following shears are computed and a moment distribution performed.

$$\overline{T}''_{10} = 0, \quad \overline{T}''_{21} = 201.34, \quad \overline{T}''_{32} = -388.97$$

	0		1		2		3
	1	0.5714	0.4286	1/2	1/2	1/2	1/2
	0	0	-201.34	201.34	388.97	-388.97	0
	0	201.96	-201.96	-102.92	102.92	-354.26	354.26
T''_n		201.96		-102.96		-354.26	
$\frac{\pi^2 T''_n h_n}{2L^2}$		1.1073	1.9378		-0.9875		-3.3991

Figure 25

Equation (40) and Figures 24 and 25 give the following expressions for the correction loads and shears.

$$B_{10} = (1.1547 + 0.6210)\, Q_{1\overline{2}} - 1.1073\ Q_{2\overline{3}} = 1.7757\ Q_{1\overline{2}} - 1.1073 Q_{2\overline{3}}$$

$$B_{21} = -2.2094\, Q_{1\overline{2}} + 2.9134\, Q_{2\overline{3}} \tag{113}$$

$$B_{32} = 2.2094\, Q_{1\overline{2}} - 3.0776\, Q_{2\overline{3}}$$

$$T''_1 = -112.73\ Q_{1\overline{2}} + 201.96\, Q_{2\overline{3}}$$

$$T''_2 = -42.74\ Q_{1\overline{2}} - 102.92\, Q_{2\overline{3}} \tag{114}$$

$$T''_3 = 215.20\, Q_{1\overline{2}} - 354.86\, Q_{2\overline{3}}$$

Since $E_{n,n-1} = A_{n,n-1} + 0.7885\, B_{n,n-1}$ the expressions for $E_{n,n-1}$ in terms of $Q_{1\bar{2}}$ and $Q_{2\bar{3}}$ are

$$E_{10} = 33.6 + 1.5118\, Q_{1\bar{2}} - 1.0771\, Q_{2\bar{3}}$$

$$E_{21} = 303.3 - 1.9470\, Q_{1\bar{2}} + 2.1223\, Q_{2\bar{3}} \qquad (115)$$

$$E_{32} = -263.4 + 1.4378\, Q_{1\bar{2}} - 1.6187\, Q_{2\bar{3}}$$

Substituting the above equations into Equations (112) gives

$$\begin{aligned} Q_{1\bar{2}} &= 849.56 - 6.4892\, Q_{1\bar{2}} + 7.6393\, Q_{2\bar{3}} \\ Q_{2\bar{3}} &= -1356.90 + 10.1073\, Q_{1\bar{2}} - 12.0719\, Q_{2\bar{3}} \end{aligned} \qquad (116)$$

or

$$\begin{aligned} 7.4892\, Q_{1\bar{2}} - 7.6393\, Q_{2\bar{3}} &= 849.56 \\ 10.1073\, Q_{1\bar{2}} = 13.1719\, Q_{2\bar{3}} &= 1356.90 \end{aligned} \qquad (117)$$

Solving these two equations for $Q_{1\bar{2}}$ and $Q_{2\bar{3}}$ gives

$$Q_{1\bar{2}} = 35.72, \quad Q_{2\bar{3}} = -76.19$$

These are the forces of two couples which determine the moments Y''_2 and Y''_3.

$$Y''_2 = 250 \text{ ft.-lbs.}, \quad Y''_3 = -283 \text{ ft.-lbs.}$$

From Equations (113) and (114), which are the general expressions for the T"s and B s these are obtained:

$$T''_1 = -19,400, \quad T''_2 = 6,320, \quad T''_3 = 34,800 \text{ lbs.}$$

$$B_{10} = 147.8, \quad B_{21} = -322.2, \quad B_{32} = 313.40 \text{ lbs.-ft.}$$

These values determine the forces N'' and moments M'' to be

$N''_1 = -19,400, \quad N''_2 = 25,720, \quad N''_3 = 28,480, \quad N''_4 = -69,600$ lbs.

$M''_1 = 53,910, \quad M''_2 = -117,550, \quad M''_3 = 114,320$ ft.-lbs.

From these values for the forces and moments the longitudinal stresses are computed as follows:

Plate 1:

$$\sigma''_0 = \frac{-19,400}{336} + \frac{53,910 \times 12}{2688} = -58 + 241 = 183 \text{ lbs./in.}^2$$

$$\sigma''_1 = -58 - 241 = -299$$

Plate 2:

$$\sigma''_1 = \frac{25,720}{252} - \frac{117,550 \times 12}{3528} = 102 - 400 = -298$$

$$\sigma''_2 = 102 + 400 = 502$$

Plate 3:

$$\sigma''_2 = 113 + 389 = 502$$

$$\sigma''_3 = 113 - 389 = -276$$

Plate 4:

$$\sigma''_3 = \frac{-69,600}{252} = -276$$

The general expressions for the longitudinal stresses along the span are obtained by combining the σ' and the σ'' and are: (See Eqn. 99)

$$\begin{aligned} \sigma_0 &= 382\, g_1(x) + 183\, g_2(x) \\ \sigma_1 &= 244\, g_1(x) - 299\, g_2(x) \\ \sigma_2 &= -675\, g_1(x) + 502\, g_2(x) \\ \sigma_3 &= 131\, g_1(x) - 276\, g_2(x) \end{aligned} \qquad g_1(x) = 4\left(\frac{x}{L} - \frac{x^2}{L^2}\right) \qquad g_2(x) = \sin\frac{\pi x}{L} \qquad (118)$$

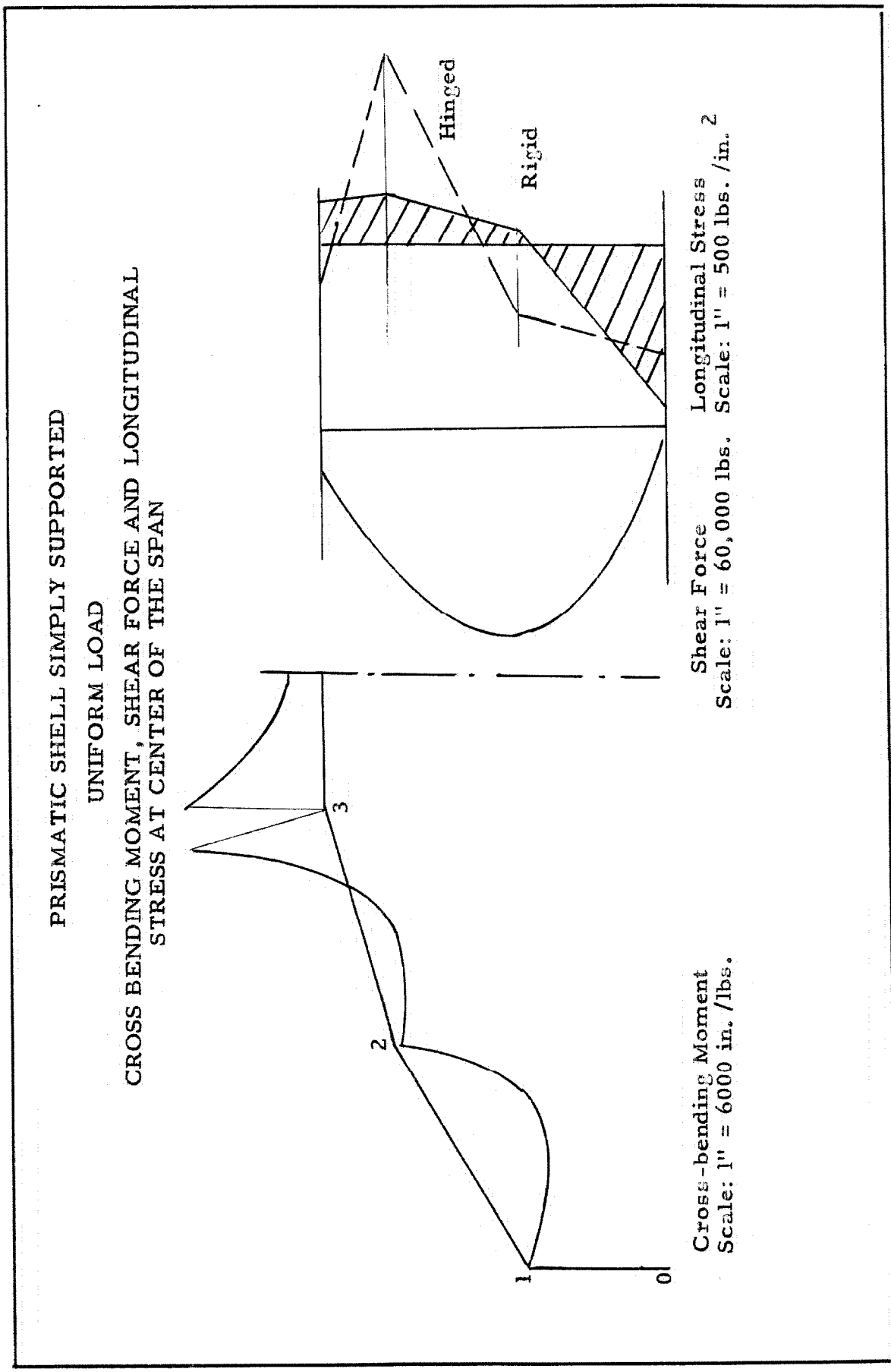
PRISMATIC SHELL SIMPLY SUPPORTED
UNIFORM LOAD
CROSS BENDING MOMENT, SHEAR FORCE AND LONGITUDINAL STRESS AT CENTER OF THE SPAN
Hinged
Rigid
0
1
2
3
Cross-bending Moment
Scale: 1" = 6000 in. /lbs.
Shear Force
Scale: 1" = 60,000 lbs.
Longitudinal Stress
Scale: 1" = 500 lbs. /in.2

Figure 26

At the center of the span the longitudinal stresses are

$\sigma_0 = 565,\ \sigma_1 = -55,\ \sigma_2 = -173,\ \sigma_3 = -145$ lbs.-in.^{2}

The corresponding general expressions for the shears are (see Eqn. 96)

$$\begin{aligned} T_1 &= 105,466\ g_1(x) - 19,400\ g_2(x) \\ T_2 &= 52,080\ g_1(x) + 6,320\ g_2(x) \\ T_3 &= -16,456\ g_1(x) + 34,800\ g_2(x) \end{aligned} \tag{119}$$

At the center of the span the shears are

$$T_1 = 86,066,\quad T_2 = 58,400,\quad T_3 = 18,344 \text{ lbs.}$$

The resultant cross-bending moments are given by Equation (100)

$$\begin{aligned} Y_1 &= 0 \\ Y_2 &= -241.1 + 250.0 \sin \frac{\pi x}{L} \text{ ft.-lbs.} \\ Y_3 &= -202.2 - 283.0 \sin \frac{\pi x}{L} \text{ ft.-lbs.} \end{aligned} \tag{120}$$

At the center of the span the moments are

$$\begin{aligned} Y_2 &= 9 \text{ ft.-lbs.} = 108 \text{ in.-lbs.} \\ Y_3 &= -485 \text{ ft.-lbs.} = -5820 \text{ in.-lbs.} \end{aligned}$$

The longitudinal stresses, the shear force and the cross-bending moments are plotted in Figure 26.

IV. DESCRIPTION OF TEST FACILITIES AND PROCEDURE

4:1 Test models

Three models were built for use in the tests described in this paper. Two of them, model A and model B were prismatic and the other, model C, was a cylindrical shell. The dimensions of the shells are shown in Figures 27 and 28.

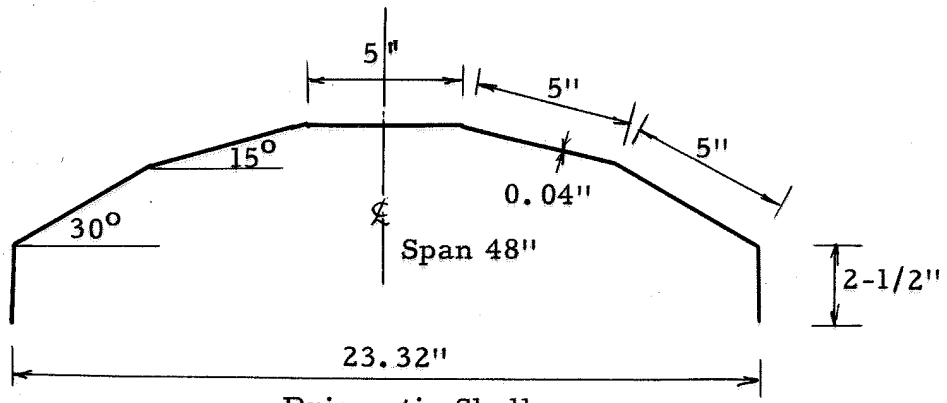

Prismatic Shell

Cross-section of Model A and B

Figure 27

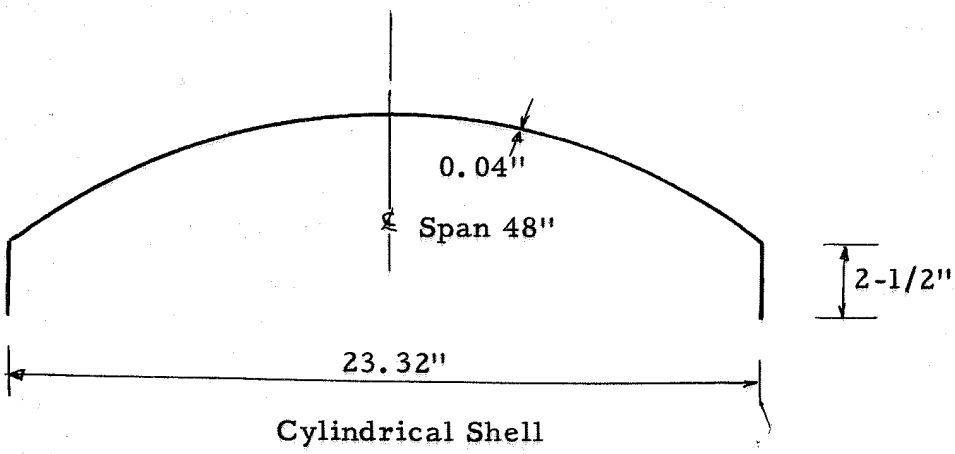

Cylindrical Shell

Cross-section of Model C

Figure 28

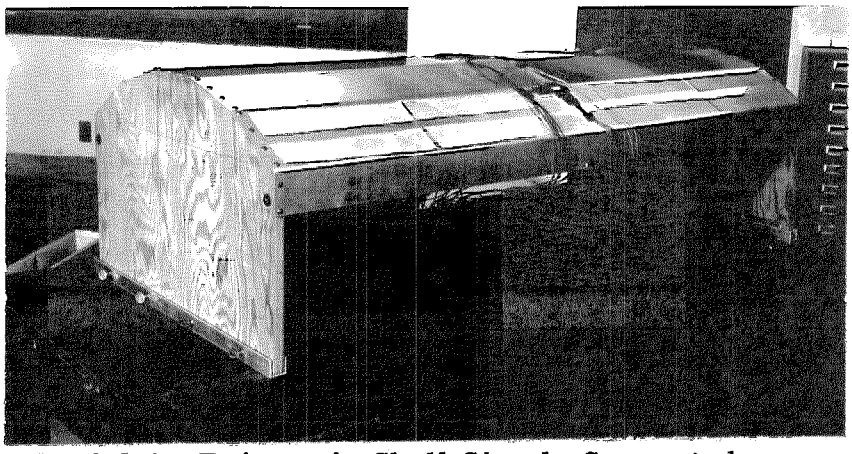

Model A, Prismatic Shell Simply Supported
Figure 29

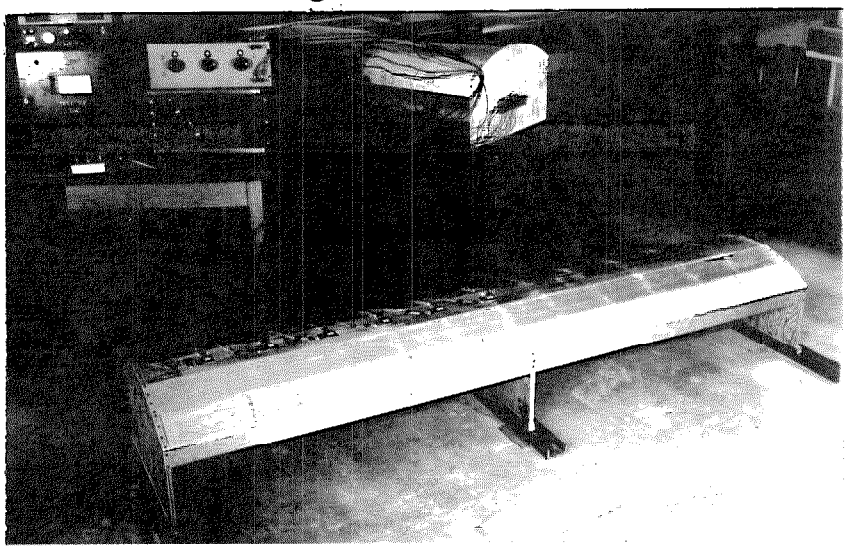

Model B, Prismatic Shell One End Fixed,
The Other Simply Supported
Figure 30

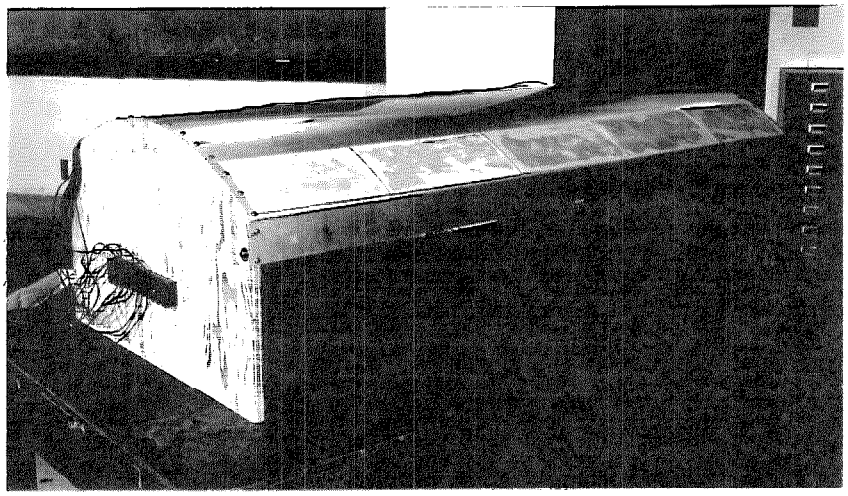

Model C, Cylindrical Shell Simply Supported
Figure 31

The shell in all models was made of a 24S-T Alclad aluminum sheet with a thickness of 0.04 inches. A thickness of three times this would have been desirable to avoid relatively large deflections of the side plates; however, the thickness of the plates was limited to 0.04 inches so that the angles of the prismatic shell could be turned with a relatively small radius.

The end frames in all models were made of 3/4 inch plywood and fastened to the shell with screws.

Model A, Figure 29, is a prismatic shell simply supported with a span of 48 inches. This model was built to check the longitudinal stress and cross-bending moment at the center of the span.

Model B, Figure 30, is a prismatic shell simply supported at one end and fixed at the other. To produce the fixed end the shell was continued over three supports with two equal spans, and when tested the load was placed symmetrically about the center support. The purpose of this model was to check the variation of the longitudinal stress and the cross-bending moment along the span.

Model C, Figure 31, is a cylindrical shell simply supported with a centerline radius such that the curve would pass through the joints of the prismatic shells, Model A and Model B. This model was built in order to determine if a cylindrical shell could be approximated satisfactorily by a prismatic shell for the purpose of stress analysis. Longitudinal stress and cross-bending moment were checked at the center of the span.

4:2 Loading of models and end supports

a) Loading

Two types of loading were used for all models. In one case

uniform load was placed along the top of the shell, extending 2-1/2" on either side of the centerline as shown in Figures 39, 47 and 55. Leadbags, weighing 25 pounds, with the approximate dimensions of 12" x 5", were used for this type of loading which will be referred to as "Uniform Load on Top". During the tests it was found that the test results were very sensitive to the variation of the loading. Extreme care had to be taken in placing the bags along the centerline and in leveling the bags off in both directions. Smaller bags than the ones mentioned above were tried, but were discarded since they introduced too much local bending.

In the second case, uniform load was placed over the entire top part of the shell as shown in Figures 43, 52 and 58. This loading will be called "Uniform Load". Leadbags, weighing 10 pounds with the approximate dimensions of 16" x 6-1/4" were used. As seen from the photographs the loading is not absolutely uniform, and it is difficult to duplicate each time the shell is loaded. Consequently a spread in the test results and a deviation from the theoretical results can be expected.

In order to increase the friction coefficient of the surface of the side plates fine sandpaper was glued to the lower 5" of the shell.

b) Supports

When testing the shell the end frames were supported on rollers, one end "pin-ended" and the other end free to roll, as shown in Figure 32.

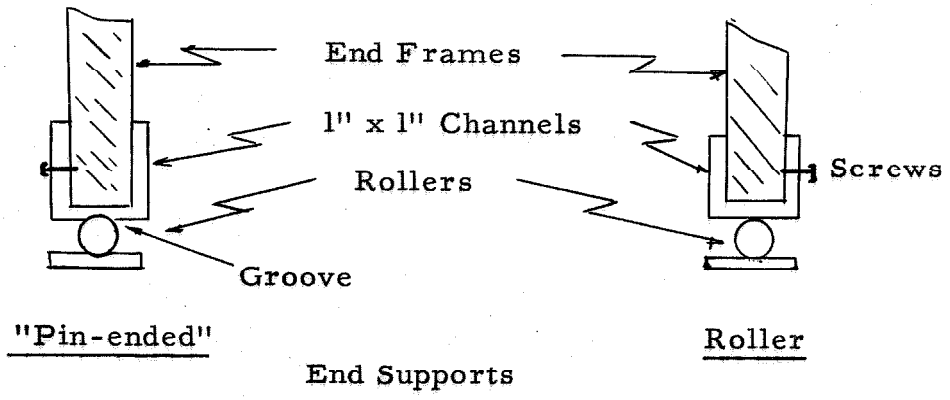

Figure 32

4:3 Strain gages

a) Type of gages

The Baldwin-Lima-Hamilton Corp. SR-4 strain gages, type A-7 and A-8, were used in determining the stress in the shell. At each particular point, where the stress was desired, four gages were mounted. Two on the top surface of the plate, one in longitudinal direction and one in crosswise direction, and two gages on the under surface of the plate in the same directions. On Model A, type A-7 gages were mounted in the longitudinal direction and type A-8 in the crosswise direction. On Model B and C only type A-7 gages were used.

All strain gages labeled with odd numbers measure strain in the longitudinal direction, gages labeled with even numbers measure strain in crosswise direction. Gages mounted on the under side of the metal are designated with the same numbers but primed.

Strain Gage Constants:	Type A-7	Res. in ohms	$120 \pm .3\%$
		Gage Factor	$1.95 \pm 2\%$
	Type A-8	Res. in ohms	$120 \pm .3\%$
		Gage Factor	$1.81 \pm 2\%$

b) Location of strain gages

The location of the gages on the three models are as shown in Figures 33, 34 and 35. In addition to the gages shown, check gages were mounted symmetrically to (1) and (6,7) on Model A (see Figure 29) and symmetrically to gage (1) on Model C (see Figure 31). These gages were only read to check the symmetry of the loading. No check gages were mounted on Model B.

Model A:

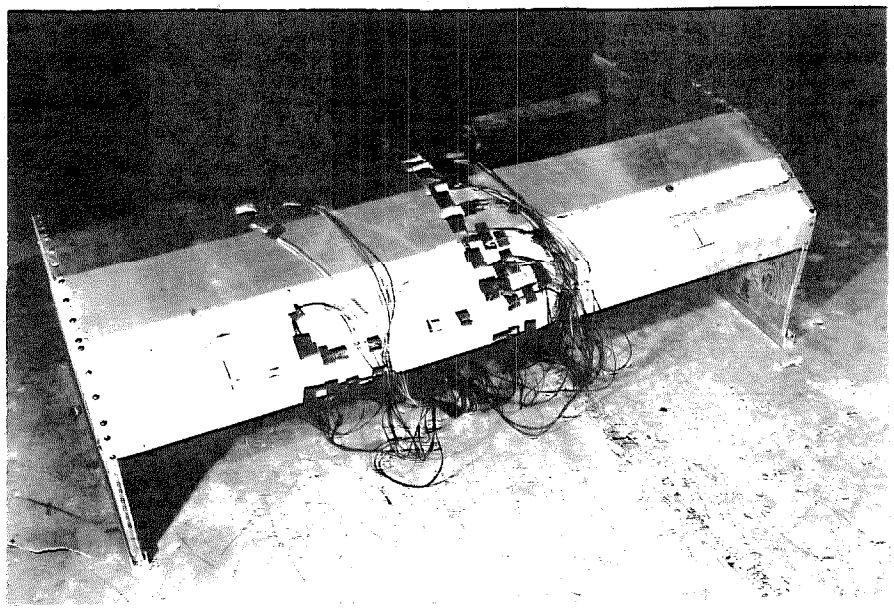

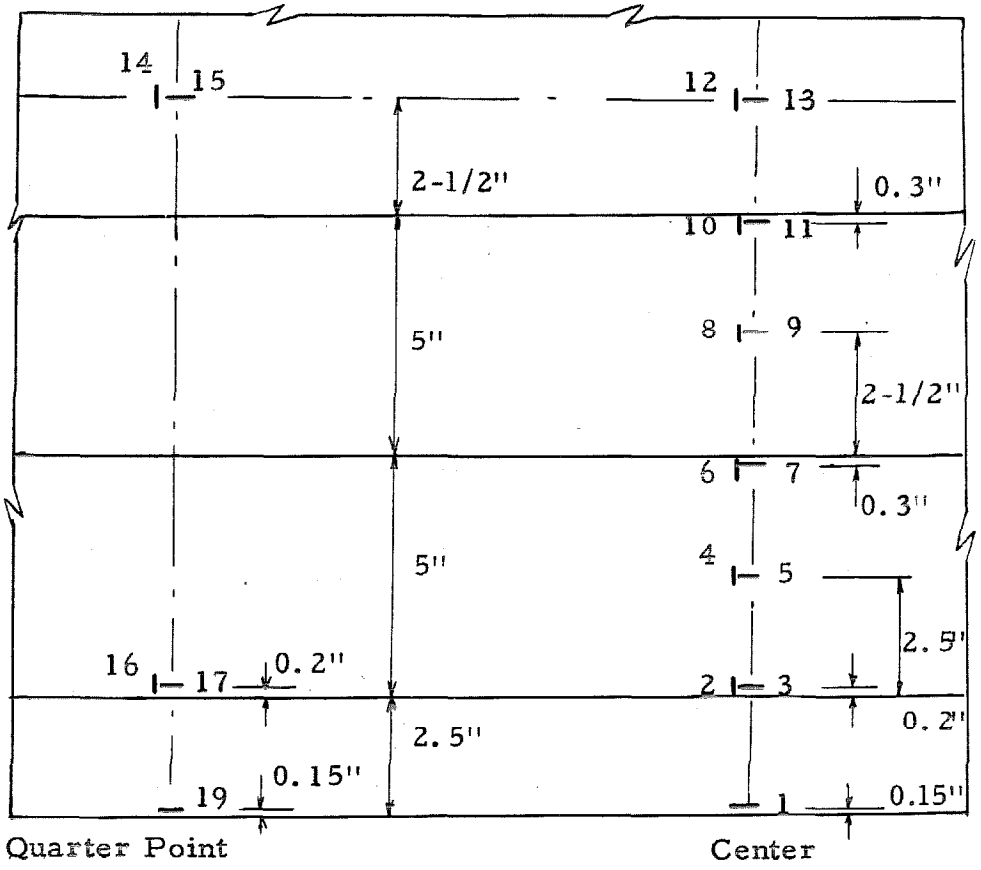

Location of Strain Gages on Model A

All even numbers are Type A-8 gages, all odd numbers Type A-7

Figure 33

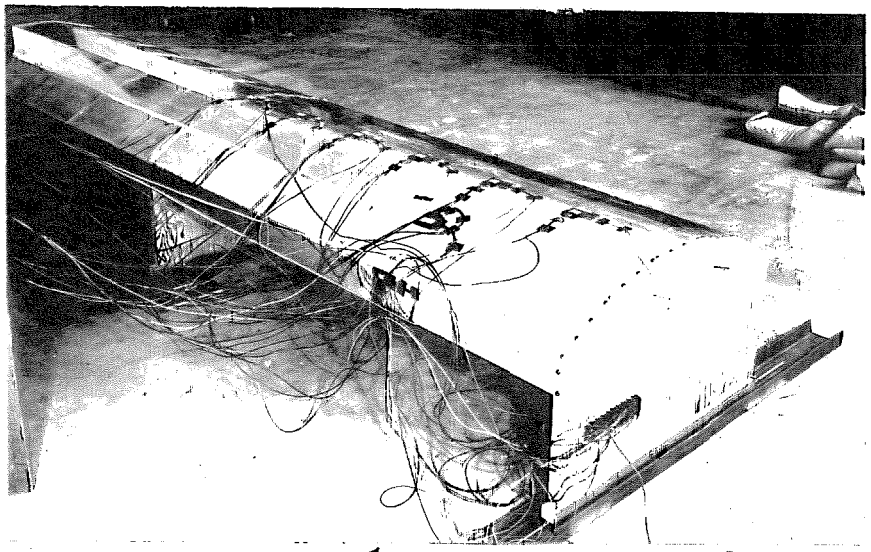

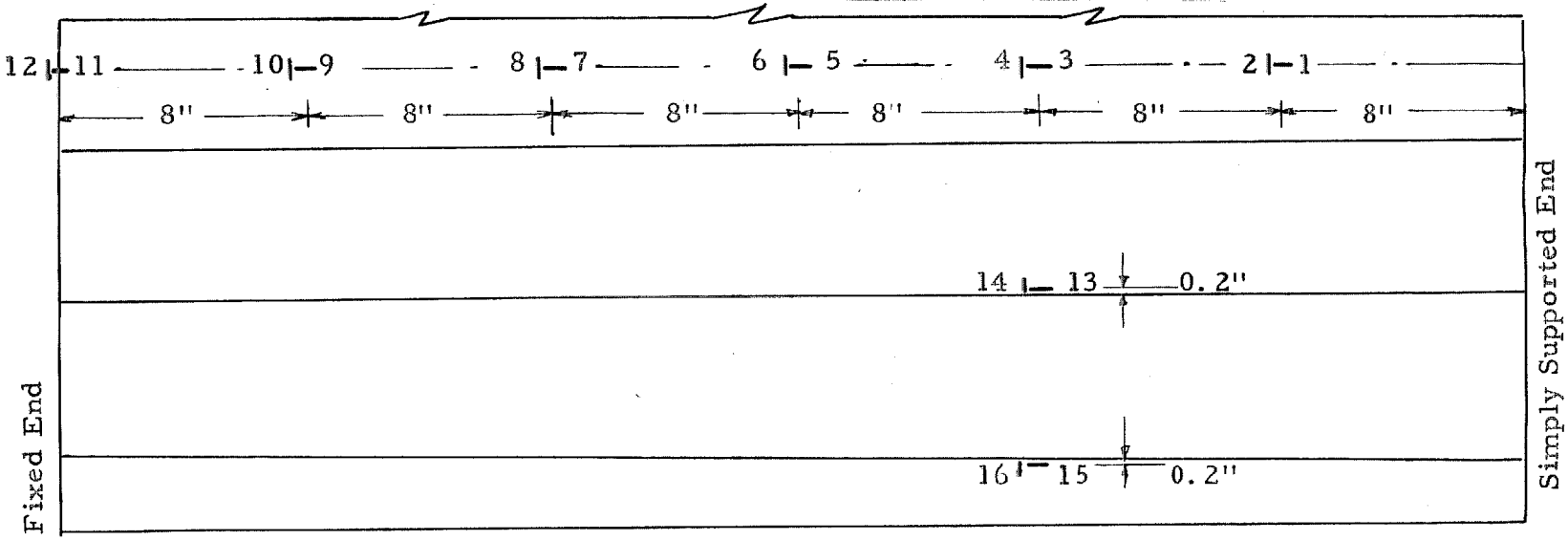

Location of Strain Gages on Model B
All Gages are Type A-7

Figure 34

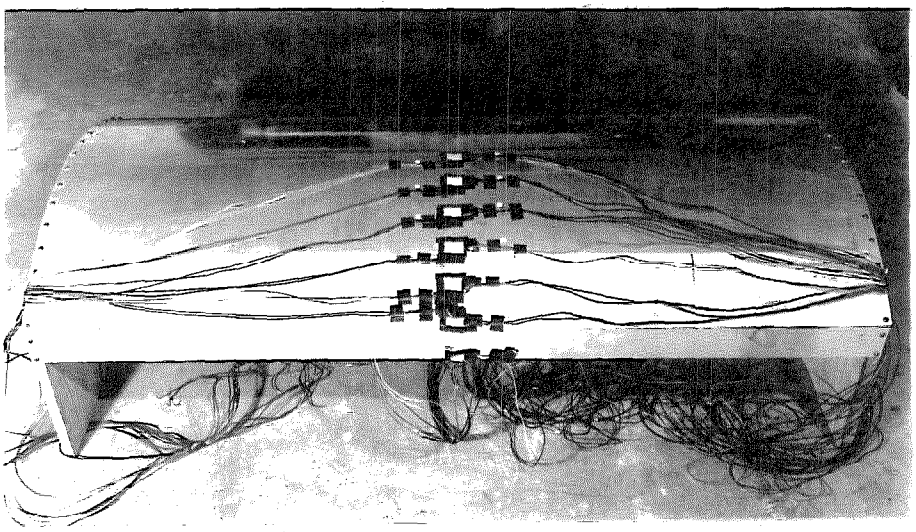

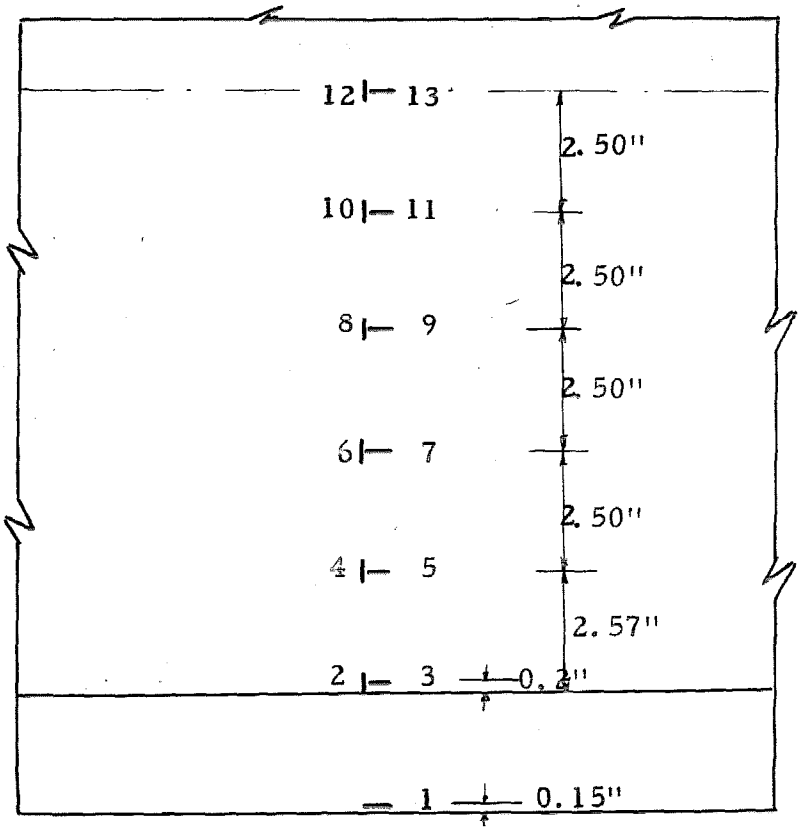

Location of Strain Gages on Model C
All Gages are Type A-7

Figure 35

4:4 Instrumentation

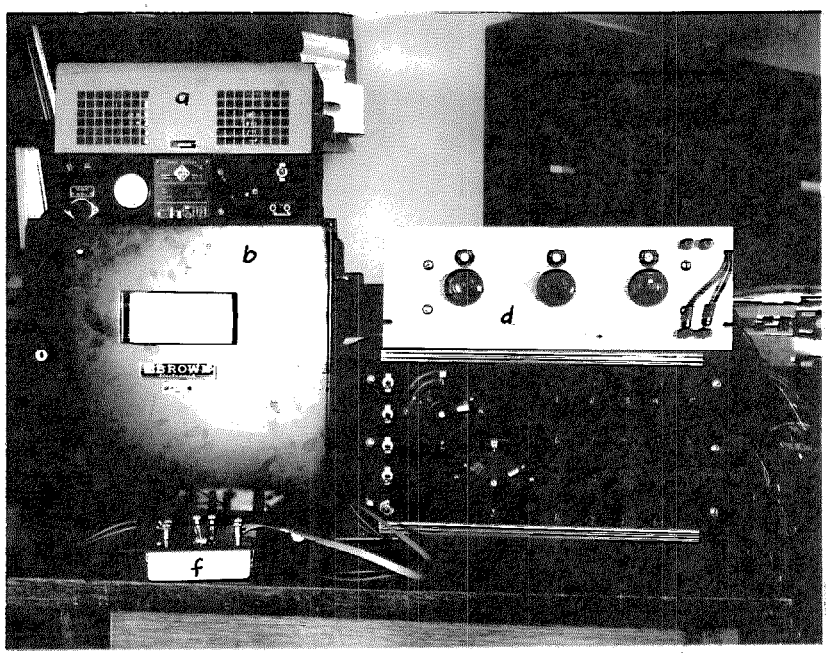

Instrument Panel
Figure 36

a) Variac Rectifier, range 0-15 volts D.C.

b) Brown Potentiometer Pyrometer, range 0-5 mv.

c) Selector switch panel with variable balancing resistors

d) Selector switch panel

e) Switch for calibration resistance

f) Double throw double pole switch

The instruments used in the experiments are shown in Figure 36. Two selector switch panels were used and are shown on the right-hand side of the figure. The lower panel has a capacity of 20 different Wheatstone bridge circuits and is equipped with a balancing resistor for each circuit. The upper panel has a capacity of 24 different bridge

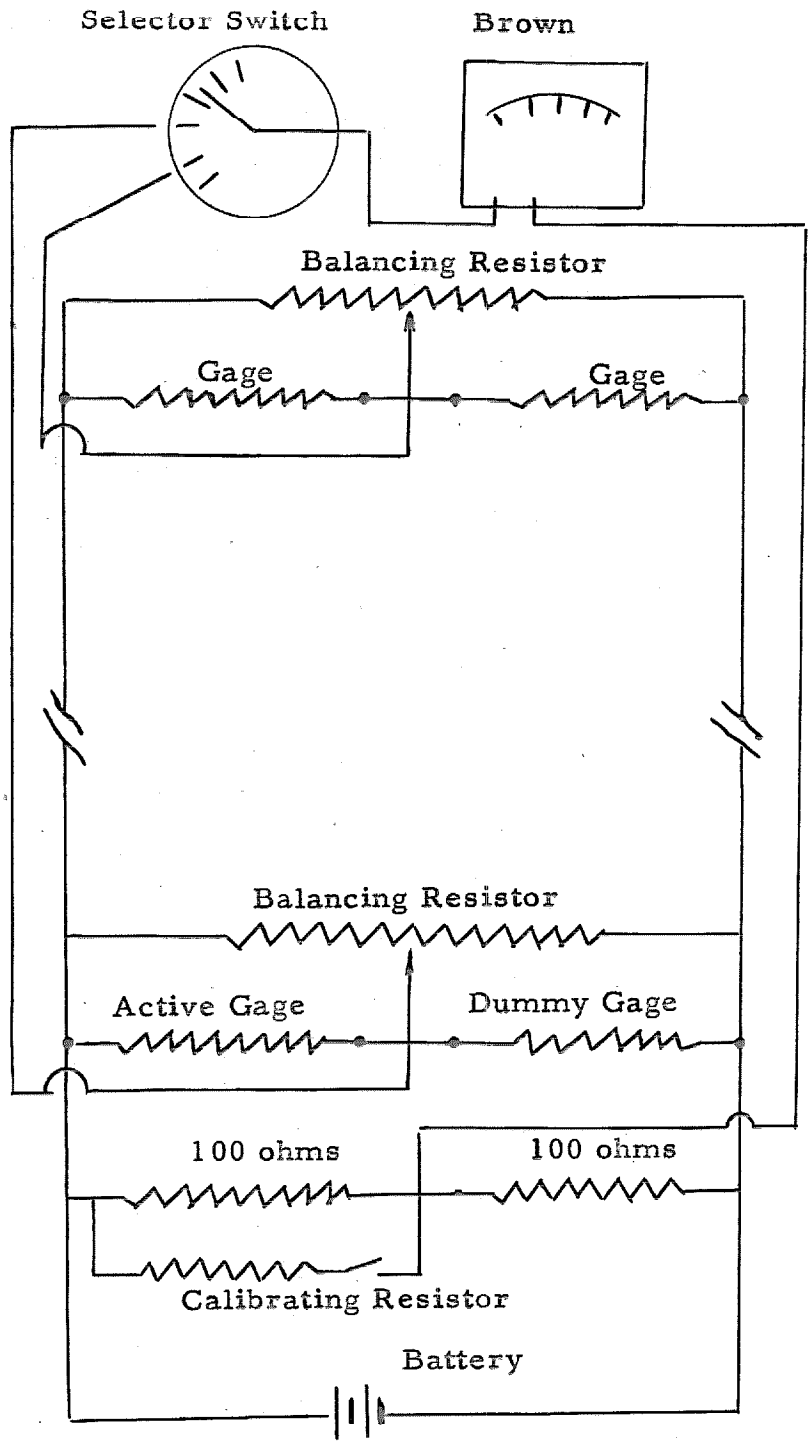

Schematic wiring diagram of the switch panel

Figure 37

circuits, but is not equipped with any balancing resistors. Figure 37 shows a schematic wiring diagram of the switch panels. The bridge output was measured with a Brown potentiometer with a range from 0-5 mv and with smallest scale division 0.01 mv. Any bridge that would balance within the range of the Brown was hooked up on the upper panel, all others were hooked up on the lower panel and balanced with the variable resistors until a reading could be otained on the Brown.

The strain gages on two models were connected at the same time. The gages on one model were connected as active gages while the gages on the other model were connected as dummy gages. One model could then be tested with the gages on the other serving as dummy gages and vice versa. Changing the load from one model to the other would, of course, produce a reading of opposite sign on the Brown potentiometer for the same stress.

During the test an automotive battery was used for input voltage, but between runs the gages were kept warm by use of a Variac Rectifier.

4:5 Calculation of Gage Output and Stresses

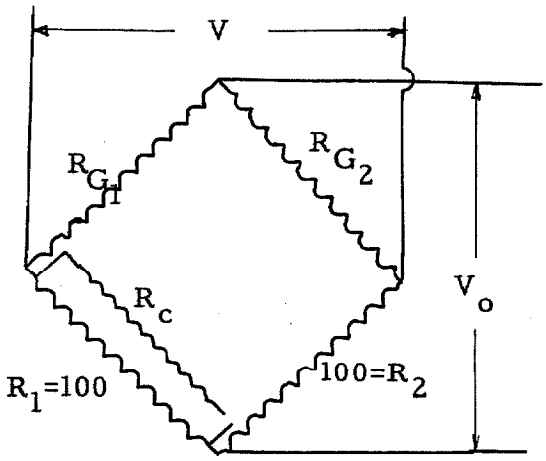

Wheatstone Bridge Circuit

Figure 38

Symbols used:

V = voltage or potential

V_o = bridge output voltage

ΔV_o = change in bridge output voltage as a result of change in strain

ΔV_c = change in bridge output voltage as a result of connecting the calibrating resistor in parallel with the built in 100 ohms resistor

R_G = gage resistance

R = built in resistance (100 ohms)

R_c = calibrating resistance

ΔR_G = change in gage resistance as a result of change in strain

ΔR = change in built in resistance (100 ohms) as a result of shunting in the calibrating resistance

From the circuit shown in Figure 38:

$$\Delta V_o = \frac{V}{2R_G}\left[R_G - \frac{2R_G}{2R_G-\Delta R_G}(R_G-\Delta R_G)\right] \doteq \frac{V}{2R_c}\Delta R_G \qquad (121)$$

$$\Delta V_c = \frac{V}{2R}\left[R - \frac{2R}{2R-\Delta R}(R-\Delta R)\right] \doteq \frac{V}{2R}\Delta R$$

Then dividing the two equations gives:

$$\frac{\Delta R_G}{R_G} = \frac{\Delta V_o}{\Delta V_c}\frac{\Delta R}{R} \qquad (122)$$

But by definition of gage factor

$$K = \frac{\Delta R_G}{R_G} \div \epsilon$$

Hence

$$K\epsilon = \frac{\Delta R_G}{R_G} \tag{123}$$

Substituting this value in Equation (122) gives:

$$\epsilon = \frac{\Delta V_o}{\Delta V_c} \frac{\Delta R}{R K} \text{ in./in.} \tag{124}$$

with a calibrating resistance of 83,233 ohms, $\Delta R = 0.12$ ohms.

Knowing the input voltage the strain can also be found as follows.

From the circuit in Figure 38:

$$V_o = V\left(\frac{R_{G_1}}{R_{G_1} - R_{G_2}} - \frac{R_1}{R_1 - R_2}\right)$$

Assuming R_1 and R_2 constant, differentiating gives

$$\Delta V_o = \frac{V}{(R_{G_1} + R_{G_2})^2} \left(R_{G_2} \Delta R_{G_1} - R_{G_1} \Delta R_{G_2}\right)$$

Assume that the change in the gage resistance due to temperature is the same in both active and dummy gages and that $R_{G_1} = R_{G_2}$. Then

$$\Delta V_o = \frac{V}{4R_G} \Delta R_G \text{ or } \frac{\Delta R_G}{R_G} = \frac{4\Delta V_o}{V}$$

Substituting this value in Equation (123) gives:

$$\epsilon = \frac{4\Delta V_o}{K V} \text{ micro in./in.} \tag{125}$$

V volts, ΔV_o millivolts

Let

ϵ_x = strain in longitudinal direction on the top surface

ϵ'_x = strain in longitudinal direction on the bottom surface

ϵ_y = strain in crosswise direction on the top surface

ϵ'_y = strain in crosswise direction on the bottom surface

σ_x = stress in longitudinal direction

Y = cross bending moment

Z = $1/6\ t^2$ section modulus

ν = Poisson's ratio

E = modulus of elasticity

K_x = gage factor for gage in longitudinal direction

K_y = gage factor for gage in crosswise direction

$$\sigma_x = \frac{E}{1-\nu^2}\left(\frac{\epsilon_x+\epsilon'_x}{2} + \frac{\epsilon_y+\epsilon'_y}{2}\right) \tag{126}$$

$$Y = -\frac{EZ}{1-\nu^2}\left(\frac{\epsilon_y-\epsilon'_y}{2} + \frac{\epsilon_x-\epsilon'_x}{2}\right) \tag{127}$$

Y positive when it produces compression in top surface.

Substitution of Equation (124) or (125) into Equations (126) and (127) gives:

$$\sigma_x = C_1\ (\Delta V_{ox} + \Delta V'_{ox}) + \frac{K_x}{K_y}\nu(\Delta V_{oy}+\Delta V'_{oy}) \tag{128}$$

$$Y = C_2\ (\Delta V'_{oy} - \Delta V_{ox}) + \frac{K_y}{K_x}\nu(\Delta V'_{ox} - \Delta V_{ox}) \tag{129}$$

where

$$C_1 = \frac{\Delta V}{2RK_x\Delta V_c}\ \frac{E}{1-\nu^2} \text{ or } C_1 = \frac{4}{2K_xV}\frac{E}{1-\nu^2} \tag{130}$$

$$C_2 = \frac{ZC_1K_x}{K_y}\ ; \qquad C_3 = \frac{K_x}{K_y}\ ;\ C_4 = \frac{K_y}{K_x}$$

Sample Calculation

Constants: $\Delta R = 0.12$ ohms, $R = 100$ ohms, $R_G = 120$ ohms

$K_y = 1.81$, $K_x = 1.95$, $E = 10.4 \times 10^6$ psi

$\nu = 0.33$

Then using (124)

$$C_1 = \frac{\Delta R\ E}{2RK_x \Delta V(1-\nu^2)} = \frac{0.12 \times 10.4 \times 10^6}{2x100x1.95x0.89} \frac{1}{\Delta V_c} = \frac{3600}{\Delta V_c} \qquad (131)$$

or using (125)

$$C_1 = \frac{4 \times E}{2V\ K_x(1-\nu^2)} = \frac{4 \times 10.4 \times 10^3}{2x\ 1.95 \times 0.89} \frac{1}{V} = \frac{12,000}{V} \qquad (132)$$

ΔV_c in millivolts, V in volts

$Z = 1/6\ t = 1/6\ 0.04^2 = 2.66 \times 10^{-4}$

$$C_2 = 2.66 \times 10^{-4} \frac{1.95}{1.81} \frac{3600}{\Delta V_c} = 1.033/\Delta V_c$$

$C_3 = 0.356$, $C_4 = 0.306$

A sample calculation of the reducing of data is shown in Table 2. The sample is taken from a test conducted on the prismatic shell simply supported with a uniform load on top. The total load was 100 lbs. or 0.416 lbs./sq. in. The stress and bending moment shown in Table 2, columns 9 and 12 respectively are due to a load of 1 lb./sq. in. which is obtained by dividing C_1 and C_2 by 0.416.

For this particular run $\Delta V = 1.785$ mv and $V = 5.952$ volts.

Then, from Equation (131),

$$C_1 = \frac{3600}{1.785} = 2018 \quad ; \qquad \text{from Equation (132), } C_1 = \frac{12,000}{5.952} = 2015$$

The constant C_1 obtained by introducing the calibration resistance in the switch panel c was then used in reducing the readings of the gages hooked up on both switch panels. Dividing by 0.416,

$$C_1' = C_1/0.416 = 4850, \quad C_2' = C \quad 0.416 = 1.394$$

In Table 2, $\sigma_x = C_1'$ x col. (8), $Y = C_2'$ x col. (11)

The test showed that $\Delta V'_{ox} - \Delta V_{ox}$ is very small and can be neglected in the calculation of Y. The gages on top and bottom in the longitudinal direction were then connected in series to limit the number of readings to be taken during the test.

1 Gage	2 ΔV	3 $\Delta V'_{ox}+\Delta V_{ox}$	4 $\Delta V'_{oy}+\Delta V_{oy}$	5 $\Delta V'_{ox}+\Delta V_{ox}$	6 $\Delta V'_{oy}-\Delta V_{oy}$	7 $C_3 x4$	8 3 + 7	9 $_x$(psi)	10 $5xC_4$	11 6+10	12 Y(in-lb)
1	-0.110	-0.216					-0.216	-1050			
1'	-0.106										
2	0.006		0		-0.012	0				-0.013	-0.018
2'	-0.006										
3	0.035	0.068		-0.002			0.068	320	-0.001		
3'	0.033										
4	0.221		-0.139		-0.581	-0.049				0.583	-0.812
4'	-0.360										
5	0.230	0.455		-0.005			0.406	1970	-0.002		
5'	0.225										
6	0.468		-0.297		-1.233	-0.106				-1.225	-1.710
6'	-0.765										
7	0.386	0.799		0.027			0.693	3360	0.008		
7'	0.413										
8	0.550		-0.059		-1.159	-0.021				-1.149	-1.600
8'	-0.609										
9	0.001	0.034		0.032			0.013	62	0.010		
9'	0.033										
10	0.410		0.177		-0.643	0.063				-0.623	-0.866
10'	-0.230										
11	-0.381	-0.695		0.067			-0.632	-3060	0.021		
11'	-0.314										
12	-1.649		0.113		3.411	0.040				3.401	4.750
12'	1.762										
13	-0.309	-0.651		-0.033			-0.611	-2980	-0.010		
13'	-0.342										

$_x$ = 4850xcol. (8)

Y = 1.394xcol. (11)

Sample Calculation

TABLE 2

C_3 = 0.356

C_4 = 0.306

V. EXPERIMENTAL RESULTS

5:1 Prismatic Shell Simply Supported, Model A, Uniform Load on Top

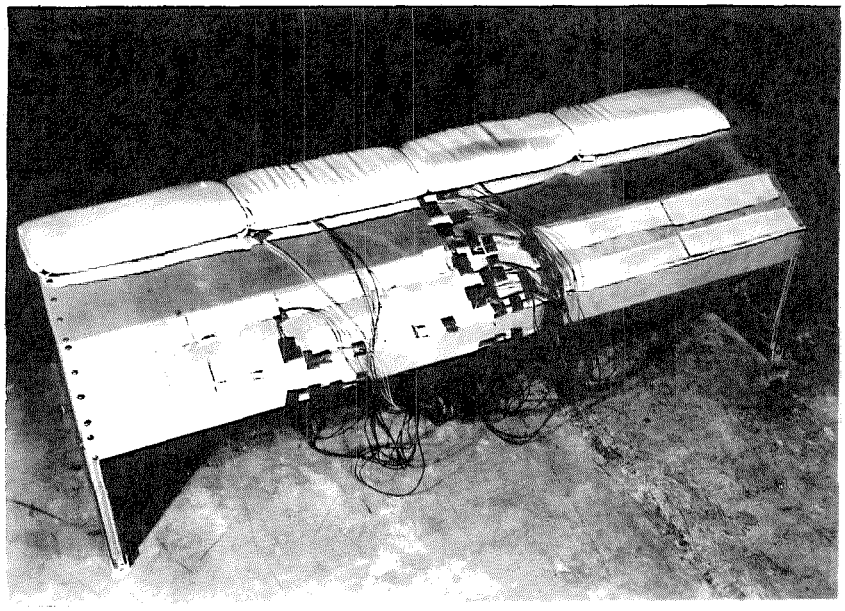

Total load 100 lbs., 0.416 lbs.-in.^{2}

Figure 39

Four 25-pound leadbags were used in loading the model as shown in Figure 39 above. Readings of the strain gage output were taken at zero load, full load and again at zero load. The results of 10 different loading cycles are shown in Tables 3, 4 and 5, and the average of these readings are plotted in Figures 40, 41 and 42. The theoretical calculations for this type of shell and loading are found in the Appendix.

TABLE 3

Prismatic Shell Simply Supported

Uniform Load on Top of Shell

Longitudinal Stress in a Section at Center of Span (psi.)

Test No.	Strain Gage Numbers						
	1	3	5	7	9	11	13
1	-1050	515	2040	3220	-138	-2840	-3120
2	- 980	386	2020	3330	-170	-2950	-3080
3	-1000	393	1960	3380	- 14	-3080	-2960
4	-1000	415	2020	3340	- 14	-3140	-3000
5	- 965	363	2080	3320	28	-3030	-2930
6	- 976	335	2050	3280	- 10	-3130	-2900
7	- 990	300	2020	3300	- 14	-3050	-2920
8	-1050	320	1970	3360	62	-3060	-2930
9	-1000	394	1980	3350	98	-3050	-2880
10	-1000	342	1990	3550	136	-3060	-2800
Average	-1000	376	2013	3343	-4	-3039	-2957

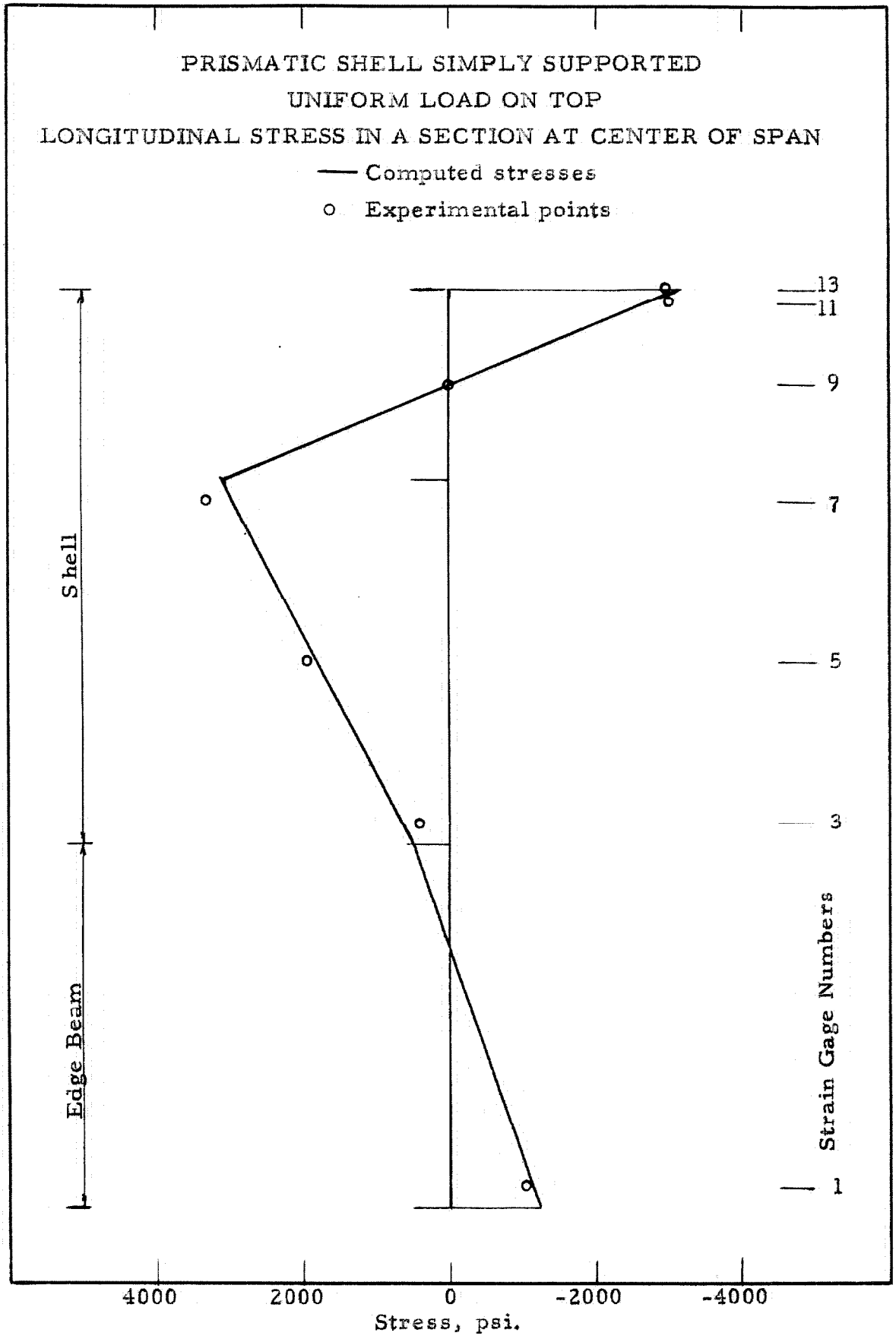
PRISMATIC SHELL SIMPLY SUPPORTED
UNIFORM LOAD ON TOP
LONGITUDINAL STRESS IN A SECTION AT CENTER OF SPAN
Computed stresses
Experimental points
Shell
Edge Beam
13
11
9
7
5
3
1
Strain Gage Numbers
4000
2000
0
-2000
-4000
Stress, psi.

Figure 40

TABLE 4

Prismatic Shell Simply Supported

Uniform Load on the Top

Cross-bending Moment at the Center of Span (in.-lbs.)

Test No.	Strain Gage Number					
	2	4	6	8	10	12
1	-0.027	-.0860	-1.870	-1.750	-0.945	5.420
2	-0.026	-0.850	-1.860	-1.700	-0.874	5.220
3	-0.031	-0.847	-1.845	-1.770	-1.040	5.330
4	-0.033	-0.840	-1.825	-1.680	-0.945	5.100
5	-0.026	-0.866	-1.840	-1.660	-0.736	5.330
6	-0.032	-0.850	-1.860	-1.680	-0.890	5.170
7	-0.026	-0.835	-1.835	-1.625	-0.835	5.420
8	-0.018	-0.583	-1.710	-1.600	-0.866	4.750
9	0.009	-0.790	-1.680	-1.620	-1.050	4.820
10	-0.009	-0.805	-1.710	-1.780	-1.180	5.400
Average	-0.021	-0.836	-1.803	-1.687	-0.936	5.196

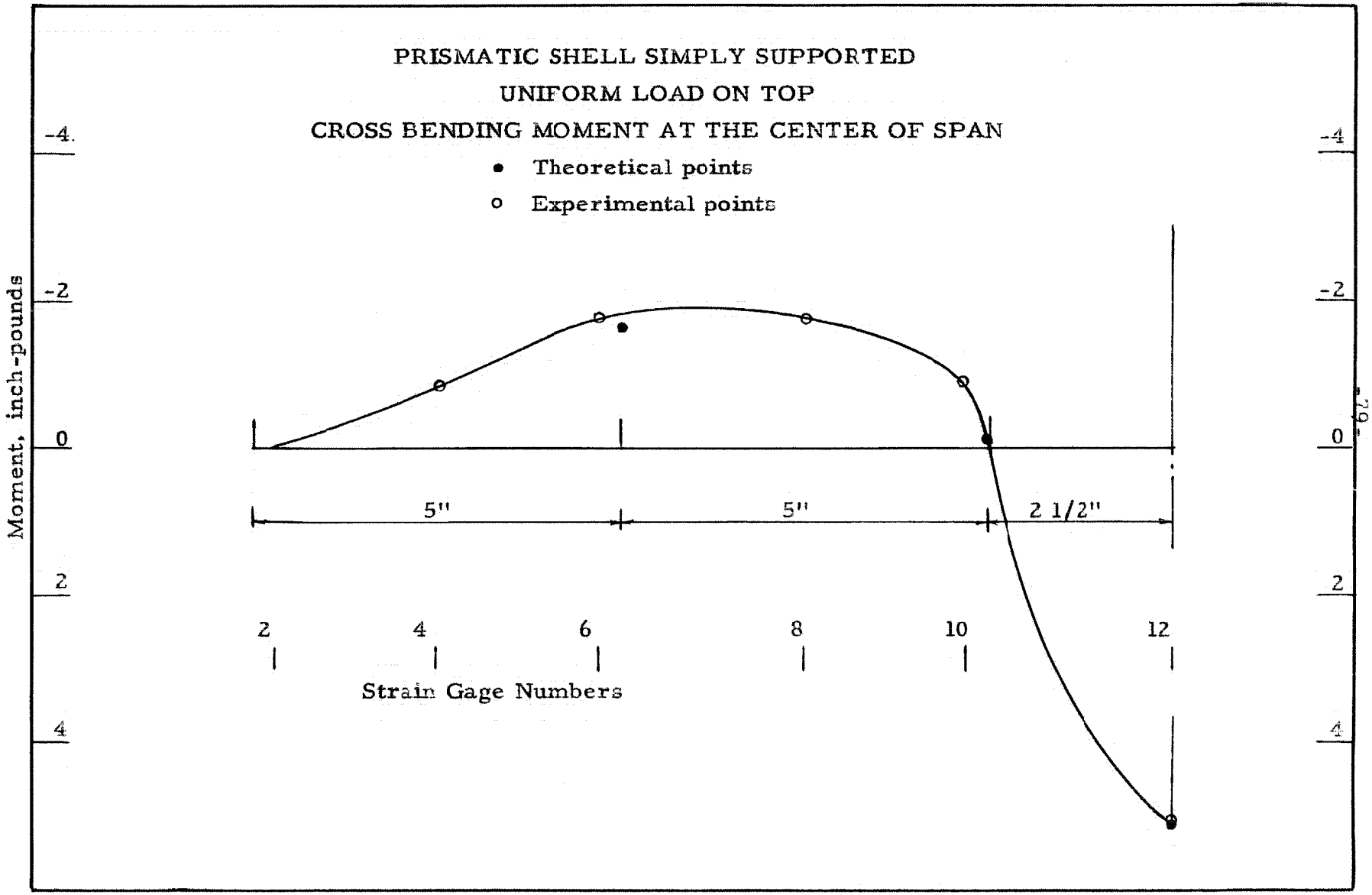
PRISMATIC SHELL SIMPLY SUPPORTED
UNIFORM LOAD ON TOP
CROSS BENDING MOMENT AT THE CENTER OF SPAN
• Theoretical points
o Experimental points
Moment, inch-pounds
-4
-2
0
2
4
5"
5"
2 1/2"
2
4
6
8
10
12
Strain Gage Numbers

Figure 41

TABLE 5

Prismatic Shell Simply Supported

Uniform Load on the Top

Longitudinal Stress at the Quarter Point (psi.)

Test No.	Strain Gage No.		
	19	17	15
1	-703	123	-2370
2	-770	147	-2450
3	-780	180	-2890
4	-713	153	-2460
5	-770	110	-2400
6	-760	90	-2410
7	-800	100	-2450
8	-740	85	-2290
9	-740	71	-2410
10	-780	180	-2770
Average	-756	124	-2490

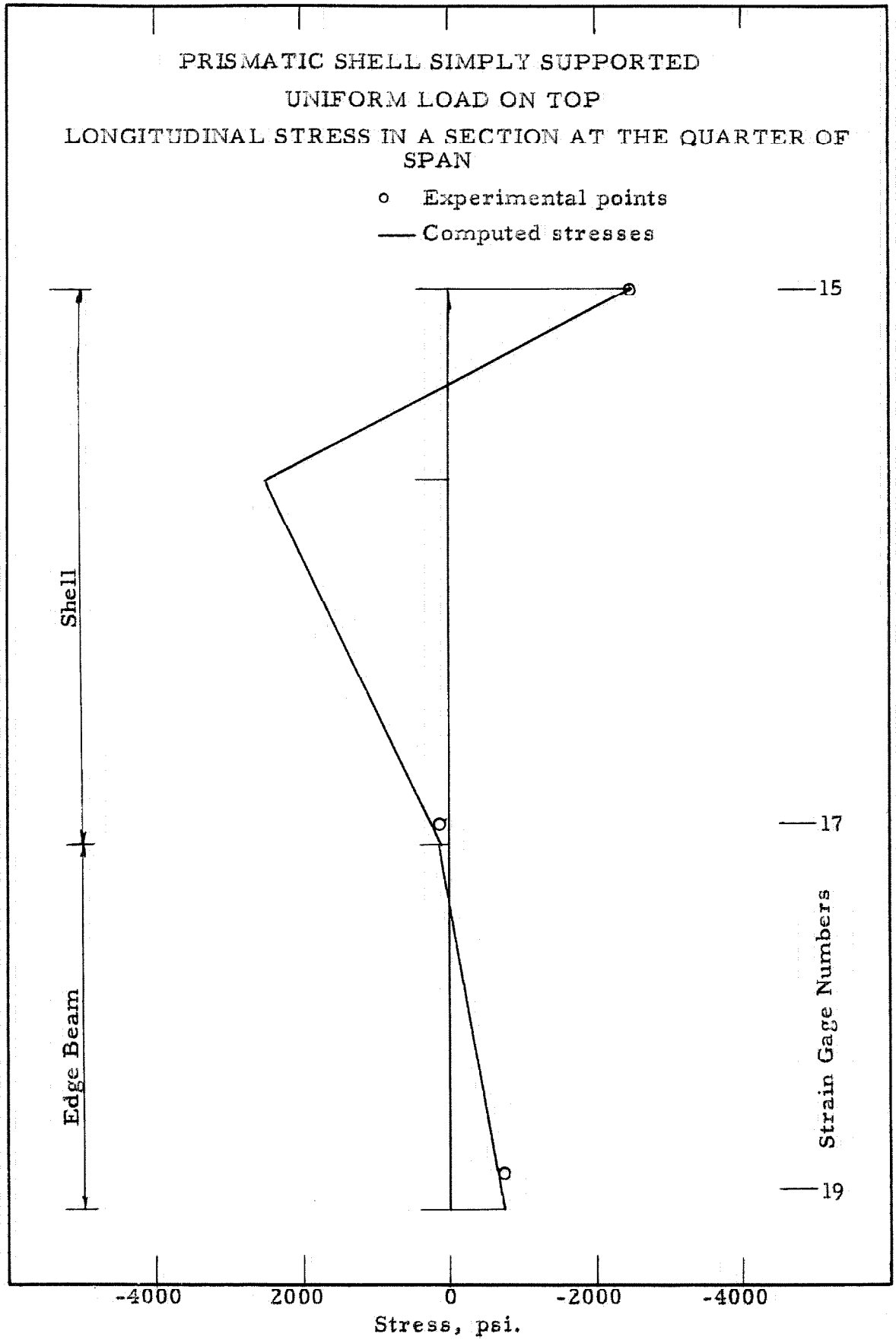
PRISMATIC SHELL SIMPLY SUPPORTED
UNIFORM LOAD ON TOP
LONGITUDINAL STRESS IN A SECTION AT THE QUARTER OF SPAN
o Experimental points
— Computed stresses
Shell
Edge Beam
15
17
19
Strain Gage Numbers
-4000
2000
0
-2000
-4000
Stress, psi.

Figure 42

5:2 Prismatic Shell Simply Supported, Model A, Uniform Load

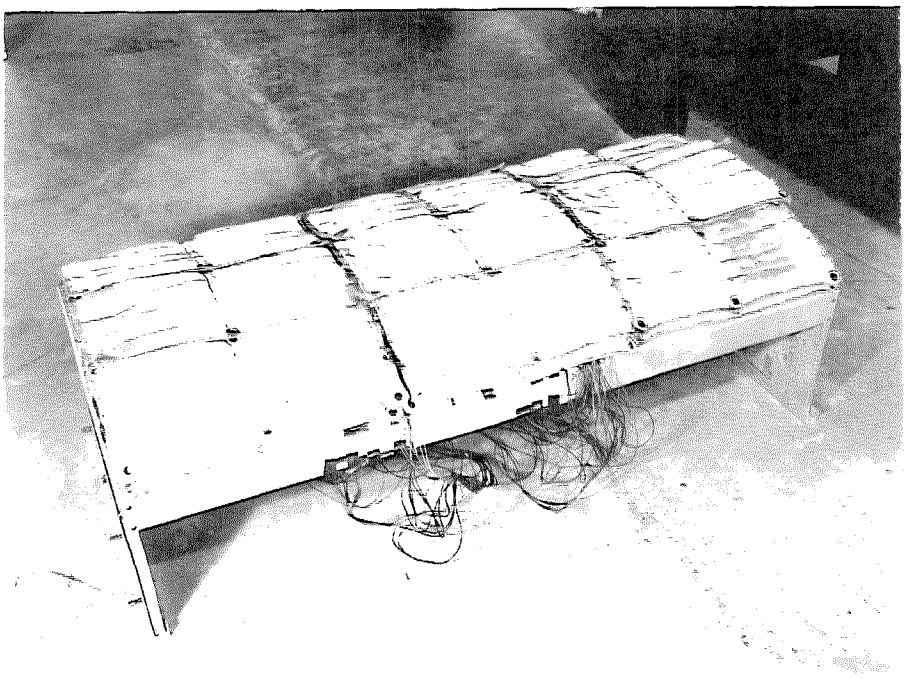

Total load 240 lbs., 0.200 lbs./in.

Figure 43

Twenty-four 10-pound leadbags were used in the loading of the model as shown in Figure 43 above. Readings of the strain gage output were taken at zero, full load and again at zero load. The results of 5 different loading cycles are shown in Tables 6, 7 and 8, and the average of these readings is plotted in Figures 44, 45 and 46. The theoretical calculation for this type of shell and loading is found in the Appendix.

TABLE 6

Prismatic Shell Simply Supported

Uniform Load

Longitudinal Stress in a Section at Center of Span (psi.)

Test No.	Strain Gage Number						
	1	3	5	7	9	11	13
1	5000	6160	830	-4730	-3120	-1800	-1550
2	4900	6900	290	-5100	-3500	-1690	-1690
3	5150	5830	690	-4680	-3040	-1640	-1710
4	5240	6470	730	-4810	-3130	-1710	-1710
5	4900	6670	805	-4660	-2850	-1740	-1750
Average	5040	6408	769	-4796	-3128	-1716	-1682

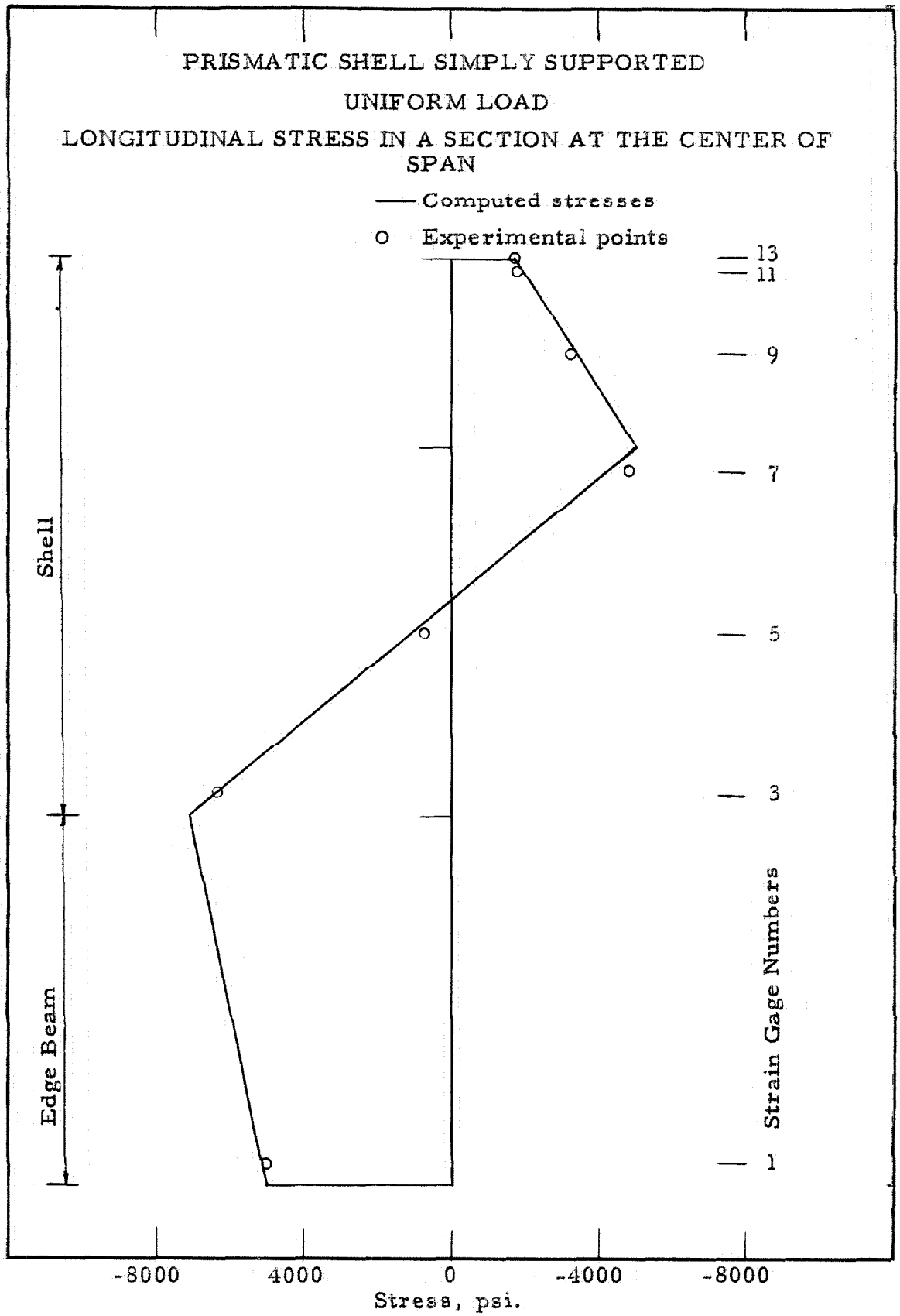
PRISMATIC SHELL SIMPLY SUPPORTED
UNIFORM LOAD
LONGITUDINAL STRESS IN A SECTION AT THE CENTER OF SPAN
Computed stresses
Experimental points
13
11
9
7
5
3
1
Strain Gage Numbers
Shell
Edge Beam
-8000
4000
0
-4000
-8000
Stress, psi.

Figure 44

TABLE 7

Prismatic Shell Simply Supported

Uniform Load

Cross-bending Moment at the Center of Span (in.- lbs.)

Test No.	Strain Gage Number					
	2	4	6	8	10	12
1	0.053	3.620	1.860	1.540	-2.900	-1.020
2	-0.096	3.350	1.520	1.590	-3.250	-0.635
3	-0.067	3.900	1.670	1.350	-3.200	-0.560
4	-0.030	3.370	1.430	2.050	-3.500	-0.734
5	-0.070	3.400	1.400	1.580	-3.850	-0.576
Average	-0.040	3.520	1.580	1.620	-3.340	-0.705

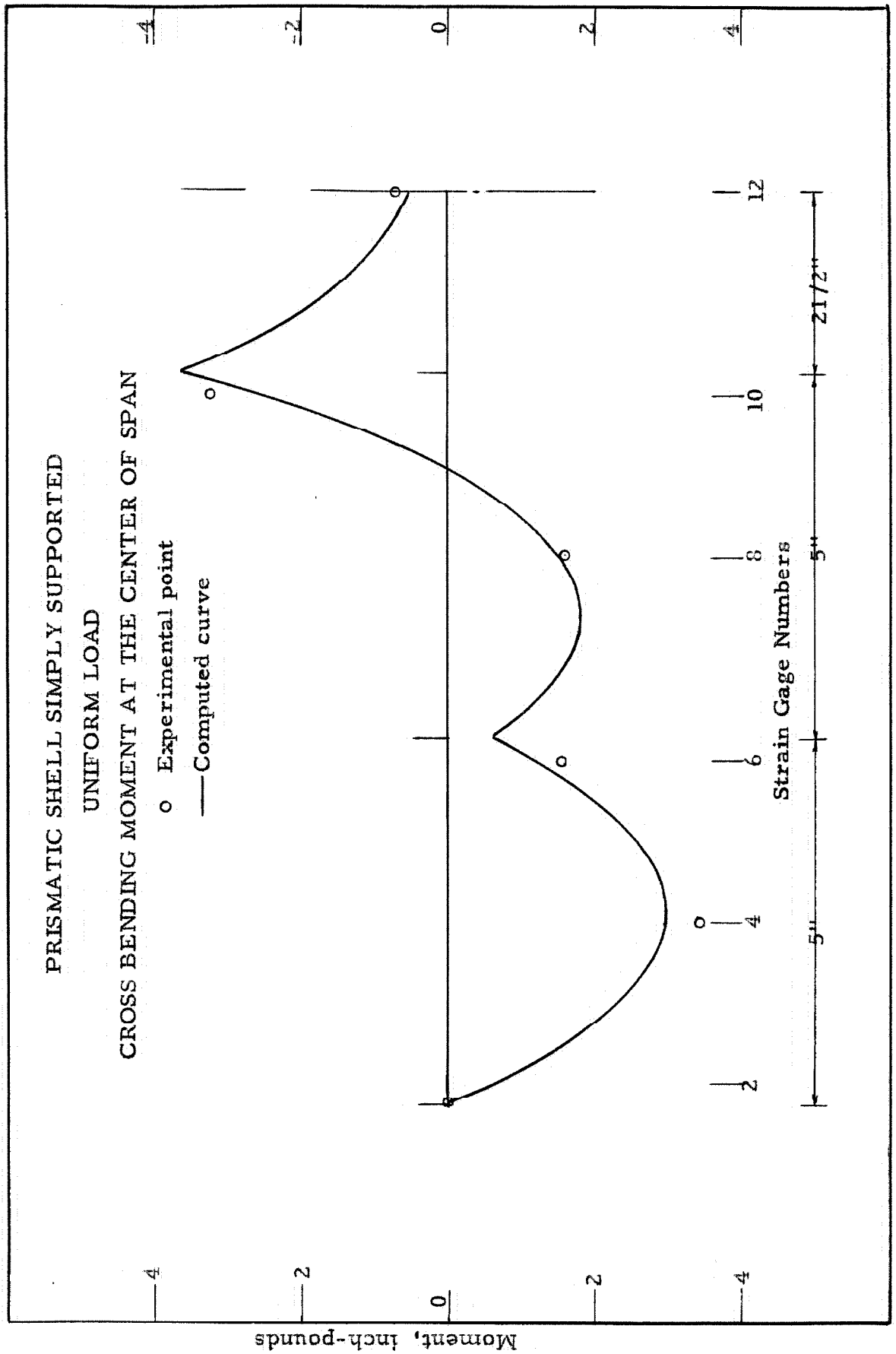
PRISMATIC SHELL SIMPLY SUPPORTED
UNIFORM LOAD
CROSS BENDING MOMENT AT THE CENTER OF SPAN
o Experimental point
—Computed curve
Moment, inch-pounds
-4
-2
0
2
4
Strain Gage Numbers
2
4
6
8
10
12
5"
5"
2 1/2"

Figure 45

TABLE 8

Prismatic Shell Simply Supported

Uniform Load

Longitudinal Stress at the Quarter Point (psi.)

Test No.	Strain Gage No.		
	19	17	15
1	3840	4590	-1045
2	3760	4650	- 820
3	3810	4820	- 780
4	3750	4800	- 965
5	3630	4640	- 976
Average	3758	4700	- 917

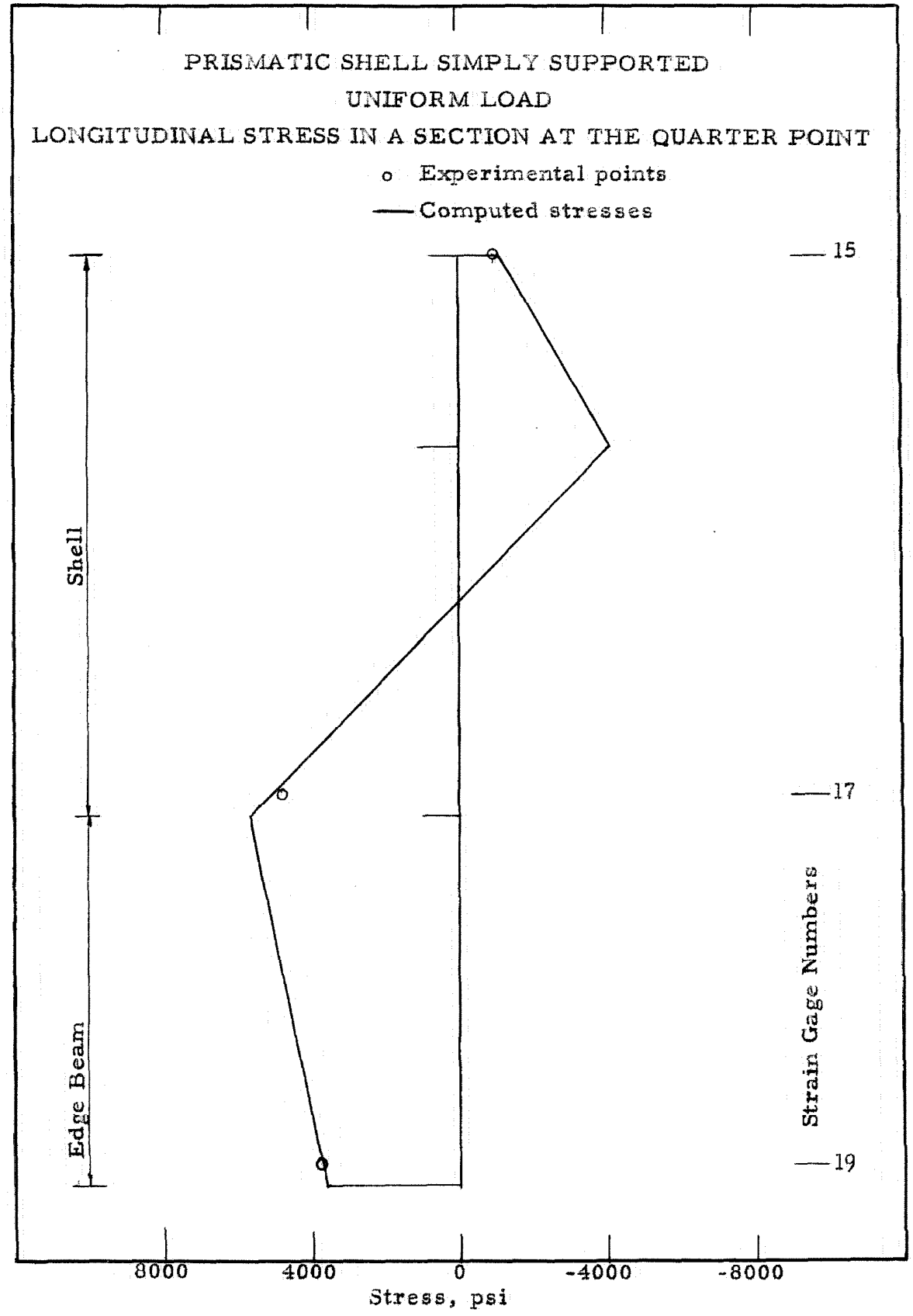
PRISMATIC SHELL SIMPLY SUPPORTED
UNIFORM LOAD
LONGITUDINAL STRESS IN A SECTION AT THE QUARTER POINT
o Experimental points
— Computed stresses
Shell
Edge Beam
15
17
19
Strain Gage Numbers
8000
4000
0
-4000
-8000
Stress, psi

Figure 46

5:3 Prismatic Shell, One End Fixed, the Other Simply Supported, Model B, Uniform Load on Top

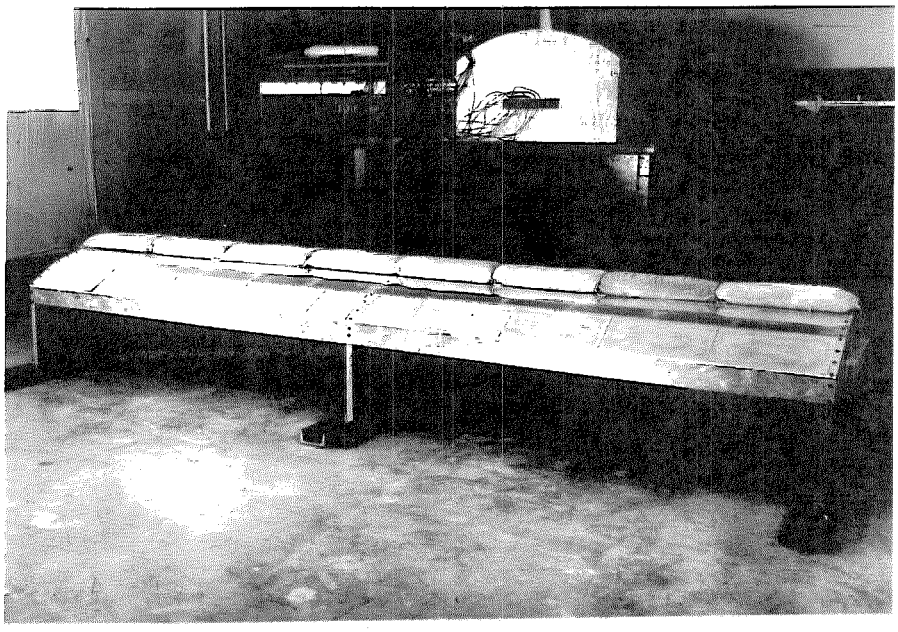

Total load in each span 100 lbs., 0.416 lbs./in.^{2}

Figure 47

Eight 25-pound leadbags, four on each span, were used in loading the model as shown in Figure 47 above. Readings of the strain gage output were taken at zero load, full load and again at zero load. The results of 10 different loading cycles are shown in Tables 9, 10, 11 and 12, and the average of the 10 readings is plotted in Figures 48, 49, 50 and 51. The theoretical calculation for this type of shell and loading is found in the Appendix.

TABLE 9

Prismatic Shell, One End Fixed, the Other Simply Supported

Uniform Load on the Top

Variation of Longitudinal Stress Along Span at the Crown (psi.)

Test No.	Strain Gage Number					
	1	3	5	7	9	11
1	-1270	-2520	-2260	-1200	1320	3600
2	-1200	-2580	-1820	- 960	1300	3730
3	-1220	-2560	-1800	-1080	1260	3760
4	-1180	-2650	-1830	-1010	1260	3730
5	-1380	-2570	-1940	-1190	1330	3720
6	-1150	-2410	-2140	-1100	1340	3800
7	-1170	-2440	-2080	-1040	1530	3820
8	-1140	-2360	-2070	-1050	1560	3860
9	-1070	-2330	-2120	- 880	1490	3800
10	-1210	-2420	-2140	- 940	1510	3860
Average	-1200	-2480	-2020	-1045	1390	3768

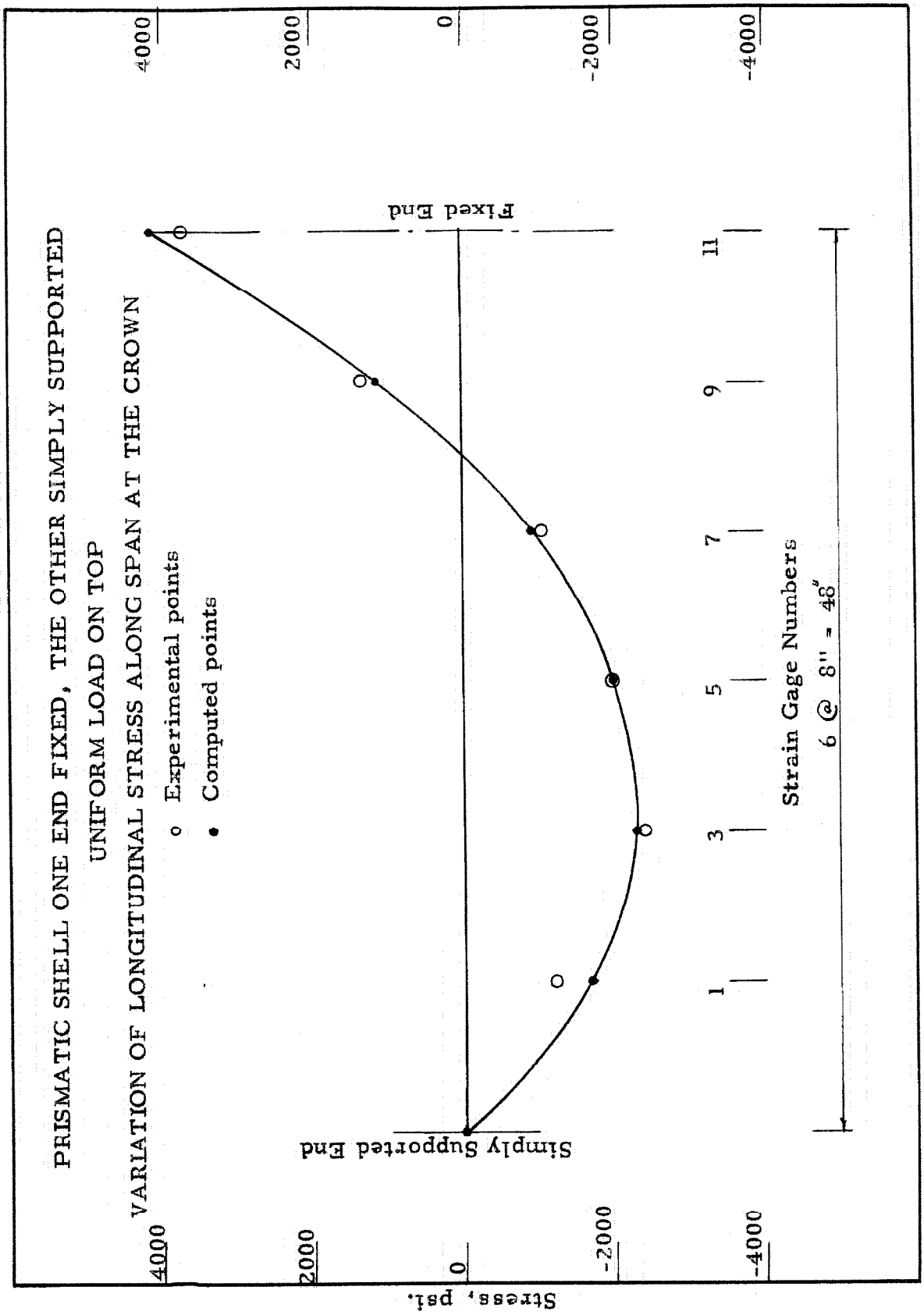
PRISMATIC SHELL ONE END FIXED, THE OTHER SIMPLY SUPPORTED
UNIFORM LOAD ON TOP
VARIATION OF LONGITUDINAL STRESS ALONG SPAN AT THE CROWN
o Experimental points
• Computed points
Stress, psi.
4000
2000
0
-2000
-4000
Simply Supported End
Fixed End
1
3
5
7
9
11
Strain Gage Numbers
6 @ 8" = 48"

Figure 48

TABLE 10

Prismatic Shell, One End Fixed, the Other Simply Supported

Uniform Load on the Top

Variation of Cross Bending Moment Along the Span at

the Crown (in.-lbs.)

Test No.	Strain Gage Number					
	2	4	6	8	10	12
1	3.680	3.900	4.260	3.600	2.870	0.585
2	3.930	3.400	4.270	3.680	2.650	0.558
3	3.870	3.620	4.030	3.630	2.720	0.573
4	3.780	3.900	4.160	3.810	2.680	0.558
5	3.730	4.150	4.090	3.640	2.880	0.572
6	3.800	4.240	3.960	3.640	3.200	0.530
7	3.850	4.050	3.770	3.560	3.160	0.536
8	3.960	4.230	4.020	3.740	3.250	0.534
9	3.860	4.060	3.810	3.780	3.080	0.546
10	4.040	4.230	3.790	3.800	3.040	0.550
Average	3.850	3.980	4.020	3.690	2.950	0.550

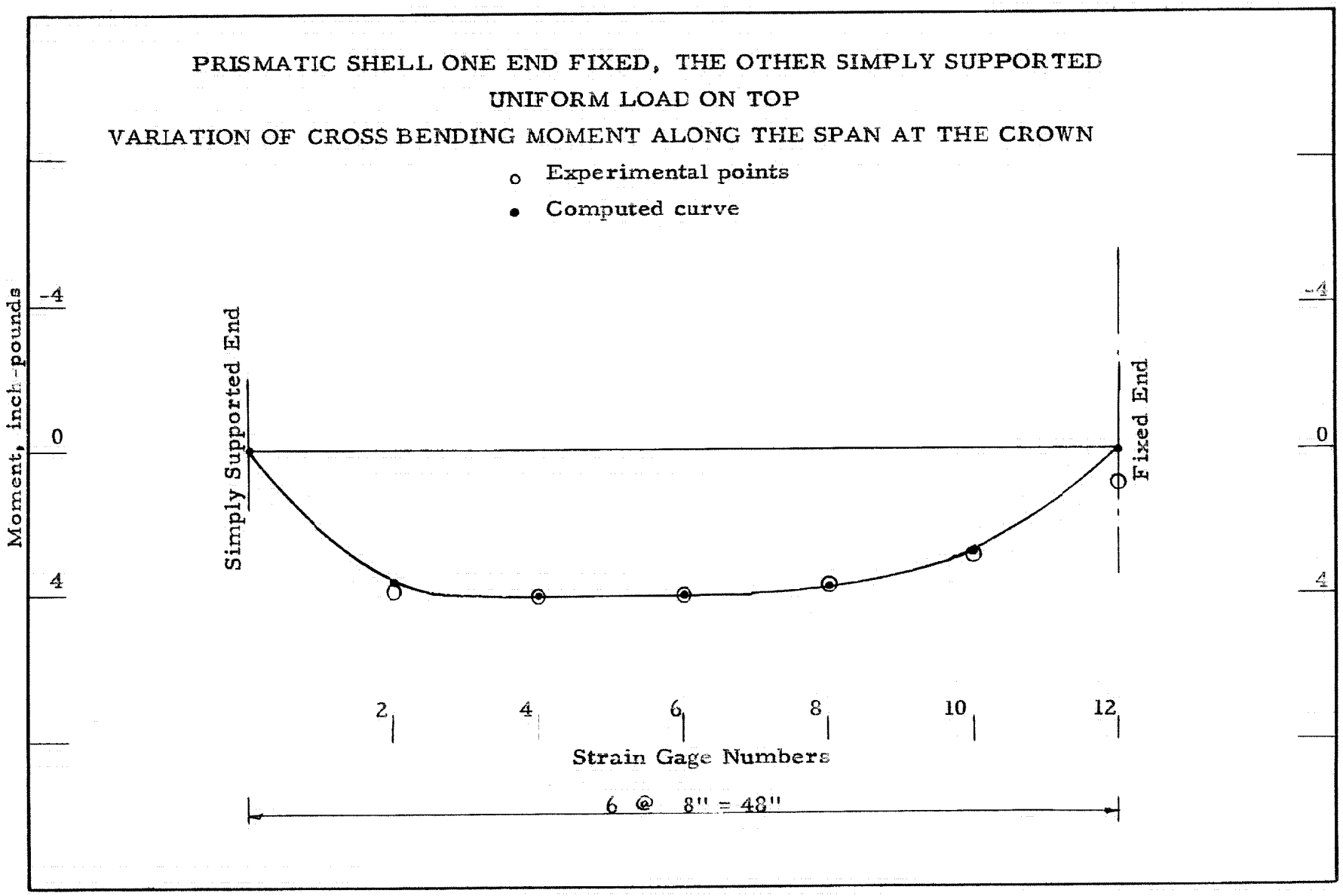
PRISMATIC SHELL ONE END FIXED, THE OTHER SIMPLY SUPPORTED
UNIFORM LOAD ON TOP
VARIATION OF CROSS BENDING MOMENT ALONG THE SPAN AT THE CROWN
o Experimental points
• Computed curve
Moment, inch-pounds
-4
0
4
Simply Supported End
Fixed End
2
4
6
8
10
12
Strain Gage Numbers
6 @ 8" = 48"

Figure 49

TABLE 11

Prismatic Shell, One End Fixed, the Other Simply Supported

Uniform Load on the Top

Longitudinal Stress in a Section at the Third Point (psi.)

Test No.	Strain Gage No.		
	3	13	15
1	-2520	2490	-542
2	-2580	2470	-625
3	-2560	2460	-635
4	-2650	2430	-606
5	-2570	2440	-695
6	-2410	2460	-625
7	-2440	2480	-690
8	-2360	2520	-600
9	-2330	2500	-583
10	-2420	2670	-616
Average	-2480	2492	-622

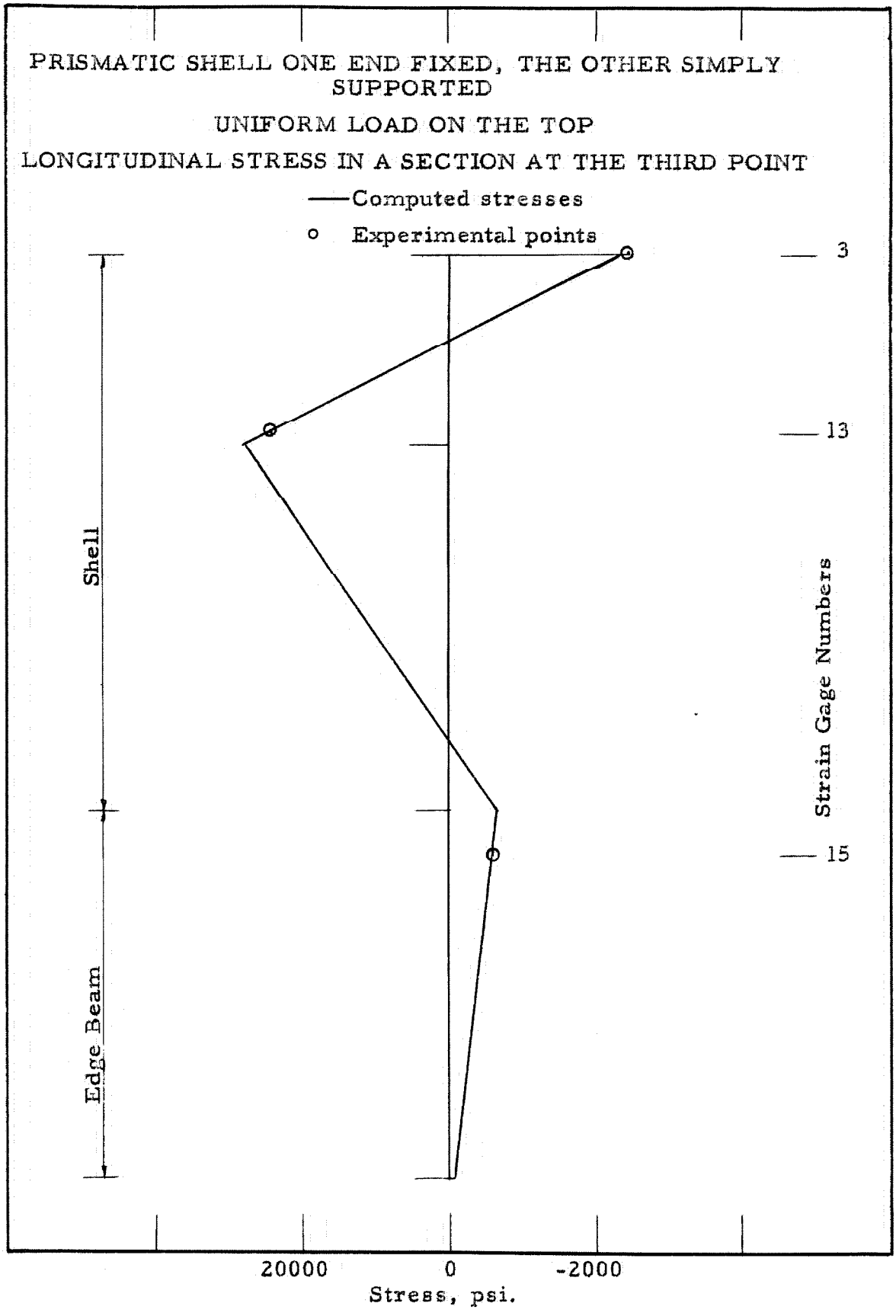
PRISMATIC SHELL ONE END FIXED, THE OTHER SIMPLY SUPPORTED
UNIFORM LOAD ON THE TOP
LONGITUDINAL STRESS IN A SECTION AT THE THIRD POINT
—Computed stresses
o Experimental points
3
13
15
Strain Gage Numbers
Shell
Edge Beam
20000
0
-2000
Stress, psi.

Figure 50

TABLE 12

Prismatic Shell, One End Fixed, the Other Simply Supported

Uniform Load on the Top

Cross Bending Moment at the Third Point (in.-lbs.)

Test No.	Strain Gage No.		
	4	14	16
1	3.900	-1.210	0.028
2	3.400	-1.070	0.031
3	3.620	-1.170	0.035
4	3.900	-1.180	-0.032
5	4.150	-1.120	0.027
6	4.240	-1.060	0.025
7	4.050	-1.100	0.024
8	4.230	1.190	0.021
9	4.060	-1.160	0.025
10	4.230	-1.110	0.027
Average	3.980	-1.140	0.028

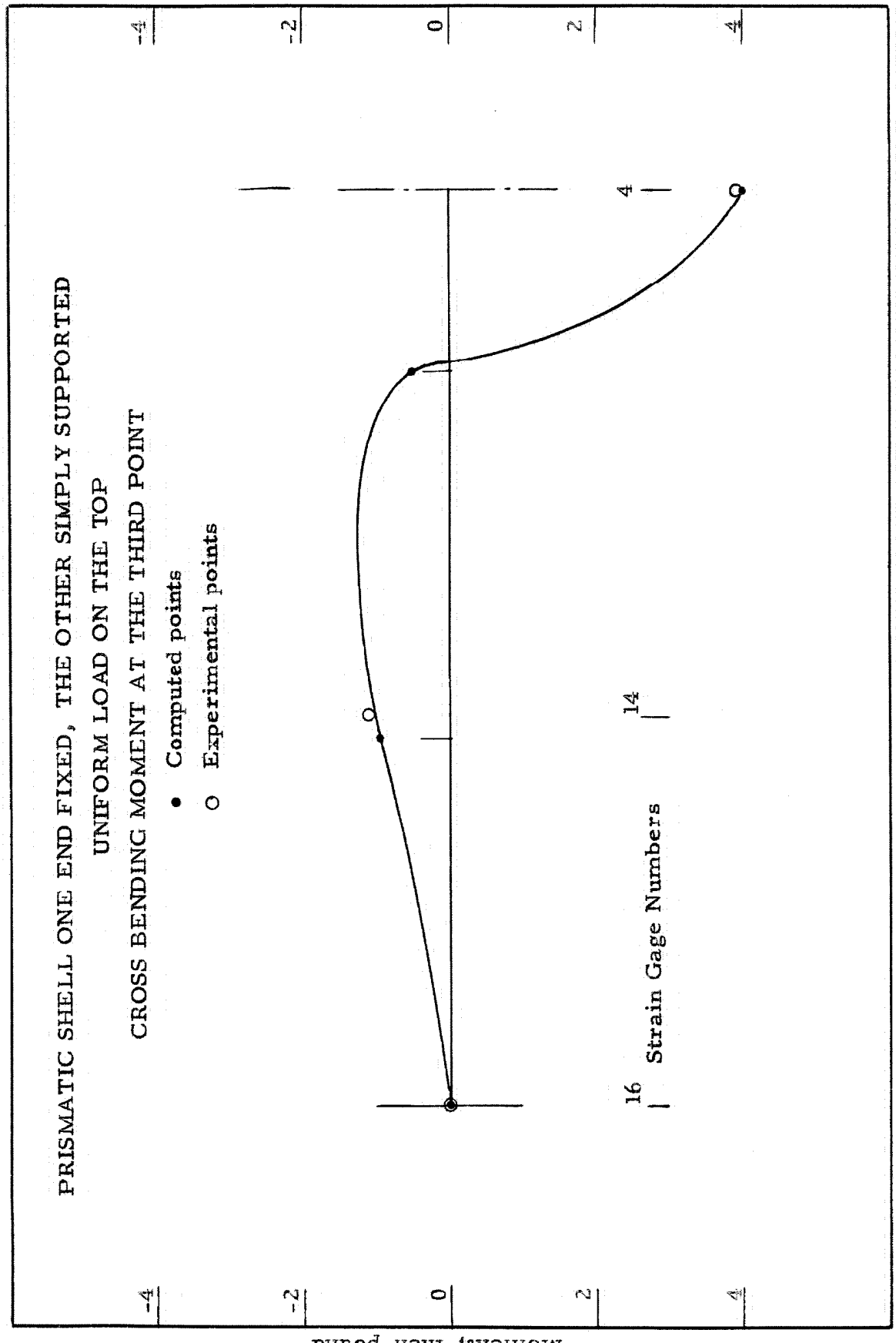
PRISMATIC SHELL ONE END FIXED, THE OTHER SIMPLY SUPPORTED
UNIFORM LOAD ON THE TOP
CROSS BENDING MOMENT AT THE THIRD POINT
• Computed points
O Experimental points
Moment, inch-pound
-4
-2
0
2
4
16
14
Strain Gage Numbers

Figure 51

5:4 Prismatic Shell, One End Fixed, the Other Simply Supported, Model B, Uniform Load

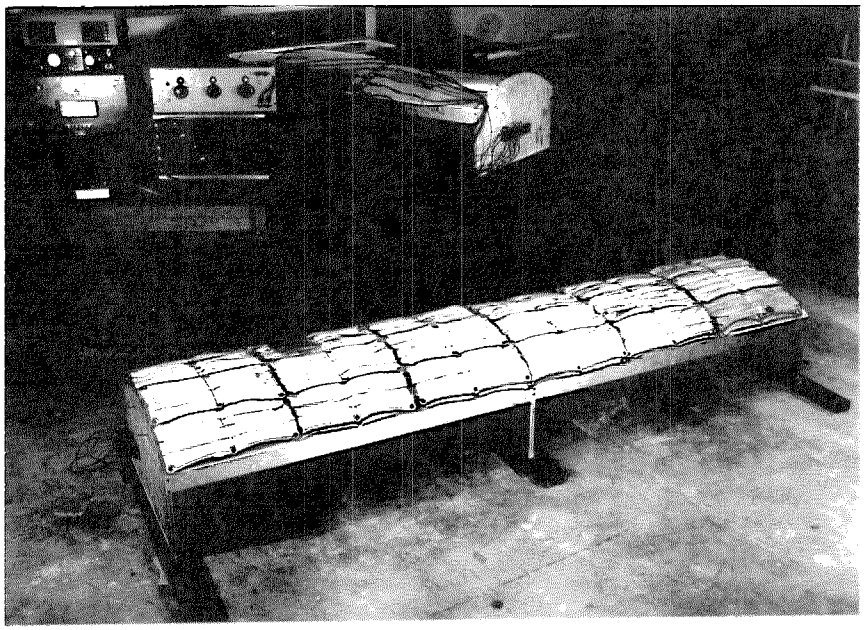

Total load on each span 240 lbs., 0.200 lbs./in.

Figure 52

Forty-eight 10-pound leadbags, twenty-four on each span, were used in loading the models as shown in Figure 52 above. Readings of the strain gage output were taken at zero load, full load and again at zero load. The results of 10 different loading cycles are shown in Tables 13, 14 and 16, and the average of the 10 readings is plotted in Figures 53 and 54. The theoretical calculation for this type of shell and loading is found in the Appendix.

TABLE 13

Prismatic Shell, One End Fixed, the Other Simply Supported

Uniform Load

Variation of Longitudinal Stress along the Span at the Crown (psi.)

Test No.	Strain Gage Numbers					
	1	3	5	7	9	11
1	- 69	- 60	-109	198	-307	-990
2	-248	50	-258	- 50	-376	-840
3	-396	- 89	- 99	-139	- 60	-585
4	-315	123	-288	50	-163	-615
5	-188	278	139	198	-168	-515
6	50	- 40	-168	129	- 60	-645
7	- 60	198	89	99	-178	-625
8	- 70	160	- 20	110	-170	-763
9	35	77	-250	- 19	- 45	-340
10	-346	- 6	-260	- 5	-105	-765
Average	-161	69	-122	- 57	-163	-688

Note: Results not shown graphically

TABLE 14

Prismatic Shell, One End Fixed, the Other Simply Supported

Uniform Load

Variation of Cross Bending Moment Along the Span at the Crown (in.-lbs.)

Test No.	Strain Gage Number					
	2	4	6	8	10	12
1	0.600	-0.179	-0.045	-0.090	0.414	0.302
2	0.317	-0.565	-0.013	-0.264	1.0 0	0.275
3	0.830	-0.230	-0.410	0.260	0.910	0.435
4	0.550	-0.466	-0.243	0.260	0.940	0.347
5	0.522	-0.685	-0.486	-0.013	1.140	0.341
6	0.940	-0.174	-0.105	-0.139	1.060	0.300
7	0.179	-0.592	-0.740	0.139	1.010	0.437
8	0.290	-0.490	-0.096	0.230	0.975	0.360
9	0.267	-0.398	0.069	0.020	1.050	0.450
10	0.540	-0.427	-0.021	-0.140	0.780	0.330
Average	0.500	-0.415	-0.210	0.026	0.929	0.358

PRISMATIC SHELL ONE END FIXED, THE OTHER SIMPLY SUPPORTED

UNIFORM LOAD

VARIATION OF CROSS BENDING MOMENT ALONG THE SPAN AT THE CROWN

o Experimental points

• Computed points

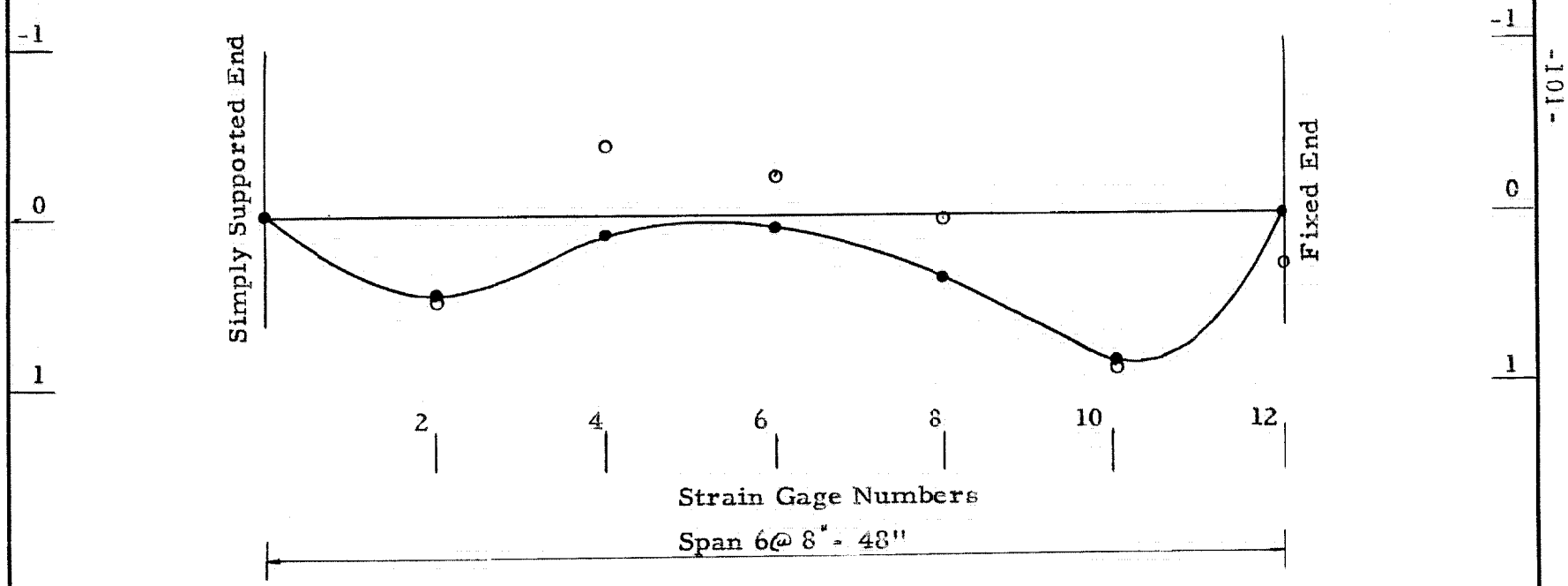

Figure 53

TABLE 15

Prismatic Shell, One End Fixed, the Other Simply Supported

Uniform Load

Longitudinal Stress in a Section at the Third Point (psi.)

Test No.	Strain Gage No.		
	3	13	15
1	- 60	-4150	4760
2	50	-4030	4920
3	- 89	-3810	4820
4	123	-3810	4760
5	278	-3880	4760
6	- 40	-3720	4720
7	198	-3760	4760
8	160	-3940	4700
9	77	-3640	4700
10	- 6	-3650	4660
Average	69	-3839	4665

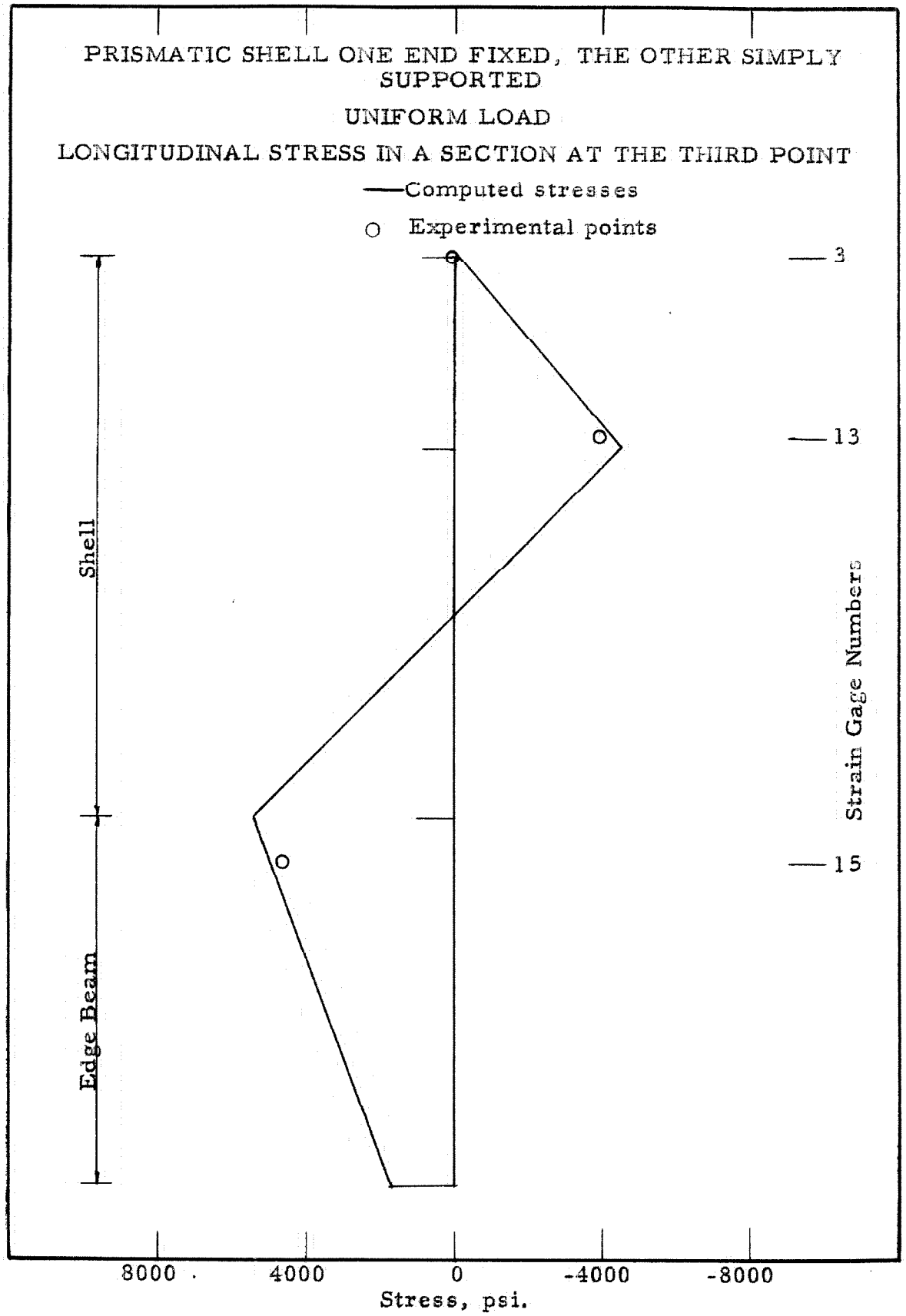
PRISMATIC SHELL ONE END FIXED, THE OTHER SIMPLY SUPPORTED
UNIFORM LOAD
LONGITUDINAL STRESS IN A SECTION AT THE THIRD POINT
—Computed stresses
○ Experimental points
Shell
Edge Beam
3
13
15
Strain Gage Numbers
8000
4000
0
-4000
-8000
Stress, psi.

Figure 54

5:5 Cylindrical Shell Simply Supported, Model C, Uniform Load on Top

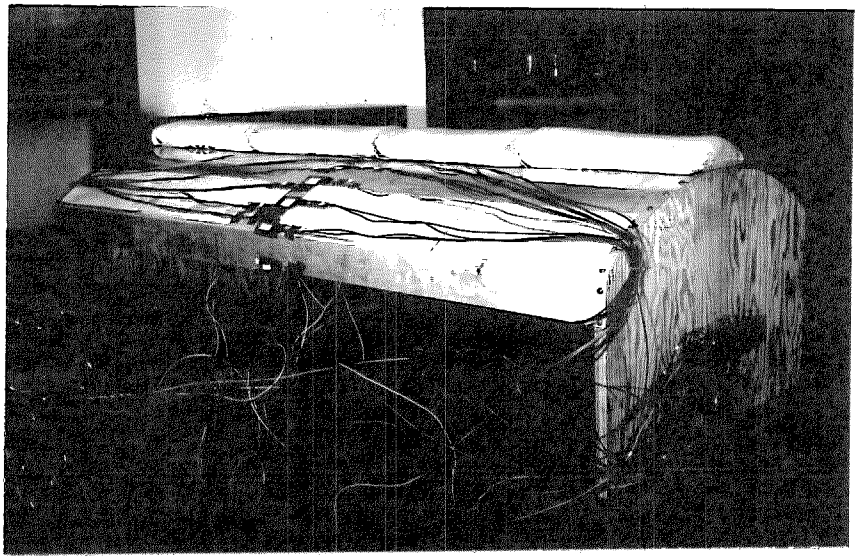

Total load 100 lbs., 0.416 lbs./in.

Figure 55

Four 25-pound leadbags were used in loading the model as shown in Figure 55 above. Readings of the strain gage output were taken at zero load, full load and again at zero load. The results of 10 different loading cycles are shown in Tables 16 and 17 and the average of the 10 readings is plotted in Figures 56 and 57. The theoretical calculation for this type of shell and loading is found in the Appendix.

TABLE 16

Cylindrical Shell Simply Supported

Uniform Load on Top

Longitudinal Stress in a Section at the Center of Span (psi.)

Test No.	Strain Gage Number						
	1	3	5	7	9	11	13
1	-870	- 53	2440	3000	287	-3020	-4100
2	-662	-200	2440	2940	400	-3050	-4230
3	-810	- 78	2410	2920	151	-3200	-4070
4	-640	- 55	2410	2920	270	-3020	-4060
5	-660	- 28	2360	2850	300	-3010	-4150
6	-716	-130	2340	2920	290	-3050	-4200
7	-680	- 23	2470	2920	386	-2990	-4070
8	-670	- 37	2480	2970	206	-3150	-4150
9	-654	- 41	2360	2900	358	-2920	-3980
10	-670	- 46	2350	2860	430	-2780	-3980
Average	-703	- 69	2406	2920	308	-3020	-4100

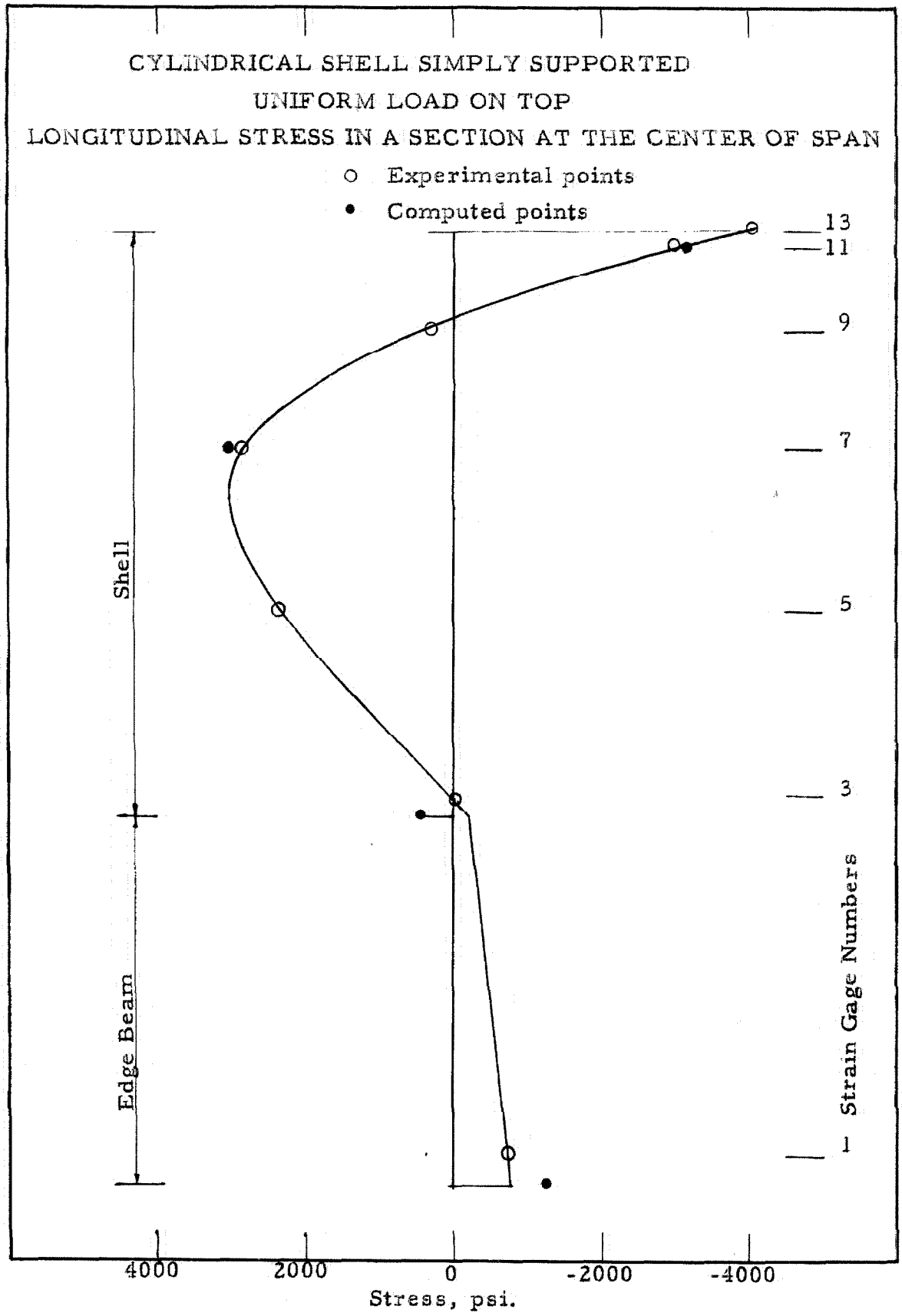
CYLINDRICAL SHELL SIMPLY SUPPORTED
UNIFORM LOAD ON TOP
LONGITUDINAL STRESS IN A SECTION AT THE CENTER OF SPAN
Experimental points
Computed points
Shell
Edge Beam
13
11
9
7
5
3
1
Strain Gage Numbers
4000
2000
0
-2000
-4000
Stress, psi.

Figure 56

TABLE 17

Cylindrical Shell Simply Supported

Uniform Load on Top

Cross Bending Moment at the Center of Span (in. -lbs.)

Test No.	Strain Gage Number					
	2	4	6	8	10	12
1	-0.013	-0.885	-2.170	-2.240	1.100	4.500
2	0.017	-0.830	-2.120	-2.305	0.851	4.550
3	-0.011	-0.845	-2.170	-2.300	1.255	4.400
4	-0.011	-0.836	-2.140	-2.260	1.080	4.390
5	-0.021	-0.852	-2.110	-2.220	0.900	4.480
6	-0.013	-0.832	-2.125	-2.270	0.955	4.520
7	-0.018	-0.855	-2.130	-2.230	1.065	4.420
8	-0.016	-0.865	-2.200	-2.280	1.290	4.450
9	-0.018	-0.820	-2.050	-2.180	1.015	4.250
10	-0.011	-0.825	-2.040	-2.150	0.870	4.370
Average	-0.012	-0.845	-2.126	-2.244	1.038	4.433

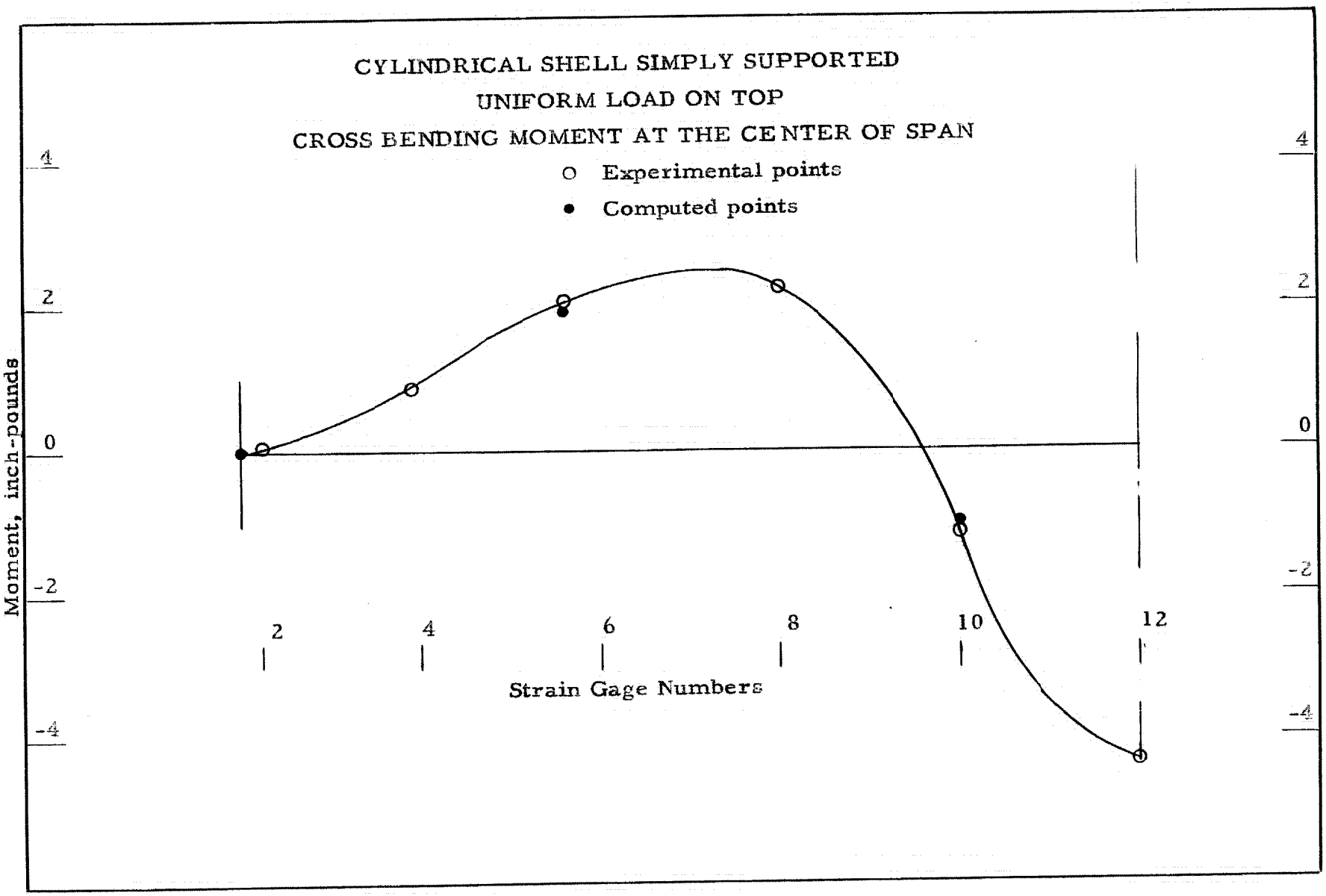
CYLINDRICAL SHELL SIMPLY SUPPORTED
UNIFORM LOAD ON TOP
CROSS BENDING MOMENT AT THE CENTER OF SPAN
o Experimental points
• Computed points
Moment, inch-pounds
4
2
0
-2
-4
2
4
6
8
10
12
Strain Gage Numbers

Figure 57

5:6 Cylindrical Shell Simply Supported, Model C, Uniform Load

Total load 240 lbs., 0.200 lbs./in.

Figure 58

Twenty-four 10-pound leadbags were used in loading the model as shown in Figure 58 above. Readings of the strain gage output were taken at zero, full load and again at zero load. The results of 5 different loading cycles are shown in Tables 18 and 19 and the average of the 10 readings plotted in Figures 59 and 60. The theoretical calculation for this type of shell and loading is found in the Appendix.

TABLE 18

Cylindrical Shell Simply Supported

Uniform Load

Longitudinal Stress in a Section at the Center of Span (psi.)

Test No.	Strain Gage Number						
	1	3	5	7	9	11	13
1	4430	7560	- 48	-4600	-4630	-2500	-1380
2	5060	7530	210	-4230	-3940	-1560	- 735
3	4980	7640	160	-4400	-4470	-1535	- 316
4	5330	7760	530	-3890	-4170	-1470	- 290
5	5630	6600	-212	-4150	-4220	-1930	- 895
Average	5080	7418	130	-4254	-4286	-1799	- 723

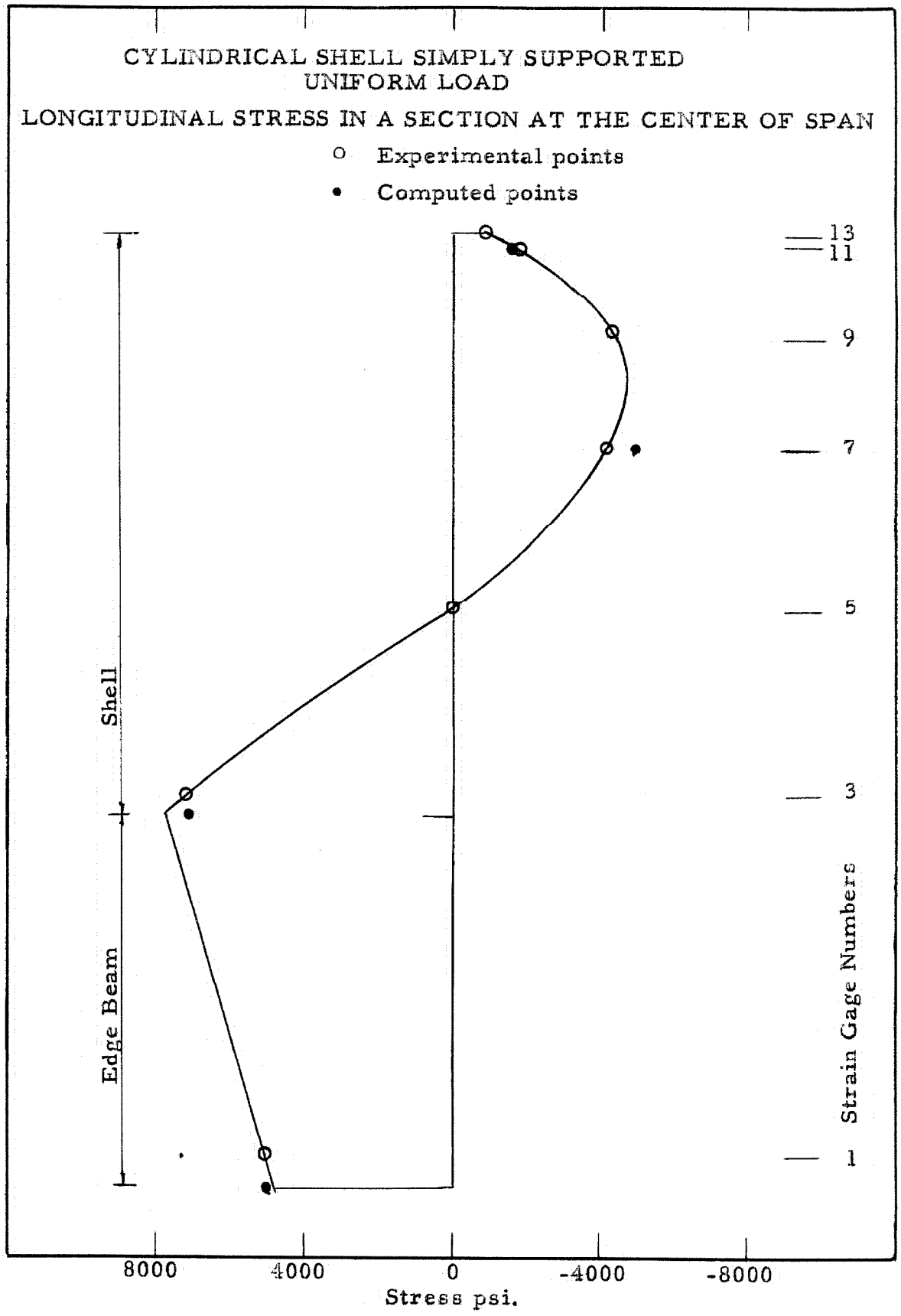
CYLINDRICAL SHELL SIMPLY SUPPORTED
UNIFORM LOAD
LONGITUDINAL STRESS IN A SECTION AT THE CENTER OF SPAN
Experimental points
Computed points
Shell
Edge Beam
13
11
9
7
5
3
1
Strain Gage Numbers
8000
4000
0
-4000
-8000
Stress psi.

Figure 59

TABLE 19

Cylindrical Shell Simply Supported

Uniform Load

Cross Bending Moment at the Center of Span (in.-lbs.)

Test No.	Strain Gage Number					
	2	4	6	8	10	12
1	-0.023	3.620	3.880	0.950	-2.135	-2.850
2	0.036	3.900	3.580	0.875	-2.290	-2.640
3	0.053	3.840	4.000	1.060	-2.420	-2.770
4	0.138	3.440	3.580	1.092	-1.900	-2.670
5	0.131	3.380	3.270	0.886	-1.940	-2.520
Average	0.067	3.636	3.662	0.973	-2.137	-2.690

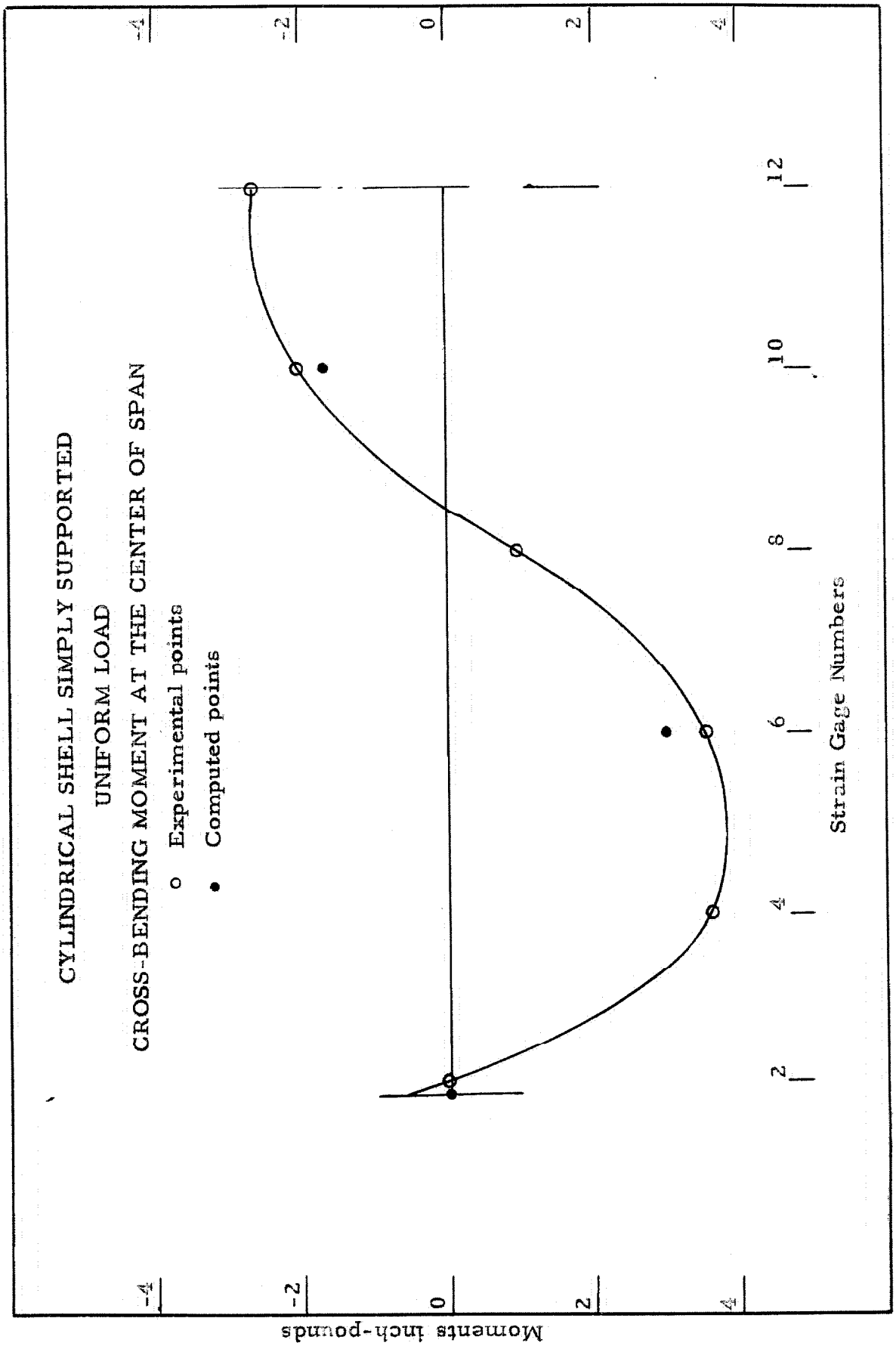
CYLINDRICAL SHELL SIMPLY SUPPORTED
UNIFORM LOAD
CROSS-BENDING MOMENT AT THE CENTER OF SPAN
o Experimental points
• Computed points
Moments inch-pounds
-4
-2
0
2
4
2
4
6
8
10
12
Strain Gage Numbers

Figure 60

5:7 Discussion of experimental results

In performing an experiment as described in this paper there are several factors which influence the accuracy of the test results. First, it is difficult to build a model with a cross-section exactly the same as assumed in the calculations. For instance, in the case of Model A, the angles were turned with an accuracy of $\pm$ 1/2 degree. Since the longitudinal stresses and cross-bending moment are sensitive to a change in the angles α, this would introduce some error in the result. Secondly, the stresses are calculated for a uniform load and this is virtually impossible to produce with lead bags. This is especially true in the case of a uniform load over the entire shell. As expected, a large spread is therefore obtained in the test results for the different runs. It was noticed that the cross-bending calculated from the test data was especially sensitive to the position of the loads on the model. Utmost care had to be taken in placing the load on the model in order to get as symmetrical a loading as possible. Thirdly, the slight change in voltage during the test introduced some error in the results. This effect shows up mostly in the case of small readings.

Since the thickness of the plate is small, the deflection perpendicular to the plates is relatively large. The transverse forces therefore produce an added cross-bending moment in the side plates between the joints which is not accounted for in the theory. However this effect would not show up in a prototype structure since the relative deflection would be about 1/10 of that in the models. It is difficult to calculate these effects in the case of the models, because it is not known how freely the joints can move toward each other.

MODEL A

The agreement is very good between the experimental results and the computed axial stresses in a section at the center of span and quarter point, both for uniform load on top and uniform load. See Figures 40, 42, 44, and 46.

In the case of uniform load on top, the cross-bending moment at the center of side plate (4) was adjusted to take into account the moment produced by the direct compression. It was assumed that the joints 3 and 4 were free to move toward each other. See Figure 41 and calculations in the Appendix. The fairly good check indicates that the joints are not free to move toward each other and thereby produce added bending moments. No modification was made in the case of the uniform load.

The fact that the longitudinal stresses on a cross-section check with the theory implies that the cross-bending must also check.

MODEL B

The reaction at the simply supported end was checked by lifting up at that end with a regular spring scale. When a sheet of paper placed under the support could be pulled free, the reading on the scale was taken. Several readings were taken for a uniform load on top (100 lbs.), and the average reading was 38 lbs. Computing the reaction with a moment of $1/8\omega L^2$ at the support gives 37.5 lbs. This indicates that the moment at the support is the same as for an ordinary beam.

The experimental results for variation of longitudinal stress

on an axial section at the center of the cross-section and in a cross-section at the third point show good agreement with the computed stresses, for both uniform load on top and uniform load. See Figures 48, 50 and 54.

In the case of uniform load on top, the cross-bending moment at the center of side plate (4) was adjusted to take into account the moment produced by direct compression. See Figure 49 and the calculation in the Appendix. No adjustment in bending moment due to direct force in the side plates was made in case of uniform load even though Figure 53 shows a fairly large disagreement between experimental and computed points. Using the computed compression forces in plate (4) and following the same procedure as shown on page 127 in calculating the added moment it is found that the correction is in the right direction, but overshoots quite a bit. This indicates that the joints (3 and 4) are not free to move toward each other and therefore has the effect of reducing the compression forces in the top plate.

MODEL C

For a uniform load on top, the longitudinal stresses in a section at the center of the span of the cylindrical shell, computed from the prismatic shell, show good agreement with the experimental stresses, except at the edge beam (Figure 5, 6). For this type of loading the edge beam is in compression and the discrepancy is attributed to buckling, which was observed during testing. In the case of uniform load the agreement between computed and experimental axial stresses is better. (Figure 59).

The cross-bending moment computed from the prismatic shell due to relative displacement of the side plates, checks well with the experimental results. The discrepancy between computed and experimental results in case of uniform load is attributed to the difficulty in obtaining the uniform loading. (See Figures 57 and 60). Most of the experimental points are within 10°/o of the computed points.

SUMMARY AND CONCLUSIONS

Cylindrical and prismatic shells may be used very economically for roof structures covering large floor areas. However, the lack of a simple design theory has retarded the general use of these structures. The previous design theories were based on the solutions of complicated differential equations involving the use of infinite series, the cylindrical shell being analysed by solving an eighth order partial differential equation, and the prismatic shell being analysed by solving "n" simultaneous differential equations of the fourth order, where "n" is the number of sides of the shell. A new method of analysis, not requiring the use of higher mathematics, is presented in this paper. The theory applies specifically to the analysis of prismatic shells, however, it is shown that cylindrical shells can also be analysed in the same manner. The method involves a certain amount of numerical calculation, but most of this consists of moment distributions which may be performed by persons without engineering training. The results of the different moment distribution processes depend only upon the geometry of the cross-section (except possibly for a constant) and are independent of the span, magnitude of loading and end conditions. The results from the distribution processes obtained in analysing one shell can thus be used in analysing other shells having geometrically similar cross sections.

The theory was verified by measuring the stresses in three different models. The difference between computed and measured stresses was well within the range of experimental error.

APPENDIX

Theoretical Calculations for Test Models

MODEL A, Uniform Load on Top

TABLE A-1

Joint No.	(1)	(2)	(3)	(4)	(5)	(6)
n	α_n	$\cos \alpha_n$	$\sin \alpha_n$	$\alpha_{n-1}-\alpha_n$	$\cot(\alpha_{n-1}-\alpha_n)$	$\operatorname{cosec}(\alpha_{n-1}\alpha_n)$
0	90	0	1	60		
1	30	0.8660	0.5000	15	0.5774	1.1547
2	15	0.9659	0.2588	15	3.7321	3.8637
3	0	1	0	15	3.7321	3.8637
4	-15	0.9659	0.2588	15	3.7321	3.8637

From Equation (47) and Table A-1:

$$\overline{Y}''_{12} = \overline{Y}''_{21} = \frac{1}{\beta} (-9.2376\ E_{10} + 4.3095 E_{21} - 3.8637 E_{32})$$

$$\overline{Y}''_{23} = \overline{Y}''_{32} = \frac{1}{\beta} (-3.8637\ E_{21} + 7.4642\ E_{32}) \qquad (A-1)$$

Distributing the coefficients of these equations as shown in the example Section 3:5 gives,

$$Y''_1 = 0$$

$$Y''_2 = \frac{1}{\beta} (-2.4347\ E_{10} + 2.3550\ E_{21} - 3.3736\ E_{32}) \qquad (A-2)$$

$$Y''_3 = \frac{1}{\beta} (+0.4803\ E_{10} - 1.2424\ E_{21} + 2.1681\ E_{32})$$

Hence the correction loads at the center of the span are:

$$Q_{1\overline{2}} = \frac{Y''_2 - Y''_1}{5} = \frac{1}{5}\,(-2.4347\,E_{10} + 2.3550\,E_{21} - 3.3736\,E_{32})$$

$$Q_{2\overline{3}} = \frac{Y''_3 - Y''_2}{5} = \frac{1}{5}\,(2.9150\,E_{10} - 3.5974\,E_{21} - 5.5417\,E_{32}) \qquad \text{(A-3)}$$

where

$$\frac{1}{5} = \frac{5L^4 t}{64H(1-\nu^2)} \quad \frac{1}{5} = \frac{1}{20.9854} \qquad \text{(A-4)}$$

From Equation (3):

$$p''_{10} = 1.1547\,R_{1\overline{2}}$$

$$p''_{21} = -0.5774\,R_{1\overline{2}} + 3.7321\,R_{2\overline{2}} + 3.8637\,R_{2\overline{3}} \qquad \text{(A-5)}$$

$$p''_{32} = -3.8637\,R_{2\overline{2}} - 3.7321\,R_{2\overline{3}} + 3.7321\,R_{3\overline{3}} + 3.8637\,R_{3\overline{4}}$$

From the external loading

$$q_2 = q_3 = 0, \quad q_4 = 1 \text{ lb/in}^2,$$

the fixed end bending moments are obtained.

$$\overline{Y}'_{34} = -\overline{Y}'_{43} = 1/12\;5^2 = 2\frac{1}{12}$$

The moment distribution is shown in Figure A-1

1	2		3		4
1	1/2	1/2	1/2	1/2	1/2
0	0	0	0	2.083	-2.083
0	0.3287	-0.3287	-1.3152	1.3152	-1.3152

Figure A-1

Then, $Y'_2 = 0.329$, $Y'_3 = -1.315$

$R_{1\overline{2}} = 0.0657$, $R_{2\overline{2}} = -0.0657$, $R_{2\overline{3}} = -0.3288$, $R_{3\overline{3}} = 0.3288$,

$R_{3\overline{4}} = 2.500$, $R_{4\overline{4}} = 2.500$

Since $p'_{10} = p'_{21} = p'_{32} = 0$, Equation (A-5) gives

$p_{10} = p''_{10} = 0.0759$, $p_{21} = p''_{21} = -1.5535$, $p_{32} = p''_{32} = 12.3573$

The fixed end "shears" $\overline{T}_{n,n-1} = \frac{1}{8} p_{n,n-1} L^2$ are:

$$\overline{T}_{10} = 8.744 \qquad \overline{T}_{21} = -89.482 \qquad \overline{T}_{32} = 712.356$$

The distribution is shown in Figure A-2.

0		1		2		3
1	1/3	2/3	1/2	1/2	1/2	1/2
-8.74	874	89.48	-89.48	-712.36	712.36	0
0	-93.01	+93.01	341.22	-341.22	598.03	-598.03
T'_n	-93.01		341.22		+598.03	
$\frac{4T'_n h_n}{L^2}$	-0.4037	-0.8074	+2.9620		+5.1912	

Figure A-2

Hence, from Figure A-2 and Equation (101a)

$$A_{10} = 0.0759 + 0.4037 = 0.4796$$

$$A_{21} = -1.5535 + 0.8074 - 2.962 = -3.7081 \qquad \text{(A-6)}$$

$$A_{32} = -12.3673 - 2.9620 - 5.1912 = 4.2141$$

The shear forces and bending moment at the center of the span are then obtained from Figure A-2 and Equation (A-6), respectively:

$T_1' = -93.0$, $T_2' = 341.2$, $T_3' = 598.0$, $N_1' = -93.0$, $N_2' = 434.2$,

$N_3' = 256.8$, $N_4' = 118.6$, $M_1' = 138.1$, $M_2' = -1067.9$, $M_3' = 1213.7$

Then since $\sigma = N/A \pm M/Z$, the longitudinal stresses at the center of the span are:

Plate 1:

$$\sigma_o' = -93 \times 10 + 138.1 \times 24 = -930 + 3314 = 2384$$

$$\sigma_1' = -930 - 3314 = -4244$$

Plate 2:

$$\sigma_1' = 434 \times 5 - 1067.9 \times 6 = 2170 - 6407 = -4237$$

$$\sigma_2' = 2170 + 6407 = 8577$$

(A-7)

Plate3:

$$\sigma_2' = 256.8 \times 5 + 1213.7 \times 6 = 1284 + 7282 = 8566$$

$$\sigma_2' = 1284 - 7282 = -5998,$$

Plate 4:

$$\sigma_3' = -2 \times 598.0 \times 5 = -5980$$

Next, determine $B_{n,n-1}$ by applying unit correction loads.

Apply correction loads $Q_{1\bar{2}} = 1$, $Q_{2\bar{2}} = -1$

Then from Equation (3):

$$w_{10} = 1.1547, \quad w_{21} = -4.3095, \quad w_{32} = 3.8637$$

The fixed end "shears" at the center of the span are:

$$\overline{T}''_{10} = \frac{48^2}{\pi^2 2.5} \times 1.1547 = 107.83, \quad \overline{T}''_{21} = -201.22, \quad \overline{T}''_{32} = 180.40$$

The distribution is shown in Figure A-3:

	0		1		2		3
	1	1/3	2/3	1/2	1/2	1/2	1/2
	-107.83	107.83	201.22	-201.22	-180.40	180.40	
	0	18.93	-18.93	-70.94	- 70.94	203.57	
T''_n		18.93		-70.94		203.57	
$\frac{\pi^2 T''_n h_n}{2L^2}$		1.1014	0.2028		-0.7597	2.1800	

Figure A-3

Apply correction loads $Q_{23} = 1$ $Q_{3\overline{3}} = -1$

Then from Equation (3):

$$w_{10} = 0 \qquad w_{21} = 3.8637 \qquad w_{32} = -7.4642$$

The fixed end shears are:

$$\overline{T}''_{10} = 0 \qquad \overline{T}''_{21} = 180.40 \qquad \overline{T}''_{32} = -348.52$$

The distribution is shown in Figure A-4:

	0		1		2		3
	1			1/2	1/2	1/2	
	0	0	-180.40	180.40	348.52	-348.52	
	0	102.09	-102.09	-70.73	70.73	-342.51	
T''_n		102.09		70.73		-324.51	
$\frac{\pi^2 T''_n h_n}{2L^2}$		0.5466	1.0932		-0.7597	2.1800	

Figure A-4

From Figures A-3, A-4 and Equation (101b) the expressions for the actual correction loads are:

$$B_{10} = (1.1547 - 0.1014) \quad Q_{1\overline{2}} - 0.5466\ Q_{2\overline{3}}$$

$$= 1.0533 \quad Q_{1\overline{2}} - 0.5466\ Q_{2\overline{3}}$$

$$B_{21} = -3.7526 \quad Q_{1\overline{2}} + 3.5278\ Q_{2\overline{3}} \qquad \text{(A-8)}$$

$$B_{32} = 2.4434\ Q_{1\overline{2}} - 3.2318\ Q_{2\overline{3}}$$

The expressions for shear at the center of the span are obtained from Figures A-3 and A-4:

$$T''_1 = 18.9338\ Q_{1\overline{2}} + 102.0928\ Q_{2\overline{3}}$$

$$T''_2 = -70.9427\ Q_{1\overline{2}} - 70.7277\ Q_{2\overline{3}} \qquad \text{(A-9)}$$

$$T''_3 = 203.7512\ Q_{1\overline{2}} - 324.5056\ Q_{2\overline{3}}$$

From Equations (A-8) and (46):

$$E_{10} = 0.4796 + 0.8305\ Q_{1\overline{2}} - 0.4310\ Q_{2\overline{3}}$$

$$E_{21} = -3.7\text{-}81 - 2.9590\ Q_{1\overline{2}} + 2.7817\ Q_{2\overline{3}} \qquad \text{(A-10)}$$

$$E_{32} = 4.2141 + 1.9267\ Q_{1\overline{2}} - 2.5483\ Q_{2\overline{3}}$$

Substituting Equations (A-10) into Equations (A-3) the following simultaneous equations are obtained:

$$20.9854\ Q_{1\overline{2}} = -15.4903\ Q_{1\overline{2}} + 16.1972\ Q_{2\overline{3}} - 24.1170$$

$$20.9854\ Q_{2\overline{3}} = \quad 23.7428\ Q_{1\overline{2}} - 25.3852\ Q_{2\overline{3}} + 38.0908 \qquad \text{(A-11)}$$

or

$$36.4757\ Q_{1\overline{2}} - 16.1972\ Q_{2\overline{3}} = -24.1170$$

$$-23.7428\ Q_{1\overline{2}} + 46.3706\ Q_{2\overline{3}} = 38.0908 \qquad \text{(A-12)}$$

The solution of these equations gives,

$Q_{1\overline{2}} = -0.3836$ $Q_{2\overline{3}} = 0.6250$, then $Y''_2 = -1.918$, $Y''_2 = 1.207$ in-lbs. (A-12a)

From Equation (A-8) and (A-9):

$$T''_1 = 56.6,\ T''_2 = -17.0,\ T''_3 = 281.0 \text{ lbs.}$$

$$B_{10} = -0.7456,\ B_{21} = 3.6444,\ B_{32} = -2.9572 \text{ lbs.}$$

Then,

$$N''_1 = 56.6,\ N''_2 = -73.6,\ N''_3 = 264.0,\ N''_4 = 562.0 \text{ lbs.}$$

$$M''_1 = 174.1,\ M''_2 = 850.8,\ M''_3 = -690.4$$

The longitudinal stresses at the center of the span produced by the correction loads are:

Plate 1: $\sigma''_o = 56.6 \times 10 - 174.1 \times 24 = 566 - 4178 = 3612$ psi.

$$\sigma''_1 = 566 + 4178 = 4744$$

Plate 2: $\sigma''_1 = -73.6 \times 5 + 850.8 \times 6 = -368 + 5105 = 4737$

$$\sigma''_2 = -368 - 5105 = -5473 \qquad \text{(A-13)}$$

Plate 3: $\sigma''_2 = -264 \times 5 - 690.4 \times 6 = -1320 - 4142 = -5462$

$$\sigma''_3 = -1320 + 4142 = 2822$$

Plate 4: $\sigma''_3 = 562 \times 5 \qquad = 2810$

Using the average of the stresses at a joint calculated from two adjacent side plates the longitudinal stresses along the span are: (See Equations (A-7), (A-13), and (99)).

$$\sigma_o = 2384\ g_1(x) - 3612\ g_2(x)$$

$$\sigma_1 = -4240\ g_1(x) + 4740\ g_2(x)$$

$$\sigma_2 = 8572\ g_1(x) - 5467\ g_2(x) \qquad \text{(A-14)}$$

$$\sigma_3 = -5989\ g_1(x) + 2816\ g_2(x)$$

where

$$g_1(x) = 4\left(\frac{x}{L} - \frac{x^2}{L^2}\right)$$

$$g_2(x) = \sin\frac{\pi x}{L} \qquad \text{(A-15)}$$

At center of the span the longitudinal stresses are:

$$\sigma_o = -1228\ \ \sigma_1 = 500\ \ \sigma_2 = 3105\ \ \sigma_3 = -3173 \text{ lbs./in.}^2$$

At quarter span the longitudinal stresses are:

$$\sigma_o = -740,\ \ \sigma_1 = 140\ \ \sigma_2 = 2580\ \ \sigma_3 = -2515 \text{ lbs./in.}^2$$

From Figure A-1 and Equation (A-12a) the cross-bending moments are

$$Y_n = Y'_n + Y''_n F_1(x)$$

$$Y_2 = 0.329 - 1.918\ F_1(x) \qquad \text{(A-16)}$$

$$Y_3 = -1.315 + 1.207\ F_1(x)$$

where $F_1(x) = \sin\frac{\pi x}{L}$

At center of the span the cross-bending moments are

$$Y_2 = -1.589, \quad Y_3 = -0.108 \text{ in.-lbs.}$$

Cross-bending moment due to transverse forces in side plate 4 in center of the span.

Consider a unit strip with compression forces and moments at the ends and loaded uniformly, as shown in Figure A-5:

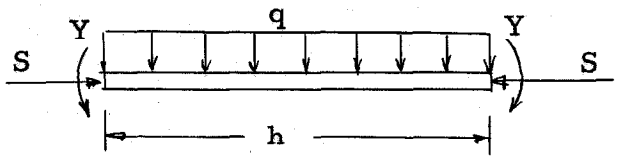

Figure A-5

The deflection at the center of the side plate (4) will then be:

$$\delta = \left(\frac{qD}{S^2} - \frac{Y}{S}\right)\left(\frac{1}{\cos\frac{uh}{2}} - 1\right) - \frac{qh^2}{8S} \qquad \text{(A-17)}$$

$$D = \frac{Et^3}{12(1-\nu^2)}; \quad u^2 = \frac{S}{D}$$

The calculations for the deflection at the center of plate 4 produced by $R_{3\overline{4}} = R_{4\overline{4}} = 2.5$ are shown below:

$$Y_3 = 0.108, \quad S = 2.5 \times 3.732 = 9.33, \quad S^2 = 87, \quad D = 62.3$$

$$p^2 = 0.1495, \quad p = 0.387, \quad \frac{uh}{2} = 0.967$$

$$\cos\frac{uh}{2} = 0.568$$

$$\delta = \left(\frac{62.3}{87} - \frac{0.108}{9.33}\right)(1.76 - 1) - \frac{25}{8 \times 9.33}$$

$$\delta = 0.535 \quad -0.335 = \quad 0.200 \text{ in.}$$

Then the moment at the center of the side plate (4) is:

$$Y = -0.108 + 1/8\, q\, L^2 + 9.33 \times 0.20$$

$$Y = -0.108 + 3.125 + 1.866 = 4.883 \text{ in.-lbs.}$$

This moment is plotted in Figure 41.

MODEL A, Uniform Load

The external loadings are:

$$q_2 = 0.8660 \frac{lb}{in^2}, \quad q_3 = 0.9659 \frac{lb}{in^2}, \quad q_4 = 1.0000 \frac{lb}{in^2}$$

$$p'_{10} = 0, \quad p'_{21} = 2.5000 \frac{lb}{in^2}, \quad p'_{32} = 1.2941 \frac{lb}{in^2}$$

From the q's the fixed bending moments are calculated as shown below:

$$\overline{Y}'_{12} = -\overline{Y}'_{21} = \frac{5^2}{12} \times 0.8660 = +1.810$$

$$\overline{Y}'_{23} = -\overline{Y}'_{32} = \frac{5^2}{12} \times 0.9659 = +2.010$$

$$\overline{Y}'_{34} = -\overline{Y}'_{43} = \frac{5^2}{12} \times 1.000 = +2.080$$

The distribution is shown in Figure A-6:

1		2		3		4
1	1/2	1/2	1/2	1/2	1/2	
+1.810	-1.810	2.010	-2.010	2.080	-2.080	
0	-2.371	-2.371	-1.985	-1.985		

Figure A-6

From the above results the values for the R's and Y's are:

$R_{1\overline{2}} = 1.691$, $R_{2\overline{2}} = 2.639$, $R_{2\overline{3}} = 2.492$, $R_{3\overline{3}} = 2.338$, $R_{3\overline{4}}=R_{4\overline{4}}=2.500$

$Y_1' = 0$, $Y_2' = -2.371$, $Y_3' = -1.985$

Substituting the values for $R_{n-1,n}$ etc. into Equation (A-5) the plate loads are:

$p''_{10} = 1.953$, $p''_{21} = 18.501$, $p''_{32} = -1.112$

Then since $p_{n,n-1} = p'_{n,n-1} + p''_{n,n-1}$

$p_{10} = 1.953$, $p_{21} = 21.001$, $p_{32} = 0.182$

The fixed end shears are:

$\overline{T}'_{10} = 224.95$, $\overline{T}_{21} = 1209.63$, $\overline{T}_{32} = 10.48$

The distribution is shown in Figure A-7:

	0		1		2		3
	1	1/3	2/3	1/2	1/2	1/2	1/2
	-225.0	225.0	.1209.6	1209.6	-10.5	10.5	256.7
		695.9	-695.9	804.6	-804.6	-256.7	256.7
T''_n			695.9		804.6		256.7
$\frac{4T''_n h_n}{L^2}$		3.020	6.040	6.984		-2.228	

Figure A-7

Hence, from Equation (101a) and Figure A-7

$$A_{10} = 1.953 - 3.020 = -1.067$$
$$A_{21} = 21.001 - 6.040 - 6.984 = 7.977 \qquad \text{(A-18)}$$
$$A_{32} = 0.182 - 6.9840 + 2.228 = -4.574$$

Then,

$$T_1' = 695.9, \quad T_2' = 804.6, \quad T_3' = -256.7$$

$$N_1' = 695.9, \quad N_2' = 108.7, \quad N_3' = -1061.3, \quad N_4 = 513.4 \qquad \text{(A-19)}$$

$$M_1' = -307.4, \quad M_2' = 2297.3, \quad M_3' = -1317.3$$

The longitudinal stresses due to $p_{n,n-1}$ are:

Plate 1:

$$\sigma_o' = 695.9 \times 10 - 307.4 \times 24 = 6959 - 7378 = -419$$

$$\sigma_1' = 6959 + 7378 = 14337$$

Plate 2:

$$\sigma_1' = 108.7 \times 5 + 2297.3 \times 6 = 543 + 13,783 = 14326$$

$$\sigma_2' = 543 - 13,783 = -13,240 \qquad \text{(A-20)}$$

Plate 3:

$$\sigma_2' = -1061.3 \times 5 - 1317.3 \times 6 = 5306 - 7904 = -13,210$$

$$\sigma_3' = -5306 + 7904 = 2598$$

Plate 4:

$$\sigma_3' = 2 \times 256.7 \times 5 = 2567$$

Using the "A's" calculated above and the same "B" as in the calculation for "uniform load on top" the equations for $E_{n,n-1}$ become:

$$\begin{aligned} E_{10} &= -1.067 + 0.8305\, Q_{1\overline{2}} - 0.4310\, Q_{2\overline{3}} \\ E_{21} &= 7.977 - 2.950\, Q_{1\overline{2}} + 2.7817\, Q_{2\overline{3}} \\ E_{32} &= -4.574 + 1.9267\, Q_{1\overline{2}} - 2.5483\, Q_{2\overline{3}} \end{aligned} \qquad \text{(A-21)}$$

Substituting into Equation (A-3) gives:

$$36.4757\ Q_{1\overline{2}} - 16.1972\ Q_{2\overline{3}} = 36.815$$

$$-23.7428\ Q_{1\overline{2}} + 46.3706\ Q_{2\overline{3}} = -57.153 \qquad \text{(A-22)}$$

The solution of these equations are,

$$Q_{1\overline{2}} = 0.598,\ Q_{2\overline{3}} = -0.926,\ Q_{2\overline{3}} = -0.926,\ Q_{1\overline{2}} = 0.598$$

Then

$$Y''_2 = 2.990 \qquad Y''_3 = -1.640$$

Substituting $Q_{1\overline{2}}$ and $Q_{2\overline{3}}$ into Equations (A-8) and (A-9) gives:

$$T''_1 = -83.26, \quad T''_2 = 23.10, \quad T''_3 = 422.44$$

$$B_{10} = 1.1362, \quad B_{21} = 5.5119, \quad B_{32} = 4.4548$$

Then

$$N'_1 = -83.3, \quad N''_2 = 106.4, \quad N''_3 = 399.3, \quad N''_4 = -844.88$$

$$M''_1 = 265.3, \quad M''_2 = -1286.8, \quad M''_3 = 1040.0$$

The longitudinal stresses are,

Plate 1:

$$\sigma''_o = -83.3 \times 10 + 265.3 \times 24 = -833 + 6367 = 5534$$

$$\sigma''_1 = -833 - 6367 = -7200$$

Plate 2:

$$\sigma''_1 = 106.4 \times 5 = 1286.8 \times 6 = 532 - 7721 = 7189 \qquad \text{(A-23)}$$

$$\sigma''_2 = 532 + 7721 = 8253$$

Plate 3:

$$\sigma''_2 = 399.3 \times 5 + 1040 \times 4 = 1996 + 6240 = 8236$$

$$\sigma''_3 = 1996 - 6240 = -4244$$

Plate 4: $\sigma''_3 = -2 \times 422.4 \times 5 = -4224$

Combine the effects due to the external loading and the correction loads and the longitudinal stresses are:

$$\sigma_o = -419\ g_1(x) + 5534\ g_2(x)$$

$$\sigma_1 = 14,332\ g_1(x) - 7195\ g_2(x)$$

$$\sigma_2 = -13,225\ g_1(x) + 8245\ g_2(x)$$

$$\sigma_3 = 2582\ g_1(x) - 4234\ g_2(x) \qquad \text{(A-24)}$$

$$T_1 = 695.9\ g_1(x) - 83.3\ g_2(x)$$

$$T_2 = 804.6\ g_1(x) + 23.1\ g_2(x)$$

$$T_3 = -256.7\ g_1(x) + 422.4\ g_2(x)$$

The cross-bending moments are:

$$Y_2 = Y_2' + Y_2'' = -2.371 + 2.990\ F_2(x)$$

$$Y_3 = Y_3' + Y_3'' = -1.985 - 2.652\ F_2(x) \qquad \text{(A-25)}$$

where $g_1(x) = 4(\frac{x}{L} - \frac{x^2}{L^2})$, $\quad g_2(x) = \sin\frac{\pi x}{L}$

$$F_2(x) = \frac{16x}{L}(1 - \frac{2x^2}{L^2} + \frac{x^3}{L^3}) \qquad \text{(A-26)}$$

The longitudinal stresses at center of the span and at the quarter point will then be:

Center of the span: $\sigma_o = 5115, \sigma_1 = 7137, \sigma_2 = -4980, \sigma_3 = -1652$ psi

Quarter point: $\sigma_o = 3600, \sigma_1 = 5640, \sigma_2 = 0\text{-}4110, \sigma_3 = -1050$ psi $\qquad \text{(A-27)}$

The cross-bending moment at the center of the span will be:

$$Y_2 = 0.620 \qquad Y_3 = -3.630 \text{ in.-lbs.}$$

MODEL B, Uniform Load on Top

From the calculation shown for the simply supported prismatic shell the longitudinal stresses due to $p_{n,n-1}$ are:

$$\sigma_0' = 2384\ g_1(x)$$

$$\sigma_1' = -4240\ g_1(x)$$

$$\sigma_2' = 8572\ g_1(x)$$

$$\sigma_3' = -5989\ g_1(x)$$

where $g_1(x) = \frac{3x}{L} - (\frac{2x}{L})^2$

Furthermore, from Equations (A-10) and (68) the equations for $E_{n,n-1}$ are:

$$E_{10} = 0.4796 + \frac{0.8101}{0.7885}(0.8305\ Q_{1\bar{2}} - 0.3965\ Q_{2\bar{3}})$$

$$E_{21} = -3.7081 - \frac{0.8101}{0.7885}(2.9590\ Q_{1\bar{2}} + 2.7817\ Q_{2\bar{3}})$$

$$E_{32} = 4.2140 + \frac{0.8101}{0.7885}(1.9267\ Q_{1\bar{2}} - 2.5483\ Q_{2\bar{3}})$$

Substituting these equations into Equation (A-3) and remembering that

$$\frac{1}{5\beta} = \frac{L^4 t^2}{(1-\nu^2)32h^5}\frac{1}{5} = 1/52.4580$$

the following simultaneous equations are obtained:

$$(52.5480 + 15.9146)\ Q_{1\bar{2}} - 16.6409\ Q_{2\bar{3}} = -24.1170$$

$$-24.3932\ Q_{1\bar{2}} + (52.4580 + 26.0806)\ Q_{2\bar{3}} = 38.0908 \qquad \text{(A-29)}$$

The solution of these equations are

$$Q_{1\bar{2}} = -0.2539, \qquad Q_{2\bar{3}} = 0.4061$$

From Equations (A-8) and (A-9)

$$T''_1 = 36.65, \quad T''_2 = -10.72, \quad T''_3 = -183.49$$

$$B_{10} = -0.4894, \quad B_{21} = 2.3856, \quad B_{32} = -1.9330$$

Then, from Equations (95) and (97)

$$N''_1 = 36.65, \quad N''_2 = -47.37, \quad N''_3 = -172.77, \quad N''_4 = 366.98$$

$$M''_1 = -114.25, \quad M''_2 = 556.94, \quad M''_3 = -451.27$$

The longitudinal stresses at the center of the span are:

Plate 1:

$$\sigma''_o = 367 - 2742 = -2375$$

$$\sigma''_1 = 367 + 2742 = 3109$$

Plate 2:

$$\sigma''_1 = -237 + 3342 = 3105$$

$$\sigma''_2 = -237 - 3342 = -3579$$

Plate 3:

$$\sigma''_2 = -864 - 2708 = -3572$$

$$\sigma''_3 = -864 + 2708 = 1844$$

Plate 4:

$$\sigma''_3 = 2 \times 183.5 \times 5 \quad 1835$$

The general expressions for longitudinal stresses are:

$$\sigma_o = 2384\, g_1(x) - 2375\, g_2(x) \qquad \text{(A-30)}$$

$$\sigma_1 = -4240\, g_1(x) + 3107\, g_2(x)$$

$$\sigma_2 = 8572\ g_1(x) - 3575\ g_2(x)$$

$$\sigma_3 = -5989\ g_1(x) + 1839\ g_2(x) \qquad \text{(A-30) Cont'd.}$$

$$g_2 = \sin\frac{\pi x}{L} - \frac{3x}{\pi L}$$

The stresses at $x = \frac{L}{2}$ will be: (the third point nearest to the simple support)

$$\sigma_o = -25,\ \sigma_1 = -650,\ \sigma_2 = 2800,\ \sigma_3 = -2325 \text{ psi.} \qquad \text{(A-31)}$$

The variation of the longitudinal stresses along the centerline on the top are as shown in Table A-2:

TABLE A-2

x/L	1/6	1/3	1/2	2/3	5/6	1
σ'_3	-2330	-3330	-2995	-1335	1665	5989
σ''_3	628	1010	962	422	-548	-1760
σ_3	-1702	-2320	-2033	-913	1117	4229

These values are plotted in Figure (48).

The cross-bending moments are:

$$Y_2 = 0.329 - 1.270\ F_1(x)$$

$$Y_3 = -1.315 + 0.760\ F_1(x) \qquad \text{(A-32)}$$

$$\text{where } F_1(x) = \frac{4x}{L}\left(1 - \frac{3x^2}{L^2} + \frac{2x^3}{L^3}\right)$$

The cross-bending moment due to the transverse forces in the side

plate (4) are determined by using equation (A-17) and performing a calculation similar to the one shown on page 127. The moments $S\delta$ are shown in Table A-3.

TABLE A-3

x/L	1/6	1/3	1/2	2/3	5/6
Y	-0.845	-0.563	-0.555	-0.790	-1.125
$1/8\ qh^2$	3.125	3.125	3.125	3.125	3.125
$S\delta$	1.300	1.510	1.510	1.330	1.070
Moment at the center of side 4.	3.580	4.072	4.075	3.665	3.070

These values for cross-bending moment are plotted in Figure 49.

MODEL B, Uniform Load

Equations (A-29) will also apply in this case except that the right-hand side of the equations will be the same as in Equations (A-22). Then,

$$\begin{aligned} 68.3726\ Q_{1\overline{2}} - 16.6409\ Q_{2\overline{3}} &= 36.815 \\ -24.3932\ Q_{1\overline{2}} + 78.5386\ Q_{2\overline{3}} &= -57.153 \end{aligned} \qquad \text{(A-33)}$$

The solution of these equations is:

$$Q_{1\overline{2}} = 0.3909, \qquad Q_{2\overline{3}} = -0.6063$$

From Equations (A-8) and (A-9)

$$T_1 = -54.50, \quad T_2 = 15.15, \quad T_3 = 276.33$$

$$B_{10} = 0.7431, \quad B_{21} = -3.6058, \quad B_{32} = 2.9147$$

Then, from Equations (95) and (97)

$$N''_1 = -54.50, \quad N''_2 = 69.65, \quad N''_3 = 261.17, \quad N''_4 = 552.66$$

$$M'_1 = 173.48, \quad M''_2 = -841.80, \quad M''_3 = 680.46$$

The longitudinal stresses at the center of the span are:

Plate 1:

$$\sigma''_o = -545 + 4164 = 3619$$

$$\sigma''_1 = -545 - 4164 = -4709$$

Plate 2:

$$\sigma''_1 = 348 - 5051 = -4703$$

$$\sigma''_2 = 348 + 5051 = 5399$$

Plate 3:

$$\sigma''_2 = 1306 + 4083 = 5389$$

$$\sigma''_3 = 1306 - 4083 = -2777$$

Plate 4:

$$\sigma''_3 = -2 \times 276.3 \times 5 = -2763$$

Combining with Equations (A-20), the total stresses are obtained.

$$\sigma_o = -419\, g_1(x) + 3619\, g_2(x)$$

$$\sigma_1 = 14,332\, g_1(x) - 4706\, g_2(x)$$

$$\sigma_2 = -13,225\, g_1(x) + 5394\, g_2(x)$$

$$\sigma_3 = 2582\, g_1(x) = 2770\, g_2(x)$$

where $g_1(x) = \frac{3x}{L} - (\frac{2x}{L})^2 \quad g_2(x) = \sin \frac{\pi x}{L} - \frac{3x}{\pi L}$

The longitudinal stresses at $x = \frac{L}{2}$ are: (the third point nearest to the simple support)

$$\sigma_o = 1747, \ \sigma_1 = 5410, \ \sigma_2 = -4470, \ \sigma_3 = -80 \text{ psi.} \qquad \text{(A-35)}$$

The variation of the longitudinal stress along the center line of the shell is:

TABLE A-4

x/L	1/6	1/3	1/2	2/3	5/6	1
σ_3'	1005	1437	1291	575	-717	-2582
σ_3''	-930	-1495	-1435	-626	808	2610
σ_3	75	-58	-144	-51	-91	28

Since the value of the stresses are small, they are not shown graphically.

The cross-bending moment will be

$$Y_2 = -2.371 + 1.954 \, F_1(x)$$

$$Y_3 = -1.985 - 1.077 \, F_1(x) \qquad \text{(A-36)}$$

where

$$F_1(x) = (\frac{4x}{L}) (1 - \frac{3x^2}{L^2} + \frac{2x^3}{L^3})$$

REFERENCES
Prismatic Shells

1. Schwyzer, H., Dipl.-Ing., Statische Untersuchung der aus ebenen Tragflachen Zusammengesetzten Raumlichen Tragwerke. Diss., Zurich 1920.

2. Craemer, Theorie der Faltwerke, B.u.E., 29, Jahrg. 1930, Heft 15, s. 276 bis 281.

3. Ehlers, George, Dipl. Ing., Ein neues Konstruktionsprinzip. Bauing, 9 Jahrg. 1930, Heft 8, S. 125 bis 132.

4. Ehlers, Die Spannungsermittlung in Flachentragwerken. Beton und Eisen, 29 Jahrg. 1930, Heft 15 und 16, S281 bis 286 und 291 - bix 296.

5. E. Gruber, Berechnung prismatischer Scheibenwerke, Intern. Assoc. Bridge & Struct. Engg. Memoires, V. 1, 1932 p. 225.

6. G. Gruening, Die Nebenspannungen in prismatischen Faltwerken, Ingenieur-Archiv. 3. Band, 1932 Heft 4, p. 319.

7. J. Goldenblatt & E. Ratz, Berechnung von Faltwerken, welche aus Scheiben mit verschiedenen statischen Systemen bestehen. Beton und Eisen 33. Jahrg. 34, Heft 23, S. 369 bis 371.

8. E. Gruber, Die Berechnung pyramidenartiger Scheibenwerke und ihre Anwendung auf Kaminkuhler. Intern. Assoc. Bridge & Struct. Engg., Memoires, V.2, 1933-34, p. 206.

9. R. Ohlig, Die Nebenspannungen der Randtrager prismatischer Faltwerke unter besonderer Berucksichtigung des U- formigen Plattenbalkens, Diss. Darmstadt. Wurzburg 1934.

10. E. Gruber, Die Berechnung ausserlich Statisch unbestimmter prismatischer Scheibenwerke. Intern. Assoc. Bridge & Struct. Engg., Memoires, V.3, 1935, p. 134.

11. R. Ohlig, Berlin, Beitrag zur Theorie der prismatischen Faltwerke. Ingenieur-Archiv, 6. Band 1935 Heft 5, S. 346 bis 354.

12. W. Petry, Scheiben und Schalen im Eisenbetonbau, Intern. Assoc. Bridge & Struct. Engg., 1st Congress, Final Report, p. 209, 1932.

13. H. Cramer, Der heutige Stand der Theorie der Scheibentrager und Faltwerke in Eisenbeton, Beton und Eisen, 36. Band 1937, Heft 16, S. 264 & 297.

14. E. Gruber, Hohltrager als Faltwerke, Intern. Assoc. Bridge & Struct. Engg., Memoires, V. 7, 1943-44, p. 139.

REFERENCES (Cont'd)

15. A. Krysztal: Hipped Plate and Shell Roof Construction in Reinforced Concrete, The Journal of the Institution of Engineers Australia, V. 22, No. 10-11, Oct.-Nov. 1950.

16. G. Winter & Minglung Pei: Hipped-plate Construction, Jour. Am. Conc. Inst., Jan. 1947.

17. Statik und Dynamik der Schalen, by W. Flugge, Berlin, Springer Verlag, 1934.

Cylindrical Shells

18. Lame, G. et Clapeyron, E., Mem. pres. par div. savants 4, 1828, p. 465.

19. Love, A.E.H., A Treatise on the Mathematical Theory of Elasticity, Cambridge (Eng.) 1892, 1893, 1906, 1920, 1927, 1944.

20. H. Rusch: Theorie der querversteiften Zylinderschalen fur schmale, unsymmetrische Kreiss-segmente, Diss. Munchen 1931.

21. U. Finsterwalder: Die Theorie der zylinderischen Schalengewolbe System Zeiss-Dywidag und ihre Anwendung auf die Grossmarkthalle in Budapest. Inernat. Assoc. Bridge & Struct. Engg. Publ. 1, 127-52, 1932.

22. F. Dischinger; Die strenge Theorie der Kreiszylinderschale in ihrer anwendung auf die Zeiss-Dywidag-Schalen. Beton und Eisen 34, 257-64 and 283-94, 1935.

23. H. Schorer: Line Load Action on Cylindrical Shells. Proc. Amer. Soc. Civ. Engr. 61, 281-316. 1935.

24. P. Nemenyi: Beitrage zur Berechnung der Schalen unter unsymmetrischer und unstetiger Belastung. Bygnungsstat. Medd 8, 53-72. 1936.

25. A. Aas-Jakobsen: Zylinderschalen mit veranderlichem Krummungshalbmesser und veranderlicher Schalenstarke. Bauing. 18, 418-22 and 436-44. 1937.

26. A. Aas-Jakobsen: Uber das Randstorungsproblem an Kreiszylinderschalen. Bauing. 20, 394-405. 1939.

27. K. Marguerre: Zur Theorie der gekrummten Platte grosser Formanderung. Proc. Fifth Internat. Congr. Appl. Mech., Cambridge (Mass.) pp. 93-101, 1939.

REFERENCES (Cont'd)

28. A. Aas-Jakobsen: Einzellasten auf Kreiszylinderschalen. Bauing. 22, 343-46, 1941.

29. F.K.G. Odquist: The Load Carrying Action on Thin Cylindrical Shells (in Swedish) Ing. Vetensk, Akad. Handl. Nr. 164, 1942.

30. A. Aas-Jakobsen: Concentrated Loads on Cylindrical Shells (in Norwegian). Bygningsstat. Medd. 15, 41-64, 1944.

31. H. Lundgren: Analytical Calculation of Anisotropic Circular Cylindrical Shells. Christiani and Nielsen Bull. No. 43. Copenhagen, 1945.

32. S. Eggwertz: Theory of Elasticity for Thin Circular Cylindrical Shells. Trans. Royal Inst. Techn. Stockholm No. 9, 1947.

33. R. S. Jenkins: Theory and Design of Cylindrical Shell Structures. Publ. by O.N. Arup, Colquhoun House, London W.1. 1947 (Modern Building Techniques - Bulletin No. 1).

34. H. Lundgren: Cylindrical Shells. Publ. by The Danish Technical Press, Copenhagen, 1951.

35. G. de Kazinczy: Design of Reinforced Concrete Cylindrical Shells. Betong Svenska Betongforenings Tidskrift, Stockholm, No. 4, 1949 (in Swedish).

36. K. Girkman: Flachentragwerke. Wien-Springer Verlag, 1946.

37. Fr. Dishinger: Neues Bauen in Eisenbeton.

38. Suchnowski: Reinforced Concrete. Moscow, 1946.

39. S. Timoshenko: Theory of Plates and Shells. New York and London, 1940.

40. E. C. Molke & I.E. Kalinka: Principles of Concrete Shell Dome Design. Jour. Am. Conc. Inst., May-June, 1938.

41. H. Savage: Reinforced Concrete Shell Roofs, Concrete and Constructional Engineering, Sept. 1930.

42. W. T. Marshall: The Elements of the Design of Cylindrical and Elliptical Shells. Concrete and Constructional Engineering, May-Sept. 1945.

43. A. I. Ashdown: Prismatic Thin-Slab Structures of one Span. Concrete and Constructional Engineering, Oct.-Nov. 1948 and Mar. 1949.

REFERENCES (Cont'd)

44. A Thin Slab Vault Roof at Dagenham. Concrete and Constructional Engineering, Dec. 1948.

45. Concrete Shell Roof used on World's Fair Building. Engg. News Record, June 4, 1934.

46. Ribbed Concrete Arch Roof Construction. Construction Review, Nov. 1943.

47. Concrete Shell and BarrelRoofs. Cement and Concrete Association, London.

48. U. Finsterwalder. Die querversteiften zylinderischen Schalengewolbe mit kreissegmentformingen Querschnitt (Segmental Cylindrical Shells with Cross Stiffeners) Ingenieur Archiv. Vol. 4, P. 43, 1933.

49. C. W. Kirkland and A. Goldstein: The Design and Construction of a Large Span Pre-stressed Concrete Shell Roof. The Structural Engineer, April 1951. Discussion Nov. 1951.

NOTATION

n = an integer

α = inclination of side plate to horizontal

h_n = width of side plate n

t_n = thickness of side plate n

L = length of shell between supports

a_n = area of cross-section of side plate

I_n = moment of inertia of plate n about the neutral axis perpendicular to plate

Z_n = section modulus of side plate n; $Z_n = \frac{2I_n}{n_n}$

$e_{n,n-1}$ = distance from neutral axis of nth plate to joint n-1

J_n = moment of inertia of cross-section of unit strip

q_n = intensity of external load component perpendicular to plate n on a unit area

$p'_{n,n-1}$ = external load component parallel to plate n on a unit length of shell. (Plate load).

$\overline{Y}'_{n-1,n}$ = fixed end cross-bending moment at joint n-1 of member n-1, n of the unit strip

Y'_n = joint cross-bending moment due to the external load on the plate

$R_{n,\overline{n}}$ = joint reaction at joint n perpendicular to plate n due to external load

$p''_{n,n-1}$ = plate load due to the R-loads

$p_{n,n-1} = p'_{n,n-1} + p''_{n,n-1}$ + (any other plate loads)

The following notation refers to the center of the span regardless of the end conditions:

$\overline{Y}''_{n-1,n}$ = fixed end cross-bending moment at joint n-1 of member n-1, n of the unit strip due to relative displacement of the joints

Y''_n = cross-bending moment at joint n due to rotation of the side plates

NOTATION (Cont'd)

$Q_{n,\overline{n}}$ = correction load at joint n perpendicular to side plate n

$w_{n,n-1}$ = plate load due to the correction loads Q

$A_{n,n-1}$ = equivalent plate load (uniform along span)

$B_{n,n-1}$ = equivalent plate load

T'_n = shear force at joint n due to p-loads

T''_n = shear force at joint n due to the w-loads

T_n = shear force at joint n

$N'_n = T'_n - T_{n-1}$ $N''_n = T''_n - T''_{n-1}$, $N_n = T_n - T_{n-1}$

$M^{0,'}_n$ = bending moment due to $p_{n,n-1}$ of side plate acting as a beam

$M^{0''}_n$ = bending moment due to $w_{n,n-1}$

M'_n = bending moment due to $p_{n,n-1}$, T'_n and T'_{n-1}

M''_n = bending moment due to $w_{n,n-1}$, T''_n and T''_{n-1}

$\overline{T}'_{n-1,n}$ = fixed end moment of the conjugate beam at joint n-1 of the member n-1, n

K = stiffness factor

y'_n = deflection of side plate n due to $p_{n,n-1}$, T'_n and T'_{n-1}

y''_n = deflection of side plate n due to $w_{n,n-1}$, T''_n and T''_{n-1}

y_n = total deflection of plate n

$\eta_{n,\overline{n+1}}$ = deflection of joint n perpendicular to plate n+1

d_n = relative displacement = $\eta_{n,\overline{n}} - \eta_{n-1,\overline{n}}$

σ = longitudinal unit stress

τ = shear per unit length